

THE INTERNATIONAL FOOD OPERATIONS & PROCESSING SIMULATION WORKSHOP

SEPTEMBER 26-28 2016
CYPRUS



EDITED BY
AGOSTINO BRUZZONE
FRANCESCO LONGO
MIQUEL ANGEL PIERA
GIUSEPPE VIGNALI

PRINTED IN RENDE (CS), ITALY, SEPTEMBER 2016

ISBN 978-88-97999-75-1 (Paperback)
ISBN 978-88-97999-83-6 (PDF)

© 2016 DIME UNIVERSITÀ DI GENOVA

RESPONSIBILITY FOR THE ACCURACY OF ALL STATEMENTS IN EACH PAPER RESTS SOLELY WITH THE AUTHOR(S). STATEMENTS ARE NOT NECESSARILY REPRESENTATIVE OF NOR ENDORSED BY THE DIME, UNIVERSITY OF GENOVA. PERMISSION IS GRANTED TO PHOTOCOPY PORTIONS OF THE PUBLICATION FOR PERSONAL USE AND FOR THE USE OF STUDENTS PROVIDING CREDIT IS GIVEN TO THE CONFERENCES AND PUBLICATION. PERMISSION DOES NOT EXTEND TO OTHER TYPES OF REPRODUCTION NOR TO COPYING FOR INCORPORATION INTO COMMERCIAL ADVERTISING NOR FOR ANY OTHER PROFIT - MAKING PURPOSE. OTHER PUBLICATIONS ARE ENCOURAGED TO INCLUDE 300 TO 500 WORD ABSTRACTS OR EXCERPTS FROM ANY PAPER CONTAINED IN THIS BOOK, PROVIDED CREDITS ARE GIVEN TO THE AUTHOR(S) AND THE CONFERENCE.

FOR PERMISSION TO PUBLISH A COMPLETE PAPER WRITE TO: DIME UNIVERSITY OF GENOVA, PROF. AGOSTINO BRUZZONE, VIA OPERA PIA 15, 16145 GENOVA, ITALY. ADDITIONAL COPIES OF THE PROCEEDINGS OF THE FOODOPS ARE AVAILABLE FROM DIME UNIVERSITY OF GENOVA, PROF. AGOSTINO BRUZZONE, VIA OPERA PIA 15, 16145 GENOVA, ITALY.

ISBN 978-88-97999-75-1 (Paperback)

ISBN 978-88-97999-83-6 (PDF)

THE INTERNATIONAL FOOD OPERATIONS & PROCESSING SIMULATION WORKSHOP, FOODOPS 2016 SEPTEMBER 26-28 2016, CYPRUS

ORGANIZED BY



DIME - UNIVERSITY OF GENOA



LIOPHANT SIMULATION



SIMULATION TEAM



IMCS - INTERNATIONAL MEDITERRANEAN & LATIN AMERICAN COUNCIL OF SIMULATION



DIMEG, UNIVERSITY OF CALABRIA



MSC-LES, MODELING & SIMULATION CENTER, LABORATORY OF ENTERPRISE SOLUTIONS



UNIVERSITY OF PARMA



MODELING AND SIMULATION CENTER OF EXCELLENCE (MSCOE)



LATVIAN SIMULATION CENTER - RIGA TECHNICAL UNIVERSITY



LOGISIM



LSIS - LABORATOIRE DES SCIENCES DE L'INFORMATION ET DES SYSTEMES



MIMOS - MOVIMENTO ITALIANO MODELLAZIONE E SIMULAZIONE



MITIM PERUGIA CENTER - UNIVERSITY OF PERUGIA



BRASILIAN SIMULATION CENTER, LAMCE-COPPE-UFRJ



MITIM - McLEOD INSTITUTE OF TECHNOLOGY AND INTEROPERABLE MODELING AND SIMULATION - GENOA CENTER



M&SNET - MCLEOD MODELING AND SIMULATION NETWORK



LATVIAN SIMULATION SOCIETY



ECOLE SUPERIEURE D'INGENIERIE EN SCIENCES APPLIQUEES



FACULTAD DE CIENCIAS EXACTAS. INEGNERIA Y AGRIMENSURA



UNIVERSITY OF LA LAGUNA



CIFASIS: CONICET-UNR-UPCAM



INSTICC - INSTITUTE FOR SYSTEMS AND TECHNOLOGIES OF INFORMATION, CONTROL AND COMMUNICATION



NATIONAL RUSSIAN SIMULATION SOCIETY



CEA - IFAC



UNIVERSITY OF BORDEAUX



UNIVERSITY OF CYPRUS

I3M 2016 INDUSTRIAL SPONSORS



CAL-TEK SRL



LIOTECH LTD

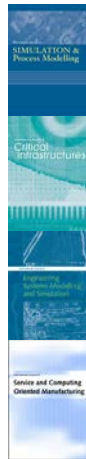


MAST SRL



SIM-4-FUTURE

I3M 2016 MEDIA PARTNERS



INDERSCIENCE PUBLISHERS – INTERNATIONAL JOURNAL OF SIMULATION AND PROCESS MODELING

INDERSCIENCE PUBLISHERS – INTERNATIONAL JOURNAL OF CRITICAL INFRASTRUCTURES

INDERSCIENCE PUBLISHERS – INTERNATIONAL JOURNAL OF ENGINEERING SYSTEMS MODELLING AND SIMULATION

INDERSCIENCE PUBLISHERS – INTERNATIONAL JOURNAL OF SERVICE AND COMPUTING ORIENTED MANUFACTURING



IGI GLOBAL – INTERNATIONAL JOURNAL OF PRIVACY AND HEALTH INFORMATION MANAGEMENT



Halldale Group



HALLDALE MEDIA GROUP: MILITARY SIMULATION AND TRAINING MAGAZINE



HALLDALE MEDIA GROUP: THE JOURNAL FOR HEALTHCARE EDUCATION, SIMULATION AND TRAINING



SAGE
SIMULATION TRANSACTION OF SCS



DE GRUYTER
INTERNATIONAL JOURNAL OF FOOD ENGINEERING

EDITORS

AGOSTINO BRUZZONE

MITIM-DIME, UNIVERSITY OF GENOA, ITALY
agostino@itim.unige.it

FRANCESCO LONGO

DIMEG, UNIVERSITY OF CALABRIA, ITALY
f.longo@unical.it

MIQUEL ANGEL PIERA

AUTONOMOUS UNIVERSITY OF BARCELONA, SPAIN
MiquelAngel.Piera@uab.cat

GIUSEPPE VIGNALI

UNIVERSITY OF PARMA, ITALY
giusppe.vignali@unipr.it

THE INTERNATIONAL MULTIDISCIPLINARY MODELING AND SIMULATION MULTICONFERENCE, I3M 2016

GENERAL CO-CHAIRS

AGOSTINO BRUZZONE, *MITIM DIME, UNIVERSITY OF GENOA, ITALY*

YURI MERKURYEV, *RIGA TECHNICAL UNIVERSITY, LATVIA*

PROGRAM CHAIR

FRANCESCO LONGO, *DIMEG, UNIVERSITY OF CALABRIA, ITALY*

THE INTERNATIONAL FOOD OPERATIONS & PROCESSING SIMULATION WORKSHOP, FOODOPS 2016

GENERAL CHAIR

GIUSEPPE VIGNALI, *UNIVERSITY OF PARMA ITALY*

PROGRAM CHAIR

FRANCESCO LONGO, *DIMEG, UNIVERSITY OF CALABRIA, ITALY*

FoodOPS 2016 INTERNATIONAL PROGRAM COMMITTEE

MATTEO AGRESTA, *UNIVERSITY OF GENOA, ITALY*
ELEONORA BOTTANI, *UNIVERSITY OF PARMA, ITALY*
AGOSTINO BRUZZONE, *DIME, UNIVERSITY OF GENOA, ITALY*
GERSON GOMES CUNHA, *COPPE UFRJ, BRAZIL*
RICCARDO DI MATTEO, *UNIVERSITY OF GENOA, ITALY*
MICHEL HAVET, *GEPEA RESEARCH UNIT, FRANCE*
FRANCESCO LONGO, *MSC-LES, UNIVERSITY OF CALABRIA, ITALY*
GIANLUCA MAGLIONE, *UNIVERSITY OF GENOA, ITALY*
FRANCESCO MARRA, *UNIVERSITY OF SALERNO, ITALY*
MARINA MASSEI, *LIOPHANT SIMULATION, ITALY*
YURI MERKURYEV, *RIGA TECHNICAL UNIVERSITY, LATVIA*
LETIZIA NICOLETTI, *CAL-TEK SRL, ITALY*
ANTONIO PADOVANO, *UNIVERSITY OF CALABRIA, ITALY*
MIQUEL ANGEL PIERA, *UNIVERSITY OF BARCELONA, SPAIN*
RUBEN MERCADE PRIETO, *SOOCHOW UNIVERSITY, CHINA*
STEFANO SAETTA, *UNIVERSITY OF PERUGIA, ITALY*
TOMAS SKOGLUND, *TETRAPAK, SWEDEN*
JACK VANDER VORST, *ORL GROUP - WAGENINGEN UNIVERSITEIT, NL*
MUSTAFA TAHSIN YILMAZ, *YILDIZ TEKNİK ÜNİVERSİTESİ, TURKEY*
GIUSEPPE VIGNALI, *UNIVERSITY OF PARMA, ITALY*

TRACKS AND WORKSHOP CHAIRS

LIQUID FOOD PROCESSING

CHAIR: TOMAS SKOGLUND, TETRAPAK, SWEDEN

SIMULATION OF FOOD SUPPLY CHAIN

CHAIR: JACK VANDER VORST, ORL GROUP - WAGENINGEN
UNIVERSITEIT, NL

MODELLING AND SIMULATION OF FOOD PROCESSING

CHAIR: MICHEL HAVET, GEPEA RESEARCH UNIT, FRANCE

MODELLING AND SIMULATION OF FOOD PROPERTIES

CHAIR: MUSTAFA TAHSIN YILMAZ, YILDIZ TEKNİK ÜNİVERSİTESİ,
TURKEY

SUSTAINABILITY OF FOOD PROCESSES

CHAIR: GIUSEPPE VIGNALI, UNIVERSITY OF PARMA, ITALY

MODELLING AND SIMULATION OF FOOD FOULING AND CLEANING TECHNIQUES

CHAIR: RUBEN MERCADE PRIETO, SOOCHOW UNIVERSITY, CHINA

MODELING OF TRANSPORT PHENOMENA IN FOOD PROCESSES ASSISTED BY MICROWAVES AND RADIO-FREQUENCIES

CHAIR: FRANCESCO MARRA, UNIVERSITY OF SALERNO, ITALY

CHAIRS' MESSAGE

WELCOME TO FOODOPS 2016!

On behalf of the Organization Committee, we would like to welcome and thank all the people who have contributed to "The international Food Operations & Processing Simulation Workshop" (FoodOPS 2016). Notwithstanding FoodOPS has now come to its second edition, thanks to the hard work of all its contributors, the workshops is growing very fast in terms of topics coverage, research contributions and challenges addressed.

As a matter of facts, this year FoodOps offers a collection of valuable works that fall under various topics in the field of Food Engineering, to cite a few sustainable food processing, artificial intelligence techniques as well as mathematical modeling, simulation and software development for food processing and process optimization.

Hence, FoodOps seeks to capture actual and future trends fostering and encouraging a forward-looking attitude. The effort to create a real value for the scientific community is further testified by the strong involvement of the IPC members that have put all their efforts in all the stages of the organization process starting from papers collection to papers review and selection. Besides, the authors' commitment in taking advantage of reviewers' suggestions cannot be overlooked.

All these aspects underpin and pave the way for a successful and fruitful Workshop.

Like its previous edition, FoodOPS 2016 is co-located with the I3M 2016 multi-conference, the ideal framework where new ideas, solutions and approaches can be profitably shared.

It takes place in the wonderful location of Larnaca, Cyprus: a great background for a great event!

At this point, all we can do is to wish all the FoodOPS and I3M attendees a fruitful conference and a wonderful stay in the breath-taking landscapes of this fantastic venue!



Giuseppe Vignali
University of Parma
Italy



Francesco Longo
University of Calabria
Italy

ACKNOWLEDGEMENTS

The FoodOPS 2016 International Program Committee (IPC) has selected the papers for the Conference among many submissions; therefore, based on this effort, a very successful event is expected. The FoodOPS 2016 IPC would like to thank all the authors as well as the reviewers for their invaluable work.

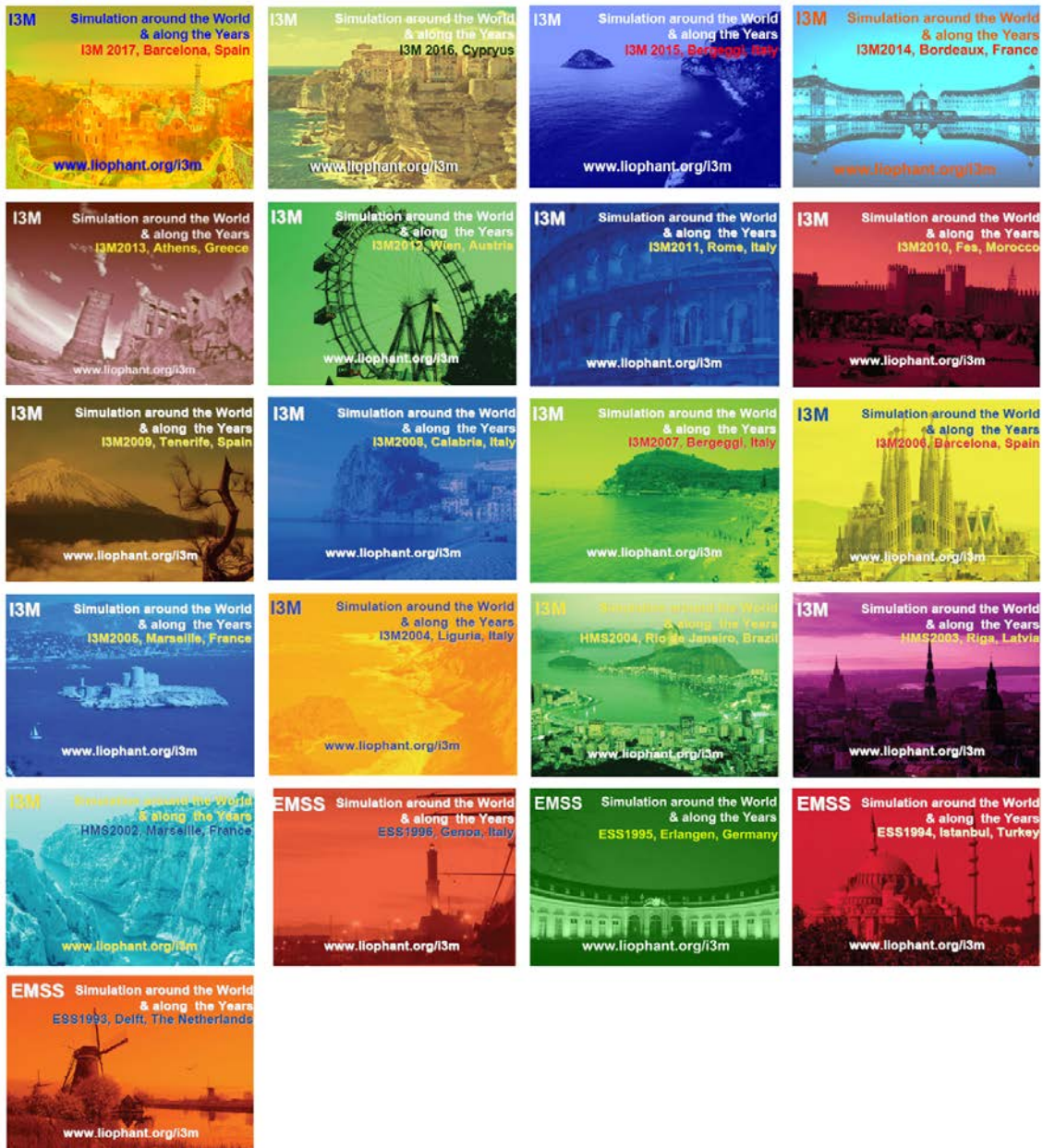
A special thank goes to all the organizations, institutions and societies that have supported and technically sponsored the event.

I3M 2016 INTERNAL STAFF

MATTEO AGRESTA, *SIMULATION TEAM, ITALY*
LUIGI BRUNO, *DIMEG, UNIVERSITY OF CALABRIA*
AGOSTINO G. BRUZZONE, *DIME, UNIVERSITY OF GENOA, ITALY*
ALESSANDRO CHIURCO, *DIMEG, UNIVERSITY OF CALABRIA, ITALY*
RICCARDO DI MATTEO, *SIMULATION TEAM, ITALY*
CATERINA FUSTO, *CAL-TEK SRL, ITALY*
FRANCESCO LONGO, *DIMEG, UNIVERSITY OF CALABRIA, ITALY*
GIANLUCA MAGLIONE, *SIMULATION TEAM, ITALY*
MARINA MASSEI, *DIME, UNIVERSITY OF GENOA, ITALY*
LETIZIA NICOLETTI, *CAL-TEK SRL, ITALY*
ANTONIO PADOVANO, *DIMEG, UNIVERSITY OF CALABRIA, ITALY*
LUCA ROTUNDO, *DIMEG, UNIVERSITY OF CALABRIA, ITALY*
CATALDO RUSSO, *CAL-TEK SRL, ITALY*
GIUSEPPE SPEZZANO, *DIMEG, UNIVERSITY OF CALABRIA, ITALY*
MARCO VETRANO, *CAL-TEK SRL, ITALY*



This International Workshop is part of the I3M Multiconference: the Congress leading Simulation around the World and Along the Years



Index

Modes for predication the mass of green bell pepper fruit with some physical characteristics F. Shahbazi, S. Rahmati	1
Discrete event simulation for sustainable batch production in food processing M. Elmasry, F. Tarek	5
Applying artificial neural network modeling for predicting postharvest loss in some common agrifood commodities M. Olaniyan, A. B. Owolabi	11
Mathematical modeling of microwave assisted fluidized bed drying of hazelnuts N. Malekjani, Z. Emam-Djomeh, S. H. Hashemabadi, G. R. Askari	19
Lifecycle modelling of an innovative durum wheat debranner D. Marchini, R. Montanari, E. Bottani, G. Tagliavini, S. Digiuni	26
CFD simulation of a co-rotating twin-screw extruder: validation of a rheological model for a starch-based dough for snack food G. Tagliavini, F. Solari, R. Montanari	32
Modelling and simulation of nitrogen injection in vegetable olive oil F. Ferrari, S. Spanu, G. Vignali	39
Joining simulation and situation awareness for an italian production system M. De Falco, V. Loia, L. Rarità, S. Tomasiello	49
Petri net model of a production process for agaricus bisporus mycelium J. I. Latorre-Biel, E. Jiménez-Macías, M. Pérez de la Parte, F. J. Leiva-Lázaro, E. Martínez-Cámara, J. Blanco-Fernández	58
Petri net modelling and operational optimization of a facility for the preparation, cultivation and production of common mushroom (agaricus bisporus) J. I. Latorre-Biel, E. Jiménez-Macías, M. Pérez de la Parte, F. J. Leiva-Lázaro, E. Martínez-Cámara, J. Blanco-Fernández	64
Feasibility study of an Augmented Reality application to enhance the operators' safety in the usage of a fruit extractor S. Spanu, M. Bertolini, E. Bottani, G. Vignali, L. Di Donato, A. Ferraro, F. Longo	70
Author's Index	79

MODES FOR PREDICATION THE MASS OF GREEN BELL PEPPER FRUIT WITH SOME PHYSICAL CHARACTERISTICS

Feizollah Shahbazi ^(a), Satar Rahmati ^(b)

^{(a),(b)} Faculty of Agriculture, Lorestan University, Khoramabaad, Iran.

^(a)shahbazi.f@lu.ac.ir

ABSTRACT

For proper design of grading systems of horticultural crops, important relationships between the mass and other properties of fruits such as length, width, thickness, volumes and projected areas must be known. The aim of this research was to measure and present some physical properties of green bell pepper fruits and correlating the mass of fruits to measured physical properties using linear, quadratic, S-curve and power models. The results showed that the effects of measured physical properties, on the mass of bell pepper fruit, were found to be statistically significant at 1% probability level. According to the results obtained in this study, the S-curve model could predict the relationships between the mass and some physical properties of green bell pepper fruits with proper values of coefficient of determination. Finally, the S-curve model based of the first projected area (PA_1) for mass predication of green bell pepper is suggested because it needs one camera, as the main part of the grading systems and it is applicable and is an economic method.

Keywords: Green bell pepper, physical characteristics, mass prediction.

1. INTRODUCTION

Green bell pepper (*Capsicum annum* L) is a fruit pod of small perennial shrub in the nightshade or *Solanaceae* family, of the genus, capsicum. It contains an impressive list of plant nutrients that are known to have disease preventing and health promoting properties and it is very low in calories and fat. Fresh bell peppers are rich source of vitamin-C. It also contains good level of vitamin-A.

Knowledge about physical properties of agricultural products and their relationships is necessary for the design of handling, sorting, processing and packaging systems. Among these properties, the dimensions, mass, volume and projected area are the most important ones in the design of grading system (Mohsenin, 1986). Consumers prefer fruits with equal weight and uniform shape. Mass grading of fruit can reduce packaging and transportation costs, and may provide an optimum packaging configuration. Fruits are often classified based on the size, mass, volume and projected areas. Electrical sizing mechanisms are more complex and expensive. Mechanical sizing mechanisms work slowly.

Therefore, it may be more economical to develop a machine, which grades fruits by their mass. Besides, using mass as the classification parameter is the most accurate method of automatic classification for more fruits. Therefore, the relationships between mass and length, width and projected areas can be useful and applicable (Khoshnam *et al.*, 2007; Lorestani *et al.*, 2012).

A number of studies have been conducted on the mass modeling of fruits based upon their physical properties. Tabatabaeefar *et al.* (2000) developed 11 models based upon dimensions, volumes and surface areas for mass predication of orange fruits. Al-Maiman and Ahmad (2002) studied the physical properties of pomegranate and developed models for predicting fruit mass while employing dimensions, volume and surface areas. A Quadratic model ($M = 0.08c^2 + 4.74c + 5.14$, $R^2 = 0.89$), to calculate the apple mass based on its minor diameter, was determined by Tabatabaeefar and Rajabipour, (2005). Lorestani and Tabatabaeefar (2006) determined models for predicting mass of Iranian kiwi fruit by its dimensions, volumes, and projected areas. They reported that the intermediate diameter was more appropriate to estimate the mass of kiwi fruit. Khanali *et al.* (2005) determined similar mass models for tangerine fruit. Naderi-Boldaji *et al.* (2008) also determined models for predicting the mass of apricot. They found a nonlinear equation ($M = 0.0019c^{2.693}$, $R^2 = 0.96$) between apricot mass and its minor diameter. Some researchers (Kingsly *et al.*, 2006; Fadavi *et al.*, 2005) reported mass models for pomegranate fruit. Lorestani and Ghari (2012) concluded that the best models for prediction the mass of fava bean were linear based on width, among the dimensional characteristics and power form based on third projected area, which perpendicular to L direction of fava bean, among the projected areas, respectively.

No detailed studies concerning mass modelling of green bell pepper fruit have yet been performed. The aims of this study were to determine the most suitable model for predicting green bell pepper mass by its physical attributes and specify some physical properties of green bell pepper to form an important database for other researches.

2. MATERIALS AND METHODS

Freshly harvested green bell peppers were obtained from Lorestan province Iran. In order to determine the physical properties, 150 green bell peppers were

randomly selected. Selected samples were healthy and free from any injuries. Samples of fruits were weighed and dried in an oven at a temperature of 78°C for 48 hours then weight loss on drying to a final constant weight was recorded as moisture content. The mass of each bell pepper (M) was measured using a digital balance with accuracy of 0.01 g. For each bell pepper, fruit, three linear dimensions were measured by using a digital caliper with accuracy of 0.01mm, including Major diameter (Length, L), Intermediate diameter (Width, W) and Minor diameter (Thickness, T) (Fig 1). Water displacement method was used for determining the fruits measured volume (V_m). Fruits geometric mean diameter (D_g) and surface area (S) were determined by using the following formulas (Mohsenin, 1986; Shahbazi, 2013), respectively:

$$D_g = (LWT)^{\frac{1}{3}} \quad (1)$$

$$S = \pi(D_g)^2 \quad (2)$$

Where: L is length (mm), W is width, T is thickness of green bell pepper (mm) S is fruit surface are (mm²) and D_g is geometric mean diameter (mm). In addition, fruit average projected areas perpendicular to dimensions (PA_1 , PA_2 and PA_3) were measured by a ΔT aremeter, MK2 model, device with accuracy of 10 mm² and then the criteria projected area (CPA) was calculated as suggested by Mohsenin (1986):

$$CPA = \frac{PA_1 + PA_2 + PA_3}{3} \quad (3)$$

Where: PA_1 (perpendicular to L direction of fruit), PA_2 (perpendicular to T direction of fruit) and PA_3 (perpendicular to W direction of fruit), are first, second and third projected areas (mm²), respectively.

The following models were considers in the estimation of mass models for green bell peppers:

Single variable regression of bell peppers mass based on fruits dimensional properties including length (L), width (W), thickness (T) and geometric mean diameter (D_g).

Single or multiple variable regression of bell peppers mass based on fruits projected areas (PA_1 , PA_2 and PA_3), surface area (S) and criteria projected are (CPA).

Singe regression of bell peppers mass based on measured volume (V_m), volume of the fruits assumed as oblate spheroid shape (V_{osp}) and volume of the fruits assumed as ellipsoid shape (V_{ellip}) (Lorestani *et al.*, 2012).

In the case of the third classification, to achieve models, which can predict the green bell pepper mass, based on volumes, three volume values were either measured or calculated. At first, measured volume (V_m) as stated earlier was measured and then the green bell pepper shape was assumed as a regular geometric shape, i.e. oblate spheroid (V_{osp}) and ellipsoid (V_{ellip}) shapes, and their volume was thus calculated as:

$$V_{osp} = \frac{4\pi}{3} \left(\frac{L}{2}\right) \left(\frac{W}{2}\right)^2 \quad (4)$$

$$V_{ellip} = \frac{4\pi}{3} \left(\frac{L}{2}\right) \left(\frac{W}{2}\right) \left(\frac{T}{2}\right) \quad (5)$$

Four models including: Linear, Quadratic, S-curve and Power models were used for mass predication of green

bell peppers based on measured physical properties, as are represented in the following expressions, respectively (Shahbazi and Rahmati, 2013 a, b):

$$M = b_0 + b_1X \quad (6)$$

$$M = b_0 + b_1X + b_2X^2 \quad (7)$$

$$M = b_0 + \frac{b_1}{X} \quad (8)$$

$$M = b_0X^{b_1} \quad (9)$$

Where M is mass (g), X is the value of an independent (physical characteristics) parameter which want to find its relationship with mass, and b_0 , b_1 , and b_2 are curve fitting parameters which are different in each equation. One evaluation of the goodness of fit is the value of the coefficient of determination (R^2). For regression equations in general, the nearer R^2 is to 1.00, the better the fit (Stroshine, 1998). SPSS 15, software was used to analyze the data and determine regression models between the physical characteristics.

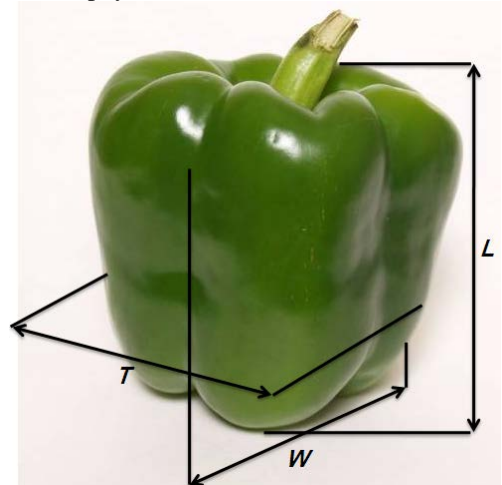


Figure1: Dimensional characteristics of green bell pepper: L, length; W, width; T, thickness.

3. RESULTS AND DISCUSSION

3.1. Physical Properties of Green Bell Peppers

Table 1 shows the measured physical properties of studied green bell peppers. The properties are measures at the moisture content of about 83.13% wet basis. As seen in Table 1, the effects of all properties, on the mass of bell pepper fruit, were found to be statistically significant at 1% probability level. The mean values of measured physical properties of studied green bell pepper fruits include: length (L), width (W), thickness (T), geometric mean diameter (D_g), surface area (S), mass (M), first projected area (AP_1), second projected area (AP_2), third projected area (AP_3), criteria projected area (CPA), measured volume (V_m), oblate spheroid volume (V_{osp}) and ellipsoid shapes volume (V_{ellip}) were 84.254 mm, 84.415 mm, 74.071 mm, 80.545 mm, 20497.90 mm², 138.541 g, 5576.82 mm², 6557.80 mm², 6490.81 mm², 6208.47 mm², 294737.01 mm³, 319383.67 mm³ and 278533.07 mm³ respectively.

Table 1. Some physical properties of green bell pepper (at 83.13% w.b. moisture content).

Properties	Value			Significant level
	Average	Maximum	Minimum	
L , mm	84.254	110.02	67.45	$P < 0.01$
W , mm	84.41	91.56	73.38	$P < 0.01$
T , mm	74.07	87.61	61.13	$P < 0.01$
D_g , mm	80.54	90.96	69.71	$P < 0.01$
S , mm ²	20497.90	25981.99	15260.12	$P < 0.01$
M , g	138.54	193.75	93.47	$P < 0.01$
PA_1 , mm ²	5576.82	7069.12	4040.31	$P < 0.01$
PA_2 , mm ²	6557.80	8484.52	4801.23	$P < 0.01$
PA_3 , mm ²	6490.80	9352.32	4888.65	$P < 0.01$
CPA , mm ²	6208.47	8156.33	4694.64	$P < 0.01$
V_m , mm ³	294737.0	392050.3	207420.	$P < 0.01$
V_{osp} , mm ³	319383.6	482682.5	190070.9	$P < 0.01$
V_{ellip} , mm ³	278533.07	393906.08	177304.95	$P < 0.01$

CPA = criteria projected area; D_g = geometric mean diameter; L = length; M = mass; PA_1 , PA_2 , PA_3 = first, second, third projected area; S = surface areas; T = thickness; V_m = measured volume; V_{osp} = oblate spheroid volume; V_{ellip} = ellipsoid shapes volume; W = width.

3.2. Mass Modeling

Table 2 shows the obtained the best models and their coefficient of determination (R^2) for mass predication of green bell peppers based on the measured physical properties. The results of the F-test and T-test in SPSS 15 software showed that all the coefficients of the models were significant at the 1% probability level.

3.2.1. Modeling Based on Dimensions

The results of mass (M) modeling of green bell pepper based on the dimensional characteristics, including: length (L), width (W), thickness (T) and geometric mean diameter (D_g), showed that S-curve model to calculate mass of bell pepper fruit based on its geometric mean diameter, had the highest R^2 among the others as:

$$M = 7.203 - \frac{183.714}{D_g} \quad R^2 = 0.908 \quad (10)$$

However, measurement of three diameters of fruit is needed for calculating the geometric mean diameter (D_g) to use this model, which makes the sizing mechanism more tedious and expensive. Among three dimensions including length (L), width (W) and thickness (T), S-curve model, which expresses the width (W) as independent variable, had the highest R^2 among the others (Table 2). Therefore, the mass model of bell pepper fruit based on width is given as S-curve form:

$$M = 7.167 - \frac{189.899}{W} \quad R^2 = 0.819 \quad (11)$$

In addition, S-curve model can predict the relationships between the mass with length (L) and thickness (T) with R^2 values of 0.512 and 0.570, respectively. Therefore, mass modeling of green bell pepper based on width is recommended. Similar model (nonlinear) suggested by Tabatabaefar *et al.* (2000) for mass predication of orange fruit mass based on fruit width too. Their recommended model was: $M = 0.069b^2 - 2.95b - 39.15$, $R^2 = 0.97$. In addition, eleven models for predicting mass of apples based on geometrical attributes were recommended by Tabatabaefar and Rajabipour (2005). They recommended an equation for calculating apple

mass based on minor diameter as $M = 0.08c^2 - 4.74c + 5.14$, $R^2 = 0.89$. Ghabel *et al.* (2010) recommended a nonlinear model for onion mass determination based on length as $M = 0.035a^2 - 1.64a + 36.137$, $R^2 = 0.96$.

3.2.2. Modeling Based on Areas

Among the investigated models based on projected areas (PA_1 , PA_2 , PA_3 and CPA), S-curve model of PA_1 was preferred because of the highest value of R^2 as:

$$M = 5.973 - \frac{572.252}{PA_1} \quad R^2 = 0.987 \quad (12)$$

For mass prediction of the green bell pepper based on surface area, the best model was S-curve with $R^2 = 0.711$ as:

$$M = 6.036 - \frac{22545.106}{S} \quad R^2 = 0.811 \quad (13)$$

However, measurement of three dimensions of green bell pepper is needed for geometric mean diameter (D_g) and surface area (S) to use this model, which makes the grading mechanisms more tedious and expensive. Therefore, mass modeling of bell pepper based on first projected area (PA_1) is recommended. Similar model (nonlinear) suggested by Shahbazi and Rahmati (2013a) for mass predication of sweet cherry fruit mass based on fruit first projected area (PA_1) too.

3.2.3. Modeling Based on Volumes

According to the results, for mass prediction of the green bell pepper based on volumes (V_m , V_{osp} and V_{ellip}), shown in Table 2, the S-curve model based on measured volume (V_m) with $R^2 = 0.984$, was the best model as:

$$M = 6.012 - \frac{187521.76}{V_m} \quad R^2 = 0.984 \quad (14)$$

4. CONCLUSIONS

The results of this study can be concluded that:

In this study, some physical properties of green bell pepper fruits and their relationships with fruit mass were presented. All considered properties were statically significant at 1% probability level.

The best model for green bell pepper s mass predication among the dimensional properties was S-curve form based on width (W) of fruit as: $M = 7.167 - \frac{189.899}{W}$, $R^2 = 0.819$.

The best model for mass prediction of green bell pepper based on three projected areas was S-curve form based on first projected area (perpendicular to L direction of fruit) as: $M = 5.973 - \frac{572.252}{PA_1}$, $R^2 = 0.987$.

S-curve model based on measured volume (V_m) with $R^2 = 0.984$, was the best model for mass prediction of the green bell pepper based on volumes as: $M = 6.012 - \frac{187521.76}{V_m}$, $R^2 = 0.984$.

At last, from economical standpoint of view, mass model of green bell pepper based on the first projected area is recommended to design and development of grading systems.

Table 2. The models for mass prediction of green bell pepper with some physical characteristics

Dependent variable	Independent variable	The best fitted model	Constant parameters			R ²
			b ₀	b ₁	b ₂	
M (g)	L (mm)	Quadratic	109.979	-0.713	0.012	0.515
M (g)	W (mm)	S-curve	7.167	-189.899	-	0.819
M (g)	T (mm)	Quadratic	-901.568	25.52	-0.154	0.570
M (g)	D _g (mm)	S-curve	7.203	-183.714	-	0.908
M (g)	PA ₁ (mm ²)	S-curve	5.973	-572.252	-	0.987
M (g)	PA ₂ (mm ²)	Quadratic	4.418	0.016	6.841×10 ⁻⁷	0.741
M (g)	PA ₃ (mm ²)	Quadratic	-496.021	0.0173	-1.104×10 ⁻⁵	0.782
M (g)	CPA (mm ²)	S-curve	6.088	-7126.03	-	0.816
M (g)	S (mm ²)	S-curve	6.036	-22545.10	-	0.811
M (g)	V _m (mm ³)	S-curve	6.012	-314783.73	-	0.984
M (g)	V _{osp} (mm ³)	S-curve	5.535	-187521.76	-	0.672
M (g)	V _{ellip} (mm ³)	S-curve	5.646	-194344.46	-	0.712

CPA=criteria projected area; D_g=geometric mean diameter; L= length; M= mass; PA₁, PA₂, PA₃ = first, second, third projected area; R² =coefficient of determination; S=surface areas; T=thickness; V_m =measured volume; V_{osp} = oblate spheroid volume; V_{ellip}=ellipsoid shapes volume; W=width.

REFERENCES

- Al-Maiman, S and Ahmad, D. 2002. Changes in physical and chemical properties during pomegranate (*Punica granatum* L.) fruit maturation. *Journal of Food Chemistry*, 76, 437–441.
- Fadavi, A., Barzegar, M., Azizi, M.H and Bayat, M. 2005. Note. Physicochemical composition of ten pomegranate cultivars (*Punicagranatum* L.) grown in Iran. *Food Science and Technology International*, 11: 113–119.
- Ghabel, R., Rajabipour, A., Ghasemi-Varnamkhasti, M and Oveisi, M. 2010. Modeling the mass of Iranian export onion (*Allium cepa* L.) varieties using some physical characteristics. *Res. Agr. Eng.* 56, 21: 33–40.
- Khanali, M., Ghasemi Varnamkhasti, M., Tabatabaeefar, A and Mobli, H. 2007. Mass and volume modelling of tangerine (*Citrus reticulata*) fruit with some physica attributes. *International Agrophysics*, 21: 329–334.
- Khoshtam, F., Tabatabaeefar, A., Varnamkhasti, M.G. and Borghei, A. 2007. Mass modeling of pomegranate (*Punicagranatum* L.) fruit with some physical characteristics. *Scientia Horticulturae*, 114: 21–26.
- Kingsly, A.R.P., Singh, D.B., Manikantan, M.R and Jain, R.K. 2006. Moisture dependent physical properties of dried pomegranate seeds (*Anardana*). *Journal of Food Engineering*, 75: 492–496.
- Lorestani, A.N. and Ghari, M. 2012. Mass Modeling of Fava bean (*vicia faba* L.) with some physical characteristics. *Scientia Horticulturae*. 133(6): 6-9.
- Lorestani, A.N. and Tabatabaeefar, A. 2006. Modeling the mass of kiwi fruit by geometrical attributes. *International Agrophysics*, 20: 135–139.
- Lorestani, A.N., Jaliliantabar, F, and Gholami, R. 2012. Mass modeling of caper (*Capparis spinosa*) with some engineering properties. *Quality Assurance and Safety of Crops & Foods*, 4: e38–e42.
- Mohsenin, N.N. 1986. *Physical Properties of Plant and Animal Materials*, revised 2nd edn. New York: Gordon and Breach Science Publications.
- Naderi-Boldaji, M., Fattahi, R., Ghasemi-Varnamkhasti, M., Tabatabaeefar, A and Jannatizadeh, A. 2008. Models for predicting the mass of apricot fruits by geometrical attributes (cv. Shams, Nakhjavan, and Jahangiri). *Scientia Horticulturae*, 118: 293–298.
- Shahbazi, F and Rahmati, S. 2013a. Mass modeling of sweet cherry (*Prunus avium* L.) fruit with some physical characteristics. *Food and Nutrition Sciences*, 4: 1-5.
- Shahbazi, F. 2013. Effective conditions for extracting higher quality kernels from walnuts. *Quality Assurance and Safety of Crops & Foods*, 5, 199-206.
- Shahbazi, F. and Rahmati, S. 2013b. Mass modeling of fig (*Ficus carica* L.) fruit with some physical characteristics. *Food Science and Nutrition*, 1: 125-129.
- Stroshine, R. 1998. *Physical Properties of Agricultural Materials and Food Products*. Course Manual. Purdue Univ., USA.
- Tabatabaeefar, A and Rajabipour, A. 2005. Modeling the mass of apples by geometrical attributes. *Scientia Horticulturae*, 105, 373–382.
- Tabatabaeefar, A., Vefagh-Nematolahee, A and Rajabipour, A., 2000. Modeling of orange mass based on dimensions. *Agric. Sci. Technol*, 2,299–305.

DISCRETE EVENT SIMULATION FOR SUSTAINABLE BATCH PRODUCTION IN FOOD PROCESSING

Mohamed Elmasry^(a), FatmaTarek^(b)

^(a)Research Assistant, Department of Civil Engineering, Qatar University, Doha, Qatar

^(b)Chief Executive Officer at Toukies, Inc, Mokattam, Cairo, Egypt

^(a)Masry@qu.edu.qa

^(b)toukies.orders@gmail.com

ABSTRACT

In a world faced with depleting resources and hazardous biodegradable food wastes, an efficient planning for the food processing operation is crucial to avoid the adverse potential impact of excess food production. This paper presents a framework for sustainable food batch production, to ensure efficient usage of raw ingredients required for producing the exact food amount required for a certain event. A discrete event simulation model is developed using STROBOSCOPE to determine the equilibrium points between the supply and demand in showcase events that involve showing food samples or products. The developed simulation model comprises two parts, namely the batch production plant and the food exhibition. To validate the model, actual case study was used to determine the amount of displayed food products in exhibitions and it was found that the MAE resulting from the model was equal to 85%. The developed simulation model and framework is expected to be a handful tool for stakeholders in small startups and young entrepreneurs in showcase events involving food sampling to minimize excess or surplus of food and raw ingredients required in food production.

Keywords: Food batch production, Sustainable Processing, Simulation, Food Exhibitions

1. INTRODUCTION

Simulation is considered as a powerful tool because of its ability to model real life situations with minimum cost and effort. Simulation tools enable users to apply what-if scenarios in which the simulation model is replicated and different alternatives can be modeled to determine the best available alternative based on the user's objective without the need to apply extra cost or time. Several simulation tools are available for that purpose such as MicroCyclone (Halpin, 1974), STROBOSCOPE (Marinez 1996), AnyLogic (AnyLogic Company), Arena (Rockwell Automation), ProModel (ProModel, Inc.), FlexSim (FlexSim Software Products, Inc.) and several others commercial and academic tools. Each of these simulation tool has advantages that make using each one of them more favorable than using the other. For instance, when using MicroCyclone, it is impossible to visualize the working

model, while on the other hand commercial packages such as AnyLogic, Arena aren't affordable for customers because they aren't open source softwares. Also some of these tools aren't easy to learn and require the user to have a strong background in simulation languages and modeling techniques because of the broad spectrum of capabilities in these tools. As such and due to these aforementioned reasons, STROBOSCOPE is envisaged to be more appealing to use when compared to these other tools because of its simplicity and its capabilities in visualizing the working model. STROBOSCOPE is a general purpose simulation programming language widely used to simulate construction processes and operations. STROBOSCOPE has the ability to access the properties of the resources and can link the different activities in the model with these properties enabling the user to understand the logic and flow of the processes in the simulation model. Therefore, STROBOSCOPE can be used to simulate and analyze different operations and processes not only in the construction industry but also in any other fields as long as the operation is well defined and known to the user. When designing any operation, complex decisions regarding the processes involved in this operation are required to be made, such as determining the appropriate number of manpower or equipment used and selecting the method by which the tasks are performed. For every decision made, cost and times are associated with this decision, hence comes the usefulness of using simulation to determine the optimum scenario or decision that would give minimum cost and time.

Several researches have addressed food processing using simulation. McGarry and Watson, (1996) developed a dynamic simulation framework to assess the resources needed and the schedule of the operation's activity to maximize managing the operation. Diefes and Okos, (2000) compared different design processes as alternatives in manufacturing whole milk powder using food operations oriented design system block library and performing economic analysis. The comparison was done with the intent of demonstrating how using food oriented design system block library can help in saving time to perform analysis of design

alternatives. The research aimed to minimize steam use in the operation and to maximize the net present worth over a 10 year planning horizon. Numerical finite element model was also used to analyze the freezing and thawing process for frozen food processing (Zhongjie and Shaoshu, 2003). In this research, the authors investigated the effect of freezing parameters on the freezing process concluding that the food shape and size, freezing air temperature and freezing air velocity are the most important factors affecting the freezing process. Longo et al., (2012) presented a simulation model to examine the behavior of industrial plants used in producing hazelnuts based products using different scenarios. The performance of the industrial plant process was investigated by using different alternatives for the plant line production capacities and machines. In this research it was concluded that the simulation model could be used in adjusting the system to improve the plant performances when using governing factors such as plant line production capacities and machines involved in the production process. In addition to the previously developed models, several models addressing food processing were introduced such as food drying, baking processes, and cold food processing (Sabarez, 2015, Flick et. al., 2015 and Tassou et. al., 2015). As for researches addressing sustainable food production, a framework was presented for industrial food processing using life cycle assessment approach while preserving environment (Sonesson et al., 2010). In this research two case studies were presented to examine using the life cycle assessment approach in industrial food processing towards sustainable environment. It can be concluded that the previously presented researches used either mathematical modeling or simulation tools to model or investigate the impact of a certain factor on the industrial food processing operations; however no research has used STROBOSCOPE for such purpose in these specific operations. The objective of this paper is to develop a generic simulation model for food production to be used in food exhibition and showcase events with the intent of minimizing the wastes as a result of surplus raw ingredients. The simulation model could help in determining the breakeven points of the processed food and the served people. The model considers the people's arrival rate, people's leaving rate, and service rate in the exhibition locations, in addition to the logistics required to transport food product from the batch plant to the exhibition yard and the food production rate. Iterations are performed to determine the governing factors in the aforementioned process and an actual data for a real food production process of sweet treats is used to validate the proposed simulation model.

2. PROPOSED SIMULATION MODEL

STROBOSCOPE is used to develop the proposed simulation model using different features of the tool; resources including manpower or equipments in STROBOSCOPE are modeled in the form of "Queue"

which represents a pool for the resource from which activities access this pool and use the available resources. Activities of different processes are modeled using "Combi" which is instantiated using a resource from the Queue. Activities represented by Combi should have duration which are interpreted by the program as a time unit (i.e.: based on the users input the program interprets the duration, so it is crucial to ensure that the units used in defining the durations are the same). Similar to the Combi a "Normal" also represents an activity, however this type of activity doesn't require a queue (i.e.: a resource) to be instantiated. The simulation model comprises to main parts namely, the batch production unit and the exhibition unit. The former represents the activities and resources used in producing, packing and loading the produced food to the truck used in transportation. While the latter represents the activities and resources used in the exhibition hall, where products are presented and sold to customers. Figure 1 shows the proposed simulation model.

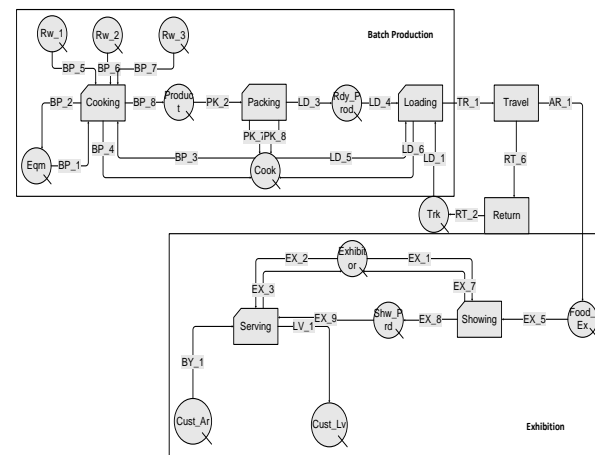


Figure 1: Proposed Simulation Model

2.1. Batch Production

The production of the food starts by the activity "Cooking" which uses the resources "Rw_1", "Rw_2", and "Rw_3" which represent the raw ingredients used in cooking the product. In addition to these resources, the "Eqm" representing the equipment used in processing/cooking the food is used by the "cook" which is the human being using the tool to perform the activity. STROBOSCOPE enables the user to define the characteristics of the different resources used, so if several equipment are used, different characteristics can be defined such as the capacity, horse power, the amount of electricity used,...etc. In this model generic type is used to define each resource where cook is defined as human being, Rw_1, Rw_2, Rw_3 are defined as raw ingredients and Eqm is defined as equipment. After food is cooked, a queue of generic type food called "Product" representing the food is introduced to the model. The activity of "Packing" then starts using the queue "Product" and "Cook" with a

By performing several runs, it was found that one of the governing resources is the exhibitor numbers. The rest of the resources turn out to be equally important. To determine which resources are effective and which are not, several iterations were performed and the outcome of the simulation model was observed from which the cost using this alternative of combination was calculated. It should be noted that increasing the amount of a resource could result in system congestion leading to an increase in the total cost and the average waiting time of these resources which means an increase in idleness and accordingly the overall simulation time.

Figure 4 shows the plot for the different alternatives between the cost on the vertical axis and the simulation time on the horizontal axis. The solid dotted line joining these three alternatives represents the pareto optimal interface which indicates that this combination would most likely result in the optimum cost and time.

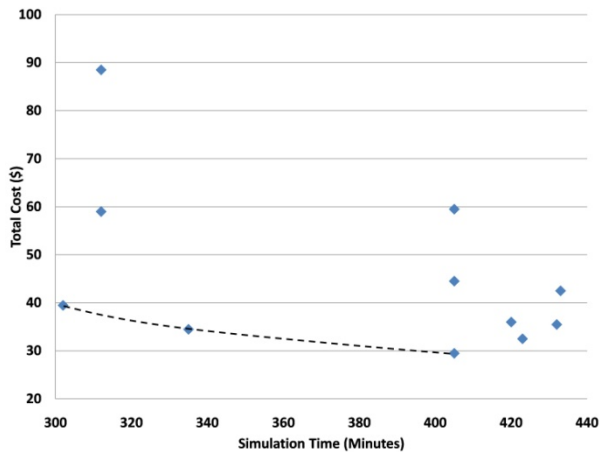


Figure 4: Optimal Resources combination Frontier

The line envelopes the three alternatives of having only one resource of the aforementioned resources, two exhibitors while having the same number of other resources and three exhibitors while having the same number of the other resources.

4.2. Breakeven Points between products and customers

Breakeven points are usually used in economics to define the point at which neither profit nor loss is made (David and Boldrin, 2008). In the context of this paper, breakeven point means the point at which the amount of raw ingredients required for processing food products that would be shown in exhibition and show case events balance the amount of customers in that event such that the waste as a result of using excess raw ingredients tend to a minimum.

To determine the number of products to be produced, the arrival, leaving and service rates in the exhibition location shall be at first calculated. The arrival rate by which the customers arrive to the location is denoted by (λ_a), while leaving rate by which the customers shall leave the showing booth is denoted by (λ_l). The service rate and as the name implies is how fast customers are

served is denoted by (μ). The different rates were computed based on different number of exhibitors to determine the plausibility of the proposed simulation model and from which the raw ingredients amount shall be computed. Table 3 shows the increase in the service rate as a result of increase in number of exhibitors. The service rates were computed based on STROBOSCOPE average waiting times for the queues of arriving and leaving customers. As such and by using the above relationships, it can be concluded that the service rate is the difference between the arrival and the leaving rates as per Equation 1.

Table 3: Different rates based on different number of exhibitors

Exhibitor	μ (1/min)
1	1/5
2	1/4
3	1/3

$$\mu = |\lambda_a - \lambda_l| \quad (1)$$

To determine the amount of products to be produced, the service rate shall be multiplied by the total duration of the exhibition denoted by (D) as per Equation 2:

$$NP = \mu * D \quad (2)$$

Where NP is the number of products to be processed for the show case, which is used to determine the exact amount of raw ingredients as per Equation 3

$$RI_i = w_i * \frac{NP}{P} \quad (3)$$

Where RI_i is the raw ingredient component amount, (w_i) is the weight of the ingredient in the mix. P is the production conversion factor, taken in this study equal to 1.45.

5. CASE STUDY

To validate the model and verify the outcomes from the simulation process a real data from a case study were used from which results were compared to the actual ones. In this case study, the distance between the plant location and exhibition is estimated to be 13 kilometers. Figure 5 shows a Google maps image for the locations of exhibition and batch production plant along with the route taken to transport food. The exhibition was only for one day starting at 10:00 AM and ending at 5:00 PM. This exhibition was designated mainly for art crafts and handmade products however there was only one booth for food products. The estimated number for customers in this exhibition was approximately 500 customers with an average arrival and leaving rates of 11/6 and 25/12. The product that was displayed in the exhibition was sweet treats that consisted of three main ingredients with weights of biscuits 17%, cream cheese 60% and topping of different flavors 23%. In this event

all the displayed products were sold out by the end of the exhibition with minimum wastes in the ingredients with a total number of 85 products.

By applying Equations 1 and 2, we find that the number of products is $(11/6 - 25/12) * 7 * 60 = 105$ units. By applying Equation 3 and using the different given weights $RI_1 = 0.17 * (45/1.45) = 5$ units, $RI_2 = 0.6 * (45/1.45) = 19$ units and $RI_3 = 0.23 * (45/1.45) = 7$ units. When comparing these findings with the actual case study data the mean average error (MAE) was found to be 84% which shows plausibility of model results and that it can be used in real cases to optimize the amount of raw food ingredients.

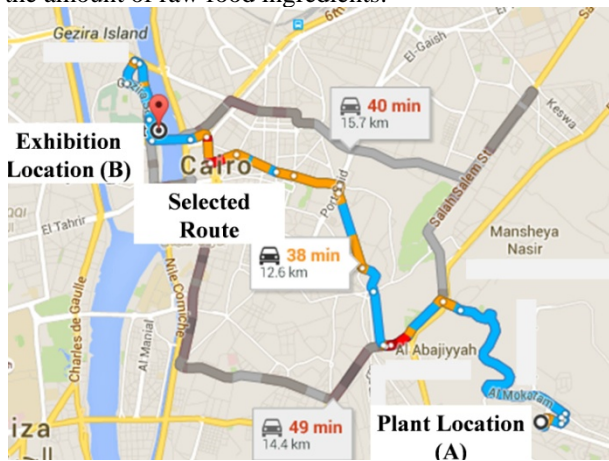


Figure 5: Google Maps imagery for the plant and exhibition location with the selected route shown

6. CONCLUSION

A discrete event simulation model is proposed for a food products and samples that will be used in exhibition and showcase events with the intent of minimizing the wastes as a result of using surplus raw ingredients. The simulation model comprised two main parts with the first part the batch production unit consisting all activities of processing, packing and loading the product, whereas the second part is the exhibition consisting all the activities and resources in the showcase event location. Different resources were examined to determine which one of them has a significant effect on the processes and the whole operation and it was found out the exhibitors are one of the governing factors that could drastically affect the duration of the activities in the event and the rate by which the products are sold. The intent of this paper was to provide a methodological framework to determine the amount of raw ingredients used in food processing to ensure sustainability by minimizing waste of raw ingredients and materials in addition to abortive work and additional electrical power required to process undesired surplus material. To achieve this goal, the service rate was linked with the duration of the event, from which the number of products can be computed. By knowing the weights for the different raw ingredients in the food product, the amount of each raw ingredient can be determined. Further investigation for the different processes and operations in the proposed

model is recommended to be added to the model to include logistics and storage activities for future work to ensure that the proposed model is comprehensive. It is also recommended to compare the results from this model with other models using other simulation tools. Also, different types of simulation such as continuous event and agent based simulations can be used in building the same model and comparing the results. The developed simulation model and framework is expected to be a handful tool for stakeholders in small startups and young entrepreneurs in showcase events involving food sampling to minimize excess or surplus of food and raw ingredients required in food production.

ACKNOWLEDGMENTS

The author would like to thank Toukies, inc. for providing the required data and for their support to produce this work.

REFERENCES

- David, L. and Boldrin, M., 2008. *Against Intellectual Monopoly*, Cambridge University Press, UK, ISBN 978-0-521-87928-6.
- Diefes, H., A., Okos, M., R., Morgan, M., T., 2000. Computer-aided process design using Food Operations Oriented Design System Block Library, *Journal of Food Engineering*, 46, 99-108.
- Flick D, Doursat C, Grenier D, Lucas T., 2015. Modelling of baking processes. Bakalis S, Knoerzer K, Fryer P, editors. *Modeling food processing operations*. Amsterdam: Elsevier Ltd., 129-61.
- Halpin, D. W. (1977). "CYCLONE—A method for modeling job site processes." *J. Constr. Div.*, 103, 489-499.
- Lomax, T., 1997. *Quantifying of congestion*, NCHRP Report 398, Transportation Research Board. National Research Council. Volume 1, Washington, USA.
- Longo F, Massei M, and Nicoletti L. 2012. An application of modeling and simulation to support industrial plants design. *International Journal of Modeling, Simulation, and Scientific Computing* 3: 1240001-1-1240001-26.
- Martinez, J., 1996. *State and Resource Based Simulation of Construction Processes Thesis Phd*, University of Michigan, MI, USA.
- McGarry, M., Watson, M., 1996. *Dynamic Computer Simulation Technology for Food Processing Engineering*, FoodPro 1996, Sydney, Australia.
- Sabarez H. 2015. *Modeling of drying processes for food materials*. Bakalis S, Knoerzer K, Fryer P, editors. *Modeling food processing operations*. Amsterdam: Elsevier Ltd., 95-127.
- Sonesson, U., Berlin, J., Hospido, A., and Ziegler, F. 2010. *Towards sustainable industrial food production using Life Cycle Assessment approaches*. Environmental assessment and management in the food industry: Life Cycle Assessment and related approaches, 165-176.

Tassou S, Gowreesunker B, Parpas D, Raeisi A. Modeling cold food chain processing and display environments. Bakalis S, Knoerzer K, Fryer P, editors. Modeling food processing operations. Amsterdam: Elsevier Ltd., 185–208.

Zhongjie, H., Shaoshu, H., Yitai, M., 2003. Numerical simulation and analysis for quick-frozen food processing Journal of Food Engineering, 60(3), 267–273.

AUTHORS BIOGRAPHY

Mohamed Elmasry: A researcher and civil Engineer with nine years experience in infrastructure design works and construction management. He holds a Bsc in civil engineering from Cairo University in Egypt and Msc in Construction management for the American University in Cairo, Egypt. He has a variety of publications in different international conference proceedings in Europe and United States of America addressing automation in construction and simulation.

Fatma Tarek: CEO and young entrepreneur in Toukies for homemade sweet treats in Cairo, Egypt. She has started this business in April, 2015 and has been working to increase her market share for that kind of industry. Since day one the mission for this startup was sustainable food production and preserving environment. She holds a Bsc in civil engineering from Cairo University in Egypt and has been involved in different social events

APPLYING ARTIFICIAL NEURAL NETWORK MODELING FOR PREDICTING POSTHARVEST LOSS IN SOME COMMON AGRIFOOD COMMODITIES

Adesoji Matthew Olaniyan^(a), Abdulhmeed Babatunde Owolabi^(b)

^(a)Department of Agricultural and Bioresources Engineering, Faculty of Engineering, Federal University, Oye Ekiti, P.M.B. 373, Oye Ekiti-371101, Ekiti State, Nigeria

^(b)Department of Agricultural Engineering Research, Nigerian Stored Products Research Institute, Asa Dam Road, P.M.B. 1489, Ilorin, Kwara State, Nigeria

^(a)amol397@hotmail.com; ^(b)owolabiabdulhameed@gmail.com

ABSTRACT

This study was carried out to predict the extent of postharvest loss in three agrifood commodities namely rice, maize and yam along the food value chain in Delta State, Nigeria. The study considered farmers, transporters, processors, marketers and consumers as the five principal actors in the value chain with farmers being the harvester. Sufficient relevant information was obtained from each of the actors with the aid of organized interviews and well-structured questionnaires. The questionnaires contain information relating to postharvest loss in each of the three commodities at every stage in the value chain - from harvest to consumption. 450 questionnaires were administered on each commodity, with 150 being handled by each actor in each commodity in each of the three senatorial districts in the state making a total of 2250 questionnaires that were administered altogether. Five types of Artificial Neural Network (ANN) topology were used for each commodity making a total of fifteen models that were used for three-layer feed-forward model (TL-FFM) with back-propagation multi-layer perception (BP-MLP) type of ANN. Data analysis was carried out by ANN-ALYUDA forecaster software under the TL-FFM with BP-MLP. Result obtained showed that transporters, processors and marketers contributed more to postharvest loss in rice, maize and yam compared with farmers and consumers. It can be inferred from this study that ANN using TL-FFM with the supervised training type BP-MLP is one of the best tools that can be used to predict postharvest loss in any agricultural commodity along the food value chain. This is due to its understanding in learning the pattern the input data followed and hence predict accurately the target output with little deviation and minimum error. Comparison between predicted values and the target output values in each of the fifteen models showed how good the ANN had been trained to predict losses that occurred along the

value chain based on the five actors that contributed to postharvest loss in each commodity.

Keywords: ANN, agrifood commodities, postharvest losses, three-layer feed-forward model, backward propagation multi-layer perception

1. INTRODUCTION

Postharvest losses are losses along the food value chain, which includes handling, storage, processing, packing, transportation, marketing and consumption. Losses are measurable reduction in foodstuffs and may affect either quantity or quality (Tyler and Gilman, 1979). They arise from the fact that freshly harvested agricultural produce is a living thing that continues with its metabolic activities even after harvest and during postharvest handling. Loss should not be confused with damage, which is the visible sign of deterioration; for example, damage restricts the use of a product, whereas loss makes its use impossible.

Total crop loss is difficult to measure because it depends upon a variety of factors, including the type of crop, the weather, and the region. In under-developed or developing countries, most food is lost well before reaching the consumer. For instance, in Nigeria, it is estimated that nearly 20 percent of produce is lost and in sub-Saharan Africa, the annual value of grain loss is estimated at \$4 billion – enough to feed 48 million people for one year (FAO, 2012).

The first distinction in agro-food losses is that between quantity and quality. Quantitative loss is a loss in terms of physical substance, meaning a reduction in weight and volume and can be assessed and measured. Qualitative loss, however, is concerned with the food and reproductive value of products and requires a different kind of evaluation. It should be noted that losses occurring during the production period and caused by various crop pests

(insects, weeds, disease) will not be considered. However, they have a major influence on food preservation conditions and account in part for the nature and size of postharvest losses.

Several authors have presented a strong argument in favour of devoting more resources to postharvest research for development efforts in developing countries (Bourne, 1983; Mukai, 1987). Although minimizing postharvest losses of already produced food is more sustainable than increasing production to compensate for these losses, less than 5% of the funding for agricultural research is allocated to postharvest research areas (Kader, 2003).

Loss assessment can be time consuming and expensive, but in many instances it is necessary to prevent inefficient use of funds. The need to assess losses in large-scale storage is in general small. In most cases unacceptable losses are very obvious without assessment. For example, in Adaptive Research on Loss Prevention in Different Postharvest Systems - the traditional method of testing, insecticides or storage structures consists of first conducting experiments at the research station level.

Artificial Neural Networks are relatively crude electronic models based on the neural structure of the brain. The brain basically learns from experience. It is a natural proof that some problems that are beyond the scope of current computers are indeed solvable by small energy efficient packages. This brain modeling also promises a less technical way to develop machine solutions.

The exact workings of the human brain are still a mystery. Yet, some aspects of this amazing processor are known. In particular, the most basic element of the human brain is a specific type of cell which, unlike the rest of the body, does not appear to regenerate. Because this type of cell is the only part of the body that is not slowly replaced, it is assumed that these cells are what provide us with our abilities to remember, think, and apply previous experiences to our every action. These cells, all 100 billion of them, are known as neurons. Each of these neurons can connect with up to 200,000 other neurons, although 1,000 to 10,000 are typical.

These artificial neural networks try to replicate only the most basic elements of this complicated, versatile, and powerful organism. They do it in a primitive way. But for the software engineer who is trying to solve problems, neural computing was never about replicating human brains. It is about machines and a new way to solve problems (Strugholtz *et al.* 2006).

Yet, all natural neurons have the same four basic components. These components are known by their biological names - dendrites, soma, axon, and synapses. Dendrites are hair-like extensions of the soma which act like input channels. These input channels receive their input through the synapses of other neurons. The soma then processes these incoming signals over time. The soma then turns that processed value into an output which is sent out to other neurons through the axon and the synapses (Strugholtz *et al.*, 2006).

2. MATERIALS AND METHODS

2.1. Validation and Reliability Procedure of Prepared Questionnaire

Structured Questionnaire were produced in order to reach out and get concise data on three (3) arable crops namely, rice, maize and yam, a necessary guide that enabled the five (5) actors namely, farmers, transporters, marketers, consumers and processors. This was done to have a record of their interaction and to encourage ease of data compilation. The validation and the reliability study of the questionnaire was done by contacting experts in the field of postharvest loss so as to be sure that the questionnaire will bring out the desired results that was needed to predicts the losses in the three arable crops.

2.2. Validation and Reliability Procedure of Prepared Questionnaire

In carrying out the postharvest loss survey experiment, the answer gotten depended very much on the questions asked. For the usefulness of the questionnaire, the data produced were trustworthy, i.e., the results were meaningful and can be applied more generally than to just the sample tested. Proving that trustworthiness for the questionnaire involved subjective experimental endpoints is not trivial, and ensuring that the resulting data reflected the "truth" has spawned an entire field of the survey experiment.

2.3. Sampling Procedure

In selecting the sampling technique for the experiment, it was virtually impossible to study every actor that contributed to postharvest losses in rice, maize and yam in Delta state. The targeted population was simply too large for the study when planning the research study. Collecting millions of questionnaires from every actor was presented with so many challenges.

2.4. Stratified Random Sampling

The sampling procedure used was stratified random sampling, the actors that contributed to postharvest losses was first identified and divided into groups based on their relevant characteristic and then the number of participant to be used was selected within those groups. Stratified random sampling was used so as to ensure that specific subgroups of the actors were adequately represented within the sample.

2.5. Method of Data Collection

Collection of data was done for three weeks in the Delta State; data collation was done for one week and data analysis using Artificial Neural Network was also done for another one week. The ANN software used to analyze and predict the data was ALYUDA forecaster using three layer feed-forward models with back-propagation multi-layer perceptron (MLP) type of neural network. Delta Central Senatorial District was taken care off for the first week, followed by Delta South for the second week, and lastly, Delta North. The ADP offices in each district were located and necessary information's on each actor was obtained from their staff.

2.6. Steps in Developing Artificial Neural Network Model

The following steps were followed in developing the Artificial Neural Network model used in this study: knowing a good model input to be used; determining the neural network type; pre-processing and partitioning of the collated data; determining network architecture to be used in running the program; defining model performance criteria to be used; training, testing and validating the model from the input data by optimizing the connection weights (Dawson and Wilby, 2001; Govindaraju, 2000; Maier and Dandy, 2000).

2.7. Inputs and Output Variables

The postharvest loss survey experiment was conducted for a period of three weeks. The five actors that contributed to postharvest loss were considered on each arable crop. In the selection of input and output variables, it was understood that in any postharvest loss, all the five aforementioned actors contributes to the losses. To achieve this, each actor was made an output variable and the other four serves as its input variables on a particular arable crop

2.8. Neural Network Topology

Five types of neural network topology were used for each of the three commodities (rice, maize and yam), making fifteen models in total for the three layer feed-forward model with back-propagation multi-layer perceptron (MLP) type of neural network . For rice, the neural network topology used for consumers, farmers, marketers, processors and transporters were 4-12-1, 4-18-1, 4-20-1, 4-24-1 and 4-24-1 as input, hidden and output layers respectively. For maize, the neural network architecture used was 4-16-1, 4-15-1, 4-18-1, 4-12-1 and 4-25-1 as input, hidden and output layers respectively. For yam, the neural network architecture used was 4-11-1, 4-17-1, 4-12-1, 4-13-1 and 4-17-1 as input, hidden and output layers respectively. This is in conformity with method Dawson and Wilby (2001) and Taylor (1979) used for determining input, hidden and output layers of neural topology.

3. RESULTS AND DISCUSSION

3.1. Rice Model Sensitivity Analysis

Figures 1 to 5 showed the sensitivity analysis result of rice consumers, rice farmers, rice marketers, rice processors and rice transporters respectively on rice crop. For rice consumers model, loss caused by processors on rice showed the highest sensitivity level with 36.673%. For rice farmers model, loss caused by processors in rice also showed the highest level of sensitivity with 44.212%. For rice marketers model, loss caused by processors in rice also showed the highest level of sensitivity with 40.524%. For rice processors model, loss caused by marketers on rice showed the highest level of sensitivity with 44.137%. Finally, for rice transporters model, loss caused by marketers on rice also showed the highest level of sensitivity with 39.425%. This implies that the major causes of postharvest loss in rice crop in Delta State are from two actors namely processors and marketers but more peculiar to processors because of inadequate processing equipments, poor road network and bad marketing structures. This is in-line with the report of Imonikebe (2013) and Talabi (1995) on methods of minimizing food losses and ensuring food security.

3.2. Maize Model Sensitivity Analysis

Figures 6 to 10 showed the sensitivity analysis result of maize consumers, maize farmers, maize marketers, maize processors and maize transporters respectively on maize crop. For maize consumers model, loss caused by processors on maize showed the highest sensitivity level with 52.166%. For maize farmers model, loss caused by processors on maize also showed the highest level of sensitivity with 33.614%.

For maize marketers model, loss caused by processors on maize also showed the highest level of sensitivity with 38.656%. For maize processors model, loss caused by marketers in maize showed the highest level of sensitivity with 28.241%. Finally, for Maize Transporters model, loss caused by processors in maize showed the highest level of sensitivity with 33.287%. This also implies that the major causes of postharvest in maize crop in Delta State are from two actors namely processors and marketers but more pronounced in processors. This is due to the attitudes of Delta State indigenes to maize crop compare with other crops which makes the processing of the produce to be less important compare to plantain. It is also due to poor road network and bad marketing structures. This is in conformity with the initial findings by Talabi (1995).

3.3. Yam Model Sensitivity Analysis

Figures 11 to 15 showed the sensitivity analysis result of yam consumers, yam farmers, yam marketers, yam processors and yam transporters respectively on yam crop. For yam consumers model, loss caused by processors in yam showed the highest sensitivity level with 29.045%. For yam farmers model, loss caused by processors in yam also showed the highest level of sensitivity with 42.367%. For yam marketers model, loss caused by processors in yam also showed the highest level of sensitivity with 34.725%. For yam processors model, loss caused by transporters in yam showed the highest level of sensitivity with 32.920%. Finally, for yam transporters model, loss caused by processors on yam showed the highest level of sensitivity with 56.126%. This also implies that the major causes of postharvest loss in yam crop in Delta State are from two actors namely processors and transporters but more prominent in processors due to lack of inadequate processing equipment in Ughelli where maize production is dominant and bad road network especially from Sapele market to Jege market which is the major market for yam tubers. This is in-line with the findings of Ebewore (2013) and Achoja (2013) on storage practices among arable farmers in Delta State, Nigeria

3.4 Implication of the Study

The study showed that majority of the respondents stated that postharvest losses in the Three (3) crops occurred mainly during processing. Other sources of losses are during transportation, and marketing. This is in conformity with the previous work done by Talabi (1995) that also identified these as the sources of postharvest losses. Poor methods of crop preservation, poor storage, processing methods and

microbial attack were some of the causes of postharvest losses identified from the study. Ukoh-Aviomoh et al. (2005) had similar findings that Improvement in the processing and transportation of arable crops will drastically reduce postharvest losses. Other causes of losses in the state are careless handling of food crops during harvesting of immature food crops and marks of cutlass on yams that leads to bruises which causes marks/injuries and microbial attack on yam. Bruises or marks on crop could result in spoilage and consequently reducing the economic value of the foodstuffs. These can be prevented by teaching farmers as one of the five (5) actors of postharvest losses to recognize maturity index of various food crops and carefulness in harvesting of root crops e.g. yam, sweet potatoes and cocoyam. Some measures for minimizing postharvest crop losses were identified from the study to ensure food security. One of such measures is avoidance of over-stacking of arable crops like rice, maize and beans. Picha. (2002) stressed the need to avoid over-stacking of food crops during transportation and storage of the crops. This is because over-stacking leads to generation of heat and deterioration of food items. The avoidance of exposure of arable crops to direct sunlight, harvesting of tuber crops e.g. yam in the morning and evening to prevent exposure to sunlight could prevent postharvest crop losses. This is because such exposure to direct sunlight led to temperature increase and deterioration (Talabi 1995). Postharvest crop losses result in food shortage and consequently food insecurity in Delta state according to the findings. The various causes of food shortage need to be identified and addressed through teaching processors and farmers effective food processing and preservation methods especially in Ughara, Ughelli South and Warri North. If this is not done, food insecurity with its attendant problems of violence, stealing, morbidity and mortality mostly of infants, children, pregnant women and elderly people will be very rampant in the state.

4. CONCLUSIONS

The data generated from this study have been able to provide evidence that:

- (i) The Artificial Neural Network using three layer feed- forward model with back propagation multi-layer perceptron were successfully used to predict postharvest losses on the three arable crops along the food value chain in Delta state.
- (ii) The level of postharvest losses in rice in Delta State are from two actors namely

processors with the highest sensitivity level of 36.673%, 44.212%, 40.524%, and marketers with highest sensitivity level of 44.137% and 39.425%. The level of postharvest losses in maize are from two actors namely processors with the highest sensitivity level of 52.166%, 33.614%, 38.656%, 33.287%, and marketers with highest sensitivity level of 28.241%.

- (iii) The level of postharvest losses in yam are from two actors namely processors with the highest sensitivity level of 29.045%, 42.367%, 34.725%, 56.126%, and transporters with the highest sensitivity level of 32.920%.
- (iv) Processors, marketers and transporters contributed immensely to the postharvest losses that occurred to rice, maize and yam in Delta state because of the aforementioned problems.
- (v) Artificial Neural Network should be used to analyze postharvest losses on all major commodities grown in Delta state in particular and Nigeria in general so that the nation can have reliable information on postharvest loss on each of the commodities and proffer solutions.
- (vi) Postharvest losses in perishable commodities such as fruits, vegetables and others should also be investigated using Artificial Neural Network to obtain information as well.

REFERENCES

Bourne M.C. 1983. Guidelines for Postharvest Food Loss Reduction Activities. United Nations Environment Programme, Industry & Environment Guidelines Series.

Dawson C.W., and Wilby R.L. 2001. Hydrological Modelling using Artificial Neural Networks. *Progress in Physical Geography*, 25 (1): 80–108.

Ebewore S.O., and Achoja F.O. 2013. Storage Practices among Arable Farmers in Delta state, Nigeria: Implication for Food Security.

FAO. 2012. High and Volatile Food Prices - FAO Support to Country Level Contingency Planning.

Food and Agriculture Organisation of the United Nations, Rome, Italy.

Govindaraju R.S. 2000. Artificial Neural Networks in Hydrology I: Preliminary Concepts. *Journal of Hydrologic Engineering*, 5 (2): 115–123.

Kader A.A. 1983. Postharvest Quality Maintenance of Fruits and Vegetables in Developing Countries. p.455-570. In: Lieberman M. (ed.), *Postharvest Physiology and Crop Preservation*. Plenum Publ. Corp., New York, NY.

Maier H.R., and Dandy G.C. 2000. Neural Networks for the Prediction and Forecasting of Water Resources Variables: A Review of Modelling Issues and Applications. *Environmental Modeling and Software* 15, 1: 101–124.

Mukai M.K. 1987. Postharvest Research in a Developing Country: A View from Brazil. *Horticultural Science*, 22:7-9.

Picha D. 2002. Post Harvest Technology for Horticultural Crops. A Paper Presented at the USDA/CSREES/USAID/FMAARD Conference held in Agriculture/Extension Development Project at Abuja, Nigeria, pp 5-10.

Strugholtz S., Panglisch S., Gebhardt J, and Gimbel R. 2006. Modeling and Optimization of Ceramic Membrane Microfiltration using Neural Networks and Genetic Algorithms. *Water Practice and Technology*, 1 (4): 102-110.

Talabi A.E. 1995. Appropriate Storage Facilities for Promoting Economic Growth and Food Security. *Proceedings of the 19th Annual Conference of the Nigerian Institute of Food Science and Technology*, 5: 19-30.

Taylor R.W.D., and Webley D.J. 1979. "Constraints on the Use of Pesticides to Protect Stored Grain in Rural Conditions," *Trop. Stored Prod. Inf.*, no. 38, pp. 1-9.

Ukoh-Aviomoh E.E., and Okoh F. 2005. Teaching Rural Families the Management of Postharvest Food Losses as a Strategy for Improving Household Food Security in Nigeria. *Journal Home Economics Research*, 6 (1):

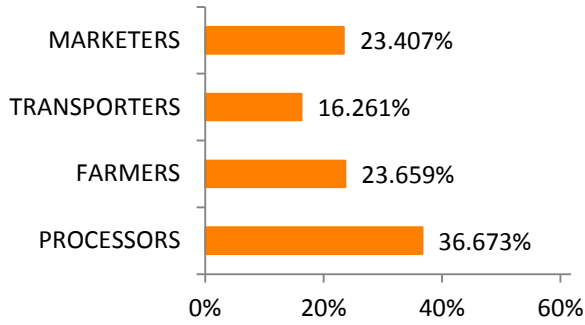


Figure 1: Sensitivity Analysis Result of Rice

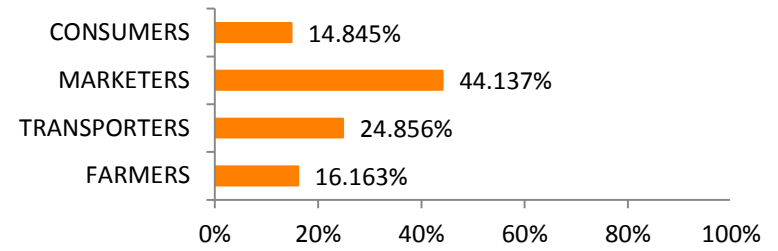


Figure 4: Sensitivity Analysis Result of Rice

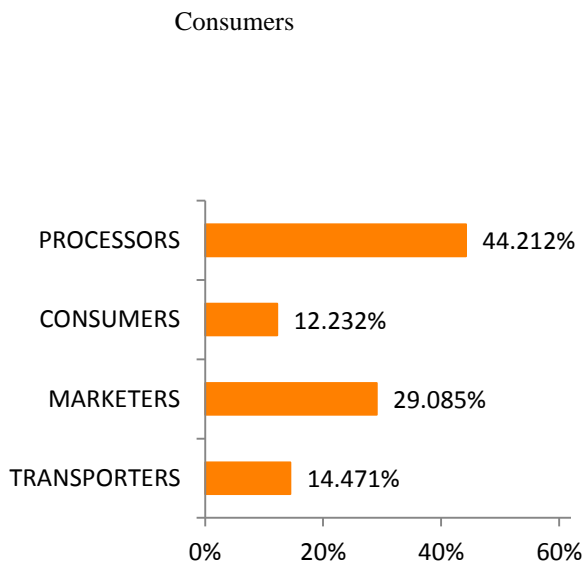


Figure 2: Sensitivity Analysis Result of Rice Farmers

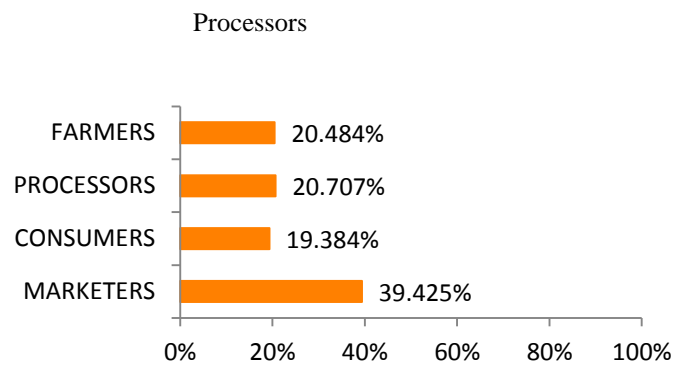


Figure 5: Sensitivity Analysis Result of Rice

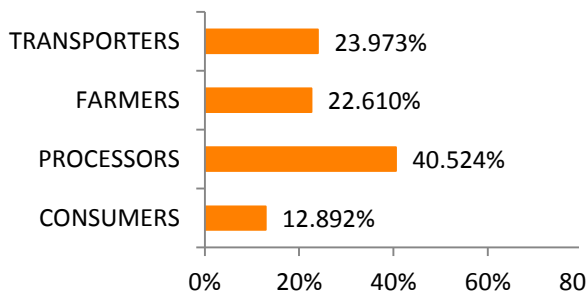


Figure 3: Sensitivity Analysis Result of Rice

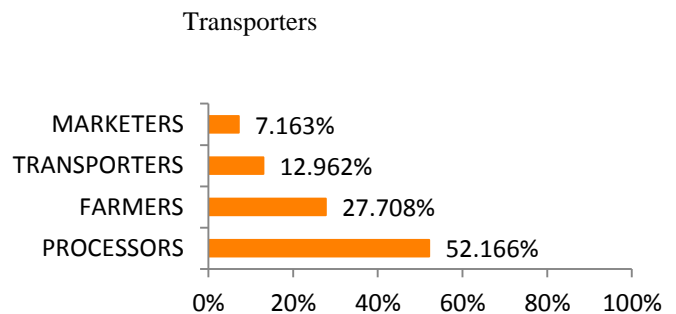


Figure 6: Sensitivity Analysis Result of Maize

Marketters

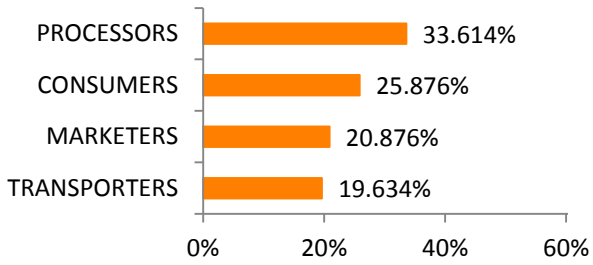


Figure 7: Sensitivity Analysis Result of Maize

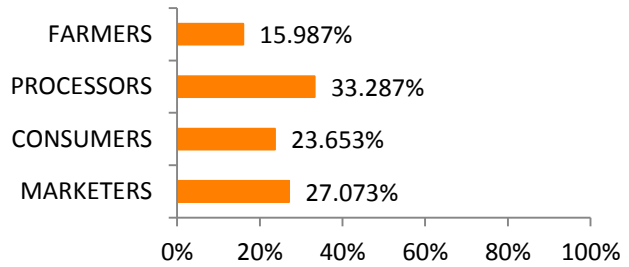


Figure 10: Sensitivity Analysis Result of Maize

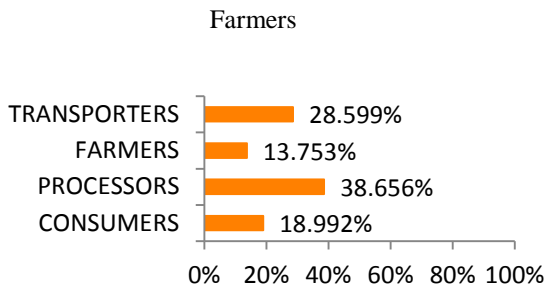


Figure 8: Sensitivity Analysis Result of Maize

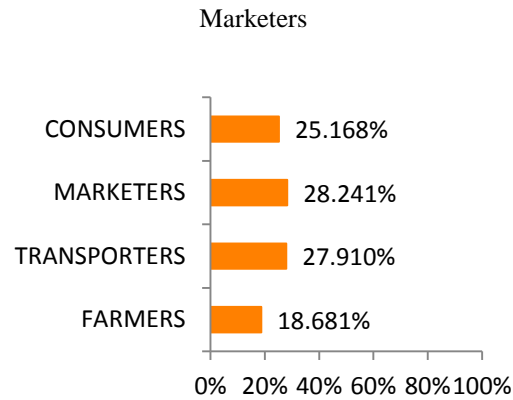
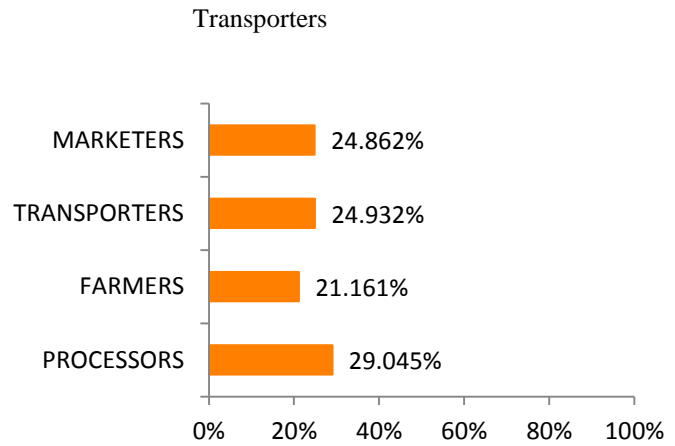


Figure 9: Sensitivity Analysis Result of Maize

Figure 11: Sensitivity Analysis Result of Yam

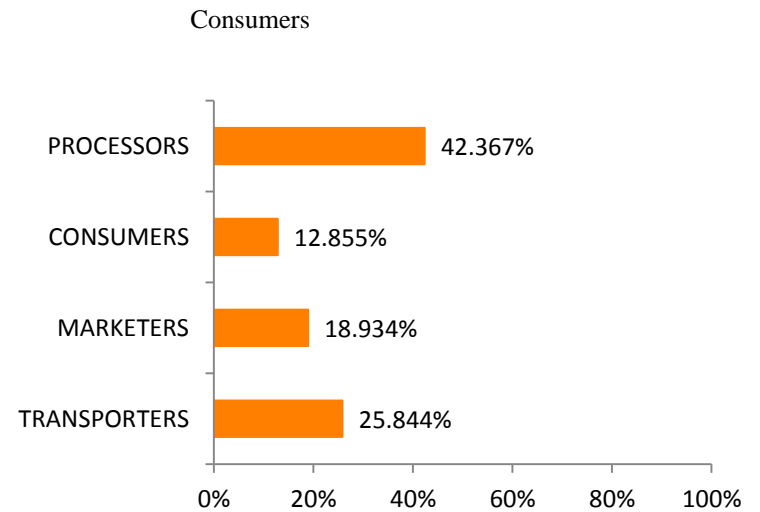


Figure 12: Sensitivity Analysis Result of Yam

Farmers

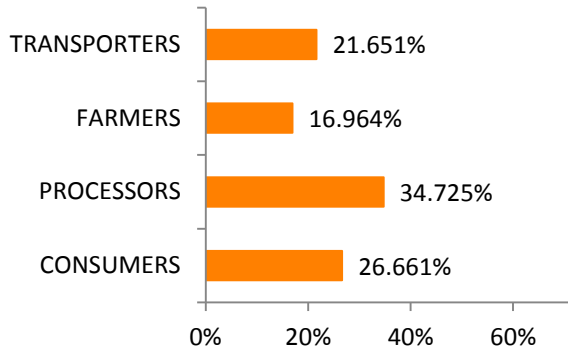


Figure 13: Sensitivity Analysis Result of Yam

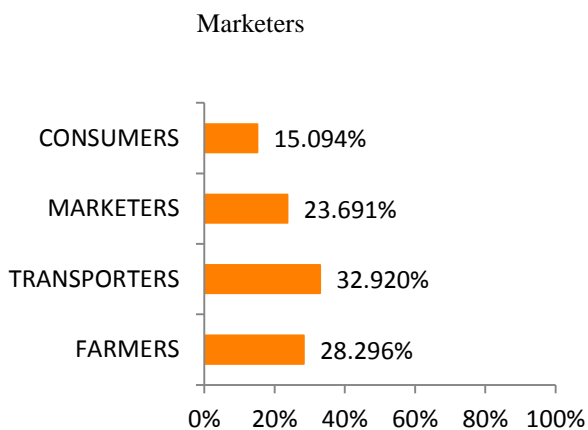


Figure 14: Sensitivity Analysis Result of Yam

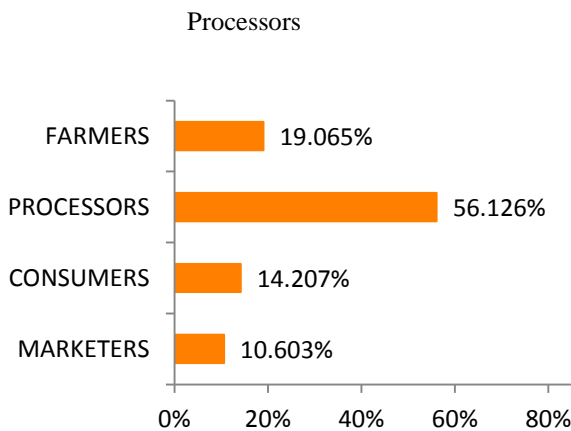


Figure 15: Sensitivity Analysis Result of Yam

BIOGRAPHY OF THE AUTHORS

1. Dr. Adesoji Matthew Olaniyan graduated with B.Eng, M.Eng and PhD in Agricultural Engineering from University of Ilorin, Nigeria in 1991, 1998 and 2006 respectively. Since 1998, he has been working on techniques, processes and equipment for processing agricultural and bioresources materials to food, fibre and industrial raw materials. Dr. Olaniyan's principal area of research is on Bioproduct Processing and Food Process Engineering, where he has carried out a number of projects and published a number of papers in local and international journals. He joined the service of the University of Ilorin in 1998 as an Assistant Lecturer in the Department of Agricultural and Biosystems Engineering and rose to the position of a Senior Lecturer in 2009. Currently, he is an Associate Professor at the Department of Agricultural and Bio-resources Engineering, Federal University Oye-Ekiti, Nigeria. Dr. Olaniyan has bagged several awards including the Award for the Best Paper (2007) in the Journal of Food Science and Technology, Mysore, India; Chinese Government Sponsorship (2008) for International Training Programme in Protected Agriculture at International Exchange Centre, Yangling, China; Netherlands Fellowship Programme (2009) for International Training Programme in Milk Processing at Practical Training Centre, Onkerk, the Netherlands; and Postdoctoral Fellowship (2011) of the Academy of Sciences of Developing Countries.

2. Mr. Babatunde Abdulhameed Owolabi graduated from the University of Ilorin with BEng and MEng degrees in Agricultural Engineering in 2010 and 2016 respectively. He is presently a Research Officer with the Nigerian Stored Products Research Institute, Ilorin with area of specialization in Crop Processing and Storage. He has carried out a number of research projects some of which are: (i) evaluation of composite packaging materials to increase the shelf life of Catfish; (ii) performance evaluation of solar cabinet dryer, solar tent dryer and smoking kiln. He has assisted other Research Engineers in the Institute to design, fabricate and instal 100 units of 50 kg and 25 kg fish smoking kilns (powered by charcoal, gas and electricity) for WAAPP-Nigeria. His work also included conducting postharvest loss survey in Delta and Edo States and training of farmers on how to preserve grains using silo as a storage structure in Ubiaja, Edo State – a programme organized by Food For All International.

MATHEMATICAL MODELING OF MICROWAVE ASSISTED FLUIDIZED BED DRYING OF HAZELNUTS

Narjes Malekjani^(a), Zahra Emam-Djomeh^(b), Seyed Hassan Hashemabadi^(c), Gholam Reza Askari^(d)

^{(a), (b), (d)} Department of Food Science, Technology and Engineering, University College of Agriculture and Natural Resources, University of Tehran, Iran.

^(c) School of Chemical Engineering, Iran University of Science and Technology, Tehran, Iran.

^(a) n.malekjani@ut.ac.ir, ^(b) emamj@ut.ac.ir, ^(c) hashemabadi@iust.ac.ir, ^(d) iraskari@ut.ac.ir

ABSTRACT

Microwave assisted fluidized bed drying is a novel drying technique which reduces drying time and yields higher quality products. In this study the effect of this method on drying kinetics of hazelnuts was studied. Drying experiments were conducted in three temperatures (40,50 and 60) and microwave power levels (0, 450 and 900W). The results showed that the effect of microwave power was more dominant than drying air temperature. Mathematical modeling was performed in order to predict the moisture changes during drying process. It was concluded that two term thin layer drying model was the best model to predict the drying kinetics of hazelnut with coefficient of determination and mean square of deviation as 0.999 and 0.02096 respectively.

Keywords: hazelnut, modeling, thin layer models, microwave, fluidized bed dryer

1. INTRODUCTION

Hazelnuts (*Corylus avellana L.*) are very important raw materials to the confectionary and chocolate industries (Kibar and Öztürk, 2009). High quality hazelnut varieties are cultivated in Northern parts of Iran. Iran is the 6th producer of hazelnut in the world (Hosseinpour et al., 2013). Hazelnuts are enriched of essential minerals, sterols, tannins, free phenolic acids, sugars, organic acids and phenolic compounds which make its unique sensory properties. High polyphenol content, makes hazelnuts an excellent source of natural antioxidants also high content of unsaturated fatty acids, α -tocopherol and carotenoids in hazelnuts have important health benefits (Ciarmiello et al., 2013).

Post-harvest storage of hazelnuts with high moisture content results in considerable qualitative and quantitative losses and drying process is required to inhibit the growth of various mycotoxins and to preserve the product (Demirtas et al., 1998). On the other hand, due to climate changes in the season of hazelnut harvest, the hazelnuts cannot be naturally dried on the tree and the nuts would be harvested with a moisture content about 25 % accordingly it should be processed to lower its

moisture content to a safe level for storage. The best moisture content to prevent the microbial growth is 7 to 8 % for unshelled hazelnuts and 4 to 5 % for shelled hazelnuts (Lopez et al., 1997). Using Conventional drying methods may have negative biochemical, chemical and organoleptic effects which decline products quality and reduce consumer acceptance (Askari et al., 2013; Demirhan and Özbek, 2015; Nadian et al., 2015).

Dipolar interaction of water molecules inside the food material causes heat generation in microwave ovens. The polar water molecules align themselves with changing electric field and the friction between oscillating molecules results in heat. This accelerated volumetric heat generation causes the pressure build up and results in rapid evaporation of water (Kumar et al., 2014). Microwave drying has various benefits such as less startup time, operation speed, energy consumption efficiency, space savings, precise process control, selective heating and for some products, superior quality of dried products (Wu and Mao, 2008). Aside from this beneficial features, microwave drying also can deteriorate product's quality if it is not used properly. The combination of microwave power with hot air convective drying has recently been proposed to overcome some limitations of single microwave processing such as possible damage to textural, color and nutritional properties, uneven heat distribution and limited penetration of the microwave radiation inside the product (Reyes et al., 2007; Askari et al., 2008).

Accurate prediction of drying process of food and agricultural products is critical to decline quality loss along with the energy consumption, and increasing the drying capacity. Thin-layer mathematical models are useful tools in designing and improvement of drying systems and analysis of mass transfer changes with time during drying process (Malekjani et al., 2013; Belghith et al., 2015). Due to complicated phenomenon and various factors required, in this study the drying kinetics have been investigated using a mathematical model. Although many attempts have been made to mathematically investigate the drying kinetic of foods during microwave and fluidized bed drying treatments

such as tomato (Belghith et al., 2015), paddy (Golpour et al., 2015), canola (Malekjani et al., 2013), pistachio (Kouchakzadeh and Shafeei, 2010), macadamia nut (Silva et al., 2006) and many other food and agricultural products, efficient models are still needed to predict the drying behavior in the microwave assisted fluidized bed drying of nuts especially hazelnut. The objective of this work is to study the effect of temperature and microwave power variations in microwave assisted fluidized bed drying on drying kinetics of hazelnuts and proposing the best model for prediction of nut moisture content with drying time.

2. MATERIAL AND METHODS

2.1. Sample Preparation

Freshly harvested hazelnut was used in this study. The hazelnuts were obtained from a local garden in Eshkevarat, Guilan, Iran and kept at 4°C refrigerator until beginning the experiments. Before the experiments hazelnut samples were unshelled manually, the poor quality hazelnuts were also removed and classified as 11–13 mm kernels using a digital micrometer.

2.2. Drying Experiments

A laboratory scale microwave assisted fluidized bed dryer was used for drying experiments (Fig. 1.). The drying air velocity, temperature and microwave power were accurately controlled in the dryer. The drying chamber consisted of a Plexiglas cylinder (10 cm diameter and 35 cm height). For all experiments, air velocity was maintained constant. For stabilization the drying parameters in the drying chamber, the dryer was run without the samples for 30 min before each experiment. Drying chamber was positioned on a digital balance with accuracy of 0.01 g (Fig. 1) and the samples were weighted when the blowing air was switched off, instead of the less reliable method of removing the sample from the drying chamber.

The drying experiments were conducted at three hot air temperature levels (40, 50 and 60°C) combined with three microwave power levels (0, 450 and 900 W). The initial moisture content of the samples was measured before the experiments and it was 24-25% (d.b). 100 gr raw unshelled hazelnut was utilized for each run. The drying experiments were continued until the moisture content of the samples reached 5-6 % which was determined by weighting the samples during drying.

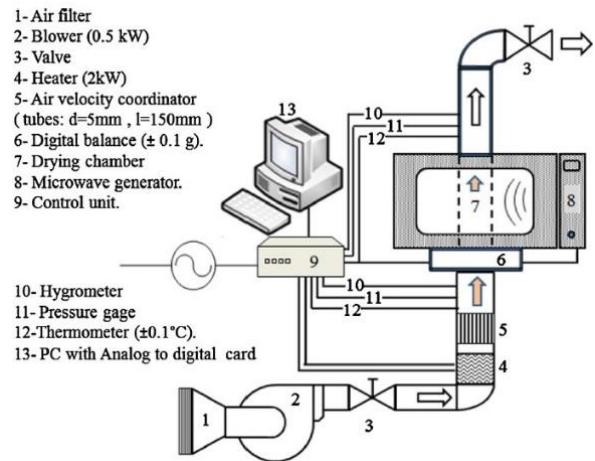


Fig 1. Drying apparatus (picture adapted by (Askari et al., 2013))

2.3. Mathematical Modeling

Moisture ratio estimated from Eq. (1):

$$\text{Moisture ratio (MR)} = \frac{M - M_e}{M_0 - M_e} \quad (1)$$

Where MR, M, M_0 , M_e are the moisture ratio, moisture content at any time, initial moisture content and equilibrium moisture content respectively.

As the value of equilibrium moisture content M_e is much smaller than M and M_0 , so, the moisture ratio may be simplified to M/M_0 (Kouchakzadeh and Shafeei, 2010). Seven popular thin layer drying models were used to describe the drying behavior of hazelnuts in different drying conditions in the microwave assisted fluidized bed dryer as table 1.

Table 1. thin layer drying models

Model name	Model
Newton	$MR = \exp(-kt)$
Page	$MR = \exp(-kt^n)$
Henderson Pabis	$MR = a \exp(-kt)$
Logarithmic	$MR = a \exp(-kt) + c$
two term	$MR = a \exp(-k_0 t) + b \exp(-k_1 t)$
two-term exponential	$MR = a \exp(-kt) + (1 - a) \exp(-kat)$
Midilli et al.	$MR = a \exp(-kt^n) + bt$

The models were evaluated and compared with experimental data using the coefficient of determination (R^2); root mean square error (RMSE) and reduced chi-square (χ^2) based on the following relationships:

$$R^2 = 1 - \frac{\sum_{i=1}^N (MR_{pre,i} - MR_{exp,i})^2}{\sum_{i=1}^N (\overline{MR}_{pre,i} - MR_{exp,i})^2}$$

$$\chi^2 = \frac{\sum_{i=1}^N (MR_{exp,i} - MR_{pre,i})^2}{N - n}$$

$$RMSE = \left(\frac{\sum_{i=1}^N (MR_{pre,i} - MR_{exp,i})^2}{N} \right)^{\frac{1}{2}}$$

where $MR_{exp,i}$ is the experimental moisture ratio, $MR_{pre,i}$ is predicted moisture ratio, N is number of observation, and n is number of constants. Non-linear regression analyses were down by using statistical computer program. The model with the highest R^2 value and lowest χ^2 and RMSE was chosen as the best model.

3. RESULTS AND DISCUSSION

The microwave assisted fluidized bed drying experiments were conducted with variations of microwave power and hot-air temperature. The initial moisture content decreased until reaching the 5-6% moisture content. Figure 2 shows the effect of drying air temperature on drying kinetics. As it is shown in Fig 2a, in the treatments without microwave power, the drying time decrease with increasing the temperature. Elevating the temperature from 40 to 50 C decreased the total drying time about 40% and further increasing of the temperature to 60 C decreased it about 62%. As it is illustrated in figure 2 b and 2c, there are not significant differences between drying curves at different temperatures. This findings were expected because of high internal heat generated in treatments with microwave power which diminished the effects of higher temperatures (Silva *et al.*, 2006).

Figure 3 shows the effects of different microwave powers at constant temperatures on drying kinetics of hazelnut. As it is illustrated the effect of microwave power is significant at all three temperatures. As the microwave power increased from 0 to 450W at 40 C, the drying time decreased about 77%, further increase of microwave power to 900W, decreased this value about 96.4 %. These decrease in drying time was 65 and 95% at 50 C and 42% and 93% at 60C respectively. The results show that the significance of microwave power is higher at lower drying temperatures. The decrease in drying time with an increase in the drying microwave power density has been reported for many foodstuffs.

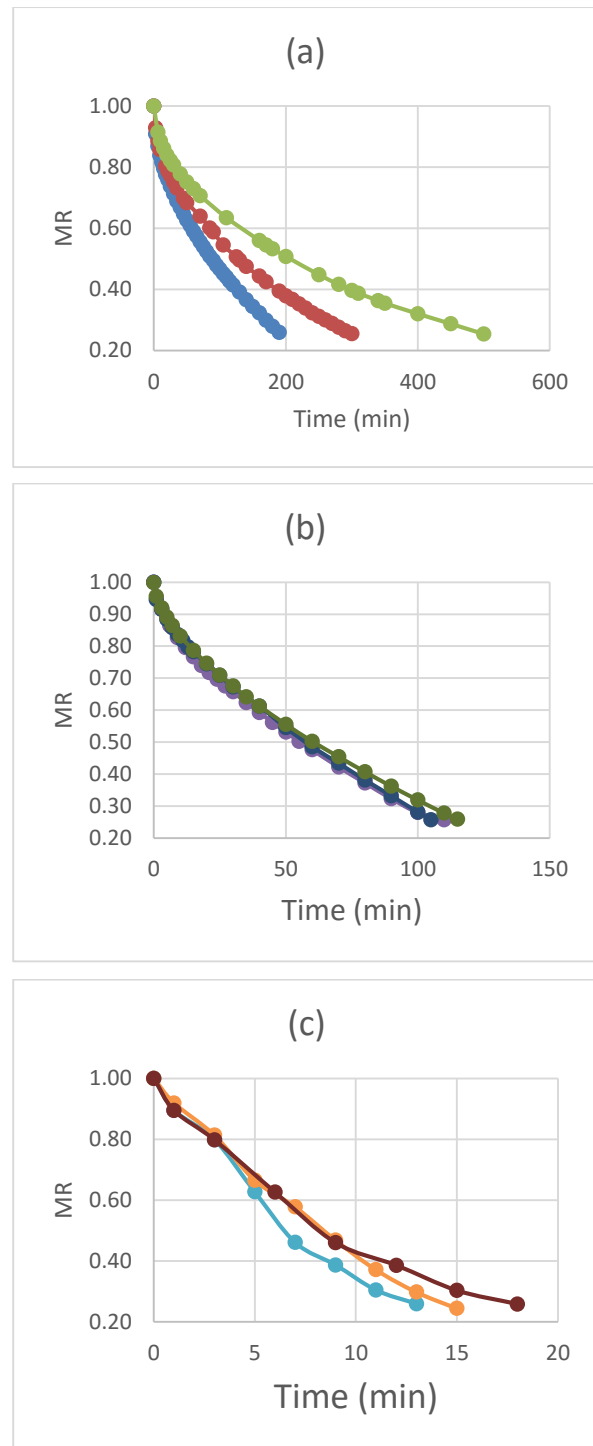


Fig 2. Effect of drying air temperature at (a) 0 W, (b) 450W, (c) 900W on hazelnut drying kinetics

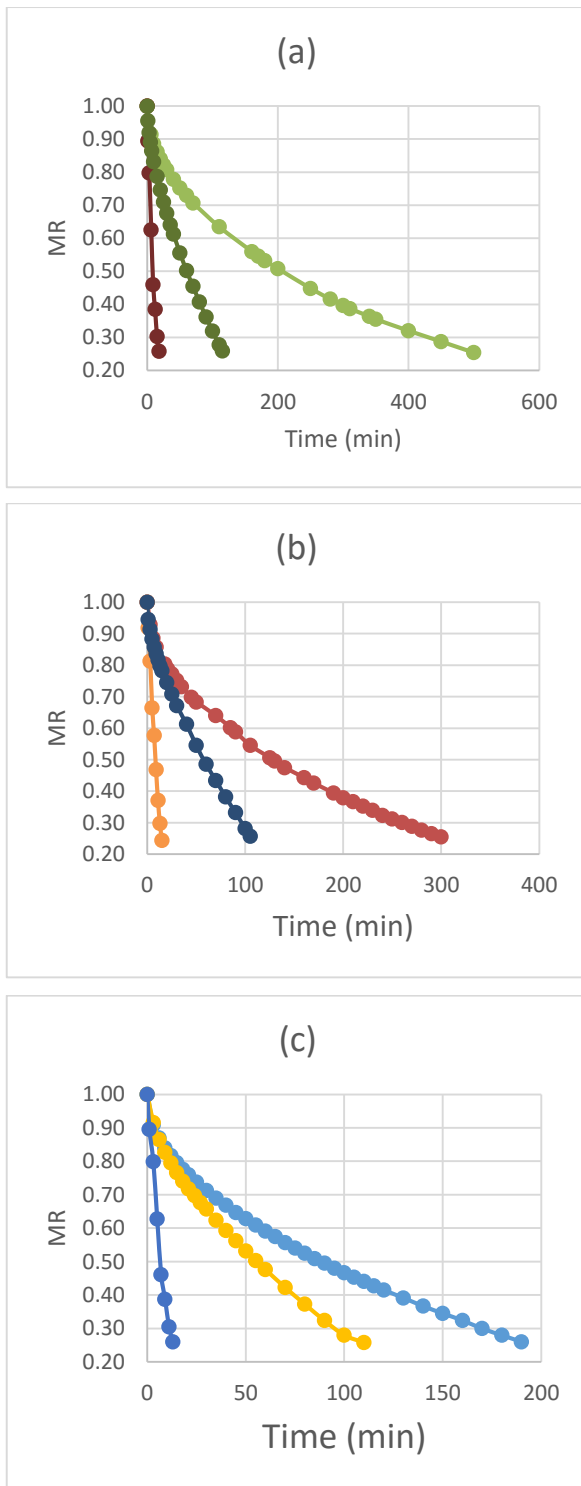


Fig 3. Effect of microwave power at (a) 40 C, (b) 50 C, (c) 60 C on hazelnut drying kinetics

The drying rates declined as the moisture content decreased and increased with the microwave power. As more heat generated within the sample due to microwave volumetric heating creating a large vapor pressure difference between the center and the surface of the product, the mass transfer within the sample was more rapid than the treatments without microwave (Fig 4). At

the beginning of the drying process, the drying rates were higher. As the moisture content of the hazelnuts was higher at initial phase of the drying more absorption of microwave power and higher drying rates took place due to the higher moisture diffusion. As the drying continued, the loss of moisture in the product resulted in a decrease in the absorption of microwave power and decreasing the drying rate (Soysal *et al.*, 2009).

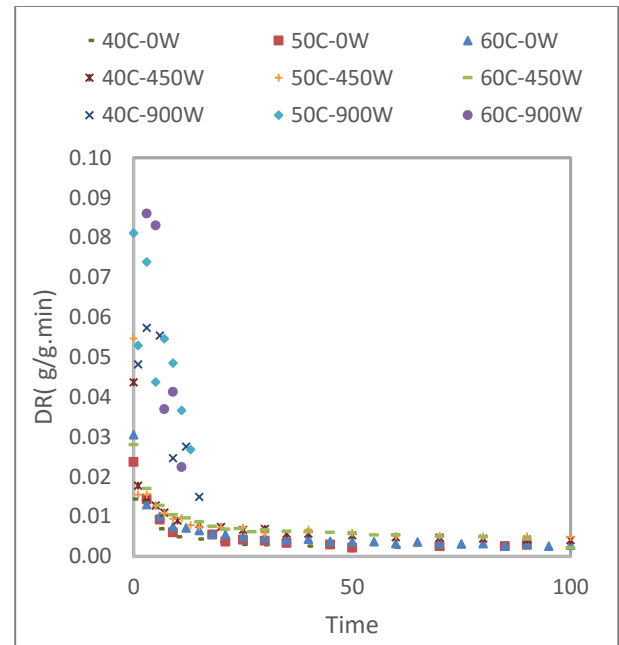


Fig 4. Drying rates at different drying condition

The statistical results from the models are shown in Table 2. In all cases, the statistical parameter estimations showed that R^2 , χ^2 and RMSE values were ranged from 0.97 to 1, 0.005 to 0.299, and 0.0000282 to 0.112, respectively. The two term model had the highest coefficient of determination and the lowest χ^2 and RMSE values. Thus, it was the best model to represent the thin layer drying characteristics of hazelnuts.

4. CONCLUSION

The drying behavior of hazelnut in a microwave assisted fluidized bed dryer was investigated at different drying times and microwave power. The results showed that microwave power has more significant effect on decreasing the drying time that drying air temperature. All treatments followed falling rate period. In order to describe the drying behavior of hazelnuts seven thin layer drying models proposed in the literature were fitted with experimental data at different conditions. Two term model was the best model fitting the experimental data with the highest R^2 and lowest RMSE and χ^2 . This model could characterize the exponential decrease in moisture ratio, as normally observed in drying behavior of agricultural and food products.

Table 2- Results of statistical analysis on the modeling of moisture contents and drying time for the microwave assisted dried hazelnuts

Model	T (C)	P(W)	Model constants		K Sq.	RMSE	R Sq.		
k									
Newton	40	0	0.0033		0.00431	0.06429	0.97528		
	40	450	0.0120		0.00105	0.03157	0.99241		
	40	900	0.0798		0.00032	0.01660	0.99619		
	50	0	0.0052		0.00374	0.06022	0.99963		
	50	450	0.0129		0.00126	0.03457	0.99176		
	50	900	0.0864		0.00061	0.02326	0.99102		
	60	0	0.0080		0.00279	0.05209	0.99977		
	60	450	0.0132		0.00120	0.03381	0.99223		
	60	900	0.1025		0.00088	0.02772	0.98799		
Page									
k n									
Page	40	0	0.0223	0.6521		0.00015	0.01189	0.99908	
	40	450	0.0244	0.8281		0.00029	0.01626	0.99795	
	40	900	0.0879	0.9589		0.00032	0.01548	0.99659	
	50	0	0.0280	0.6705		0.00024	0.01496	0.99998	
	50	450	0.0253	0.8314		0.00049	0.02108	0.99686	
	50	900	0.0605	1.1608		0.00016	0.01105	0.99819	
	60	0	0.0317	0.6965		0.00023	0.01469	0.99998	
	60	450	0.0274	0.8159		0.00029	0.01620	0.99819	
	60	900	0.0778	1.1338		0.00062	0.02157	0.99338	
k a									
Handerson and Pabis	40	0	0.0027	0.8954		0.00087	0.02823	0.99487	
	40	450	0.0110	0.9499		0.00028	0.01574	0.99806	
	40	900	0.0786	0.9895		0.00033	0.01570	0.99647	
	50	0	0.0043	0.8896		0.00078	0.02710	0.99992	
	50	450	0.0116	0.9478		0.00033	0.01735	0.99787	
	50	900	0.0889	1.0199		0.00058	0.02119	0.99303	
	60	0	0.0066	0.8961		0.00051	0.02198	0.99996	
	60	450	0.0118	0.9383		0.00033	0.01745	0.99789	
	60	900	0.1049	1.0166		0.00094	0.02651	0.98960	
k a c									
Logaritmic	40	0	0.0045	0.7155	0.2018		0.00055	0.02140	0.99699
	40	450	0.0119	0.9094	0.0439		0.00023	0.01384	0.99852
	40	900	0.0787	0.9848	0.0035		0.00009	0.00885	0.99894
	50	0	0.0067	0.7393	0.1737		0.00074	0.02492	0.99995
	50	450	0.0116	0.9478	0.0000		0.00029	0.01552	0.99829
	50	900	0.0889	1.0199	0.0000		0.00019	0.01272	0.99786
	60	0	0.0092	0.7641	0.1498		0.00061	0.02263	0.99997
	60	450	0.0129	0.8957	0.0475		0.00031	0.01612	0.99814
	60	900	0.1049	1.0166	0.0000		0.00027	0.01500	0.99694
a k0 k1 b									
Two Term	40	0	0.8400	0.0025	0.0692	0.1502	0.00005	0.00642	0.99973
	40	450	0.9277	0.0105	0.4572	0.0686	0.00006	0.00704	0.99962

	40	900	0.9398	0.0874	0.0000	0.0548	0.00011	0.00937	0.99887
	50	0	0.8412	0.0040	0.1338	0.1542	0.00003	0.00475	1.00000
	50	450	0.9340	0.0113	0.9568	0.0652	0.00015	0.01100	0.99915
	50	900	0.6553	0.0889	0.0888	0.3646	0.00025	0.01422	0.99739
	60	0	0.8585	0.0061	0.1955	0.1370	0.00003	0.00501	1.00000
	60	450	0.9135	0.0112	0.3564	0.0872	0.00008	0.00776	0.99960
	60	900	0.5004	0.1049	0.1049	0.5161	0.00035	0.01677	0.99638
			k	a					
Two Term Exponential	40	0	0.0239	0.1169			0.00174	0.03998	0.99002
	40	450	0.1424	0.0745			0.00021	0.01390	0.99851
	40	900	0.1132	0.4962			0.00031	0.01532	0.99667
	50	0	0.0352	0.1246			0.00138	0.03603	0.99986
	50	450	0.1727	0.0663			0.00036	0.01789	0.99776
	50	900	0.1209	1.6976			0.00012	0.00975	0.99858
	60	0	0.0568	0.1171			0.00088	0.02874	0.99993
	60	450	0.1341	0.0847			0.00021	0.01397	0.99866
	60	900	0.1404	1.6702			0.00060	0.02124	0.99359
			a	k	n	b			
Midilli et al.	40	0	0.9737	0.0159	0.7075	0.0000	0.00016	0.01120	0.99924
	40	450	0.9697	0.0170	0.9034	0.0000	0.00021	0.01287	0.99871
	40	900	1.0139	0.1133	0.8587	0.0000	0.00021	0.01295	0.99783
	50	0	0.6442	0.1015	0.1042	0.0000	0.08314	0.25790	0.99553
	50	450	0.9593	0.0150	0.9427	0.0000	0.00035	0.01666	0.99803
	50	900	1.0000	0.0687	1.1012	0.0000	0.00010	0.00895	0.99897
	60	0	0.5137	0.1040	0.1048	0.0000	0.11167	0.29890	0.99229
	60	450	0.9691	0.0200	0.8818	0.0000	0.00028	0.01486	0.99852
	60	900	0.9947	0.0784	1.1271	0.0000	0.00023	0.01362	0.99761

REFERENCES

- Askari, G., Emam-Djomeh, Z., and Mousavi, S. 2008. Investigation of the effects of microwave treatment on the optical properties of apple slices during drying. *Drying Technology* 26, 1362-1368.
- Askari, G., Emam-Djomeh, Z., and Mousavi, S. 2013. Heat and mass transfer in apple cubes in a microwave-assisted fluidized bed drier. *Food and Bioproducts Processing* 91, 207-215.
- Belghith, A., Azzouz, S., and Elcafsi, A. 2015. Desorption isotherms and mathematical modeling of thin layer drying kinetics of tomato. *Heat and Mass Transfer*, 1-13.
- Ciarmiello, L.F., Piccirillo, P., Gerardi, C., Piro, F., De Luca, A., D'imperio, F., Rosito, V., Poltronieri, P., and Santino, A. 2013. Microwave irradiation for dry-roasting of hazelnuts and evaluation of microwave treatment on hazelnuts peeling and fatty acid oxidation. *Journal of Food Research* 2, 22.
- Demirhan, E., and Özbek, B. 2015. Color Change Kinetics of Tea Leaves During Microwave Drying. *International Journal of Food Engineering* 11, 255-263.
- Demirtas, C., Ayhan, T., and Kaygusuz, K. 1998. Drying behaviour of hazelnuts. *Journal of the Science of Food and Agriculture* 76, 559-564.
- Golpour, I., Amiri Chayjan, R., Amiri Parian, J., and Khazaei, J. 2015. Prediction of Paddy Moisture Content during Thin Layer Drying Using Machine Vision and Artificial Neural Networks. *Journal of Agricultural Science and Technology* 17, 287-298.
- Hosseinpour, A., Seifi, E., Javadi, D., Ramezanpour, S.S., and Molnar, T.J. 2013. Nut and kernel characteristics of twelve hazelnut cultivars grown in Iran. *Scientia Horticulturae* 150, 410-413.
- Kibar, H., and Öztürk, T. 2009. The effect of moisture content on the physico-mechanical properties of some hazelnut varieties. *Journal of Stored Products Research* 45, 14-18.
- Kouchakzadeh, A., and Shafeei, S. 2010. Modeling of microwave-convective drying of pistachios. *Energy conversion and management* 51, 2012-2015.

- Kumar, D., Prasad, S., and Murthy, G.S. 2014. Optimization of microwave-assisted hot air drying conditions of okra using response surface methodology. *Journal of food science and technology* *51*, 221-232.
- Lopez, A., Pique, M., Boatella, J., Parcerisa, J., Romero, A., Ferrá, A., and Garcí, J. 1997. Influence of drying conditions on the hazelnut quality. I. Lipid oxidation. *Drying technology* *15*, 965-977.
- Malekjani, N., Jafari, S.M., Rahmati, M.H., Zadeh, E.E., and Mirzaee, H. 2013. Evaluation of thin-layer drying models and artificial neural networks for describing drying kinetics of canola seed in a heat pump assisted fluidized bed dryer. *International Journal of Food Engineering* *9*, 375-384.
- Nadian, M.H., Rafiee, S., Aghbashlo, M., Hosseinpour, S., and Mohtasebi, S.S. 2015. Continuous real-time monitoring and neural network modeling of apple slices color changes during hot air drying. *Food and Bioproducts Processing* *94*, 263-274.
- Reyes, A., Ceron, S., Zuniga, R., and Moyano, P. 2007. A comparative study of microwave-assisted air drying of potato slices. *Biosystems Engineering* *98*, 310-318.
- Silva, F., Marsaioli, A., Maximo, G., Silva, M., and Goncalves, L. 2006. Microwave assisted drying of macadamia nuts. *Journal of Food Engineering* *77*, 550-558.
- Soysal, Y., Ayhan, Z., Eşturk, O., and Arıkan, M. 2009. Intermittent microwave-convective drying of red pepper: Drying kinetics, physical (colour and texture) and sensory quality. *Biosystems Engineering* *103*, 455-463.
- Wu, T., and Mao, L. 2008. Influences of hot air drying and microwave drying on nutritional and odorous properties of grass carp (*Ctenopharyngodon idellus*) filets. *Food Chemistry* *110*, 647-653.

LIFECYCLE MODELLING OF AN INNOVATIVE DURUM WHEAT DEBRANNER

Davide Marchini^(a), Roberto Montanari^(b), Eleonora Bottani^(c), Giorgia Tagliavini^(d), Simona Digiuni^(e)

^{(a),(b),(c),(d),(e)} Department of Industrial Engineering, University of Parma

^(a) davide.marchini@unipr.it, ^(b) roberto.montanari@unipr.it, ^(c) eleonora.bottani@unipr.it

ABSTRACT

Debranning is a very common technique in the grinding process of many cereals. It has the aim of removing part of the outer layers from the kernels prior to the milling process, improving production yield and product refinement. Debranning is performed using specific machines with vertical configuration. They consist of a cylindrical perforated stator and of several rotating grinding wheel arranged in series. This study focuses on the substitution of the silicon carbide grinding wheels, traditionally used in debranning systems, with innovative diamond wheels. We exploited a set of key performance indicators (KPIs) to compare the two alternatives and to develop a life-cycle model of the diamond wheels. This model allowed to obtain some important technical and economic findings, and demonstrated that diamond wheels have potential to provide more effective results compared to the traditional wheels, from both the economic and reliability perspective.

Keywords: life-cycle modeling, debranning, diamond wheels, wheat milling

1. INTRODUCTION

Wheat kernel structure, as shown in Figure 1, consists of three essential constituents: bran, endosperm and germ. Endosperm, the major constituent, contains mainly starch granules embedded in a protein matrix and accounts for 81–84% of the grain. Germ contains the embryo and the scutellum and accounts for 2–3% of the grain. Bran, which forms 14–16% of the grain, consists of all outer layers including the aleurone layer, which is usually removed along with the other bran layers during milling (MacMasters, Bradbury, & Hinton, 1964).

Debranning is a well-established technology in the processing of bracted cereals as rice, oat and barley (Dexter and Wood, 1996). This process, in fact, effectively removes only the outer hull layers of the covered grains, allowing the recovery of intact kernels that will be differently processed in successive stages. Durum wheat debranning aims to the sequential and controlled removal of the outer layers of cereal kernels to a desired level prior to milling, thus simplifying the milling process itself, since less bran remains in the kernel to be removed during milling (Mousia et al. 2004). To facilitate the separation of the outer layers, the debranning is usually preceded by humidification operations, with the addition of small amounts of water.

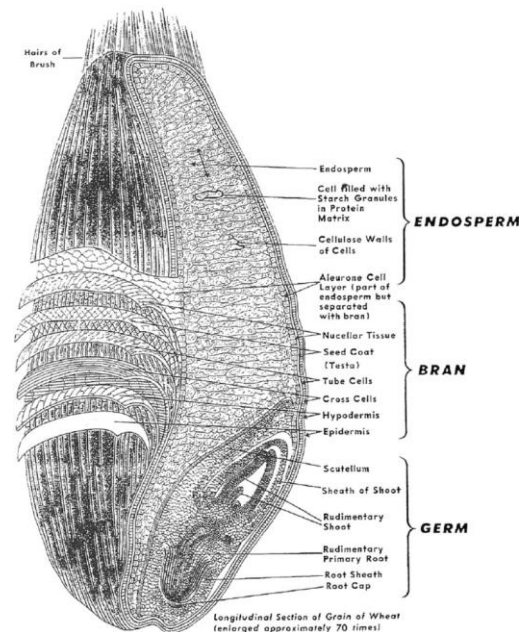


Figure 1 - Typical wheat kernel structure and composition (published on line by North America Millers' Association).

Increasing number of industrial and research studies (Dexter et al., 1994; Dexter & Sarkar 2004; Fellers, Mossman, Johnston, & Wheeler, 1976; McGee, 1995; Sekon, Singh, & Singh, 1992) reports the advantages of debranning prior to milling.

- It improves the yield and refinement of semolina in durum wheat milling, as the quantity of bran that contaminates the product will be significantly lower (Bass 1988, Dexter and Sarkar 1993);
- It ensures a higher chemical safety of the products, as the main contaminants rate is contained in the bran layers (e.g. mycotoxins) (Wilson, 2000);
- It can lower capital investment because mill flow is shortened (it needs less break and separation phases) (Dexter and Sarkar, 2004);
- It speeds up the hydration process of grain prior to the milling phase, as without the pericarp layers, the water penetration is faster and more homogeneous (Hemery et al. 2007).

Debranning is performed using particular machines with vertical configuration, consisting of a cylindrical perforated stator and of several rotating grinding wheel arranged in series. The kernels can be fed from below or above and pass through the space between the rotor and the stator. The abrasion is due to the rubbing of the grains against the walls of the machine (wheels and stator) and against other grains. Internal air pressure helps the removal of by-products through the screen (the perforated stator). As mentioned, the wheels are arranged in series vertically and can be in a variable number.

Usually, the grinding wheels are made of silicon carbide. The main limitations of this type of machine are often exactly due to the mineral nature of this material, and consequently to its poor reliability and short life-cycle. A recent technology suggests the substitution of these traditional wheels with a new kind of grinding wheels, with a thin surface deposition of synthetic diamonds on a metallic layer. The diamonds size varies with a given distribution around a particular value guaranteed by the manufacturer. This kind of modification, which could seem minimal, can lead to a longer useful-life of the device, with a more controllable process.

The aim of the study is to derive a lifecycle model that could describe the performance of diamond grinding wheels over time. Moreover, some comparisons with the silicon carbide wheels will be made, taking into account both the operational and economic points of view.

All the debranners and devices used for the tests described in this paper were provided by OCRIM S.p.A., an Italian company that acts as a world-wide leading plant producer for the milling sector. The company supported us in this study as it was interested in investigating the performance improvement achievable with the new technology, to ponder the adoption of this solution to its machines.

2. MATERIALS AND METHODS

The experimental tests were conducted partially at the Department of Industrial Engineering of the University of Parma (Italy) and partially at a production site, a Durum wheat mill sited in North Dakota (USA). The mill is equipped with two debranning machines, each one with 7 grindstone wheels. One of the debranning machines was equipped with the traditional silicon carbide package, while in the other the two lower wheels, more subjected to wear, were replaced with the innovative diamond wheels (Figure 2). This was a compromise solution: it is easy to realise that diamond wheels are more expensive than traditional ones, and then they were used only in the critical areas of the machine, for economic reasons.

The debranning rate that can be obtained is mainly a function of the power absorption of the machine. By regulating the energy absorption of the wheels, the employee can determine the product level inside the machine, and thus, at a constant global wheat flow-rate, the residence time and the debranning rate.

The evaluation of the debranning performance was carried out taking into account two KPIs, referring to the efficiency in removing bran from the kernels and to the wear over time of the wheels.

- The first KPI (KPI1) is termed “Debranning Ratio” and is computed as the ratio between the global processed mass of wheat and the relative separated mass of bran;
- The second KPI (KPI2), called “Wear Index”, is an indicator of the wear of the wheels, calculated via image analysis. A digital microscope was used to collect a sequence of pictures, from which it was possible to find out the size distribution of the diamonds and the average coverage of the surface of the wheels.



Figure 2 - 3D rendering of the grindstone package with 2 diamond wheels.

To compute the two KPIs, and to build up a life-cycle model for the new diamond wheels, we planned and implemented an important experimental campaign. A total of five measuring interventions took place at the test milling plant over a period of 26 months.

The wheels packs of the two machines were installed together in January 2014. The first measurement campaign was made immediately after the installation (2-3 days later). The second measurement was made after two months, the third one after one year (January 2015), the fourth one after 16 months and the last one after 26 months (March 2016). All the samples were collected during the normal operating cycle of the milling plant. Each intervention took three days, with two daily sampling moments, one in the morning and one in the afternoon.

2.1. KPI1: Debranning Ratio

As mentioned, KPI1 reflects the ratio between the flow-rate of the processed wheat and the flow-rate of the separated bran. To compute this indicator, we collected a series of 5 samples per sampling moment. Samples were collected by taking the bran output from the machines for

1 minute. Then, the bran was weighed and compared to the global productivity of the machine to derive the Debranning Ratio. The measurements were carried out both on the machine with the traditional wheels and on the machine with diamond wheels, at three different levels of energy absorption. At a constant flow rate, energy absorption can be assumed to be proportional to the residence time of the wheat into the debranner. Thus, during the three days of test, a total of 90 samples were collected on both the debranning lines, 30 for each energy absorption rate. This made it possible to derive statistically significant results.

2.2. KPI2: Wear Index of the wheels

The second KPI is a measure of the surface wear. It was calculated only for the innovative grindstone package with diamond wheels, in line with the fact that the analysis aims at developing a life-cycle model of this new device (while the behaviour of traditional wheels is already known and documented). As mentioned, the new grindstone package was equipped with 2 diamond wheels. In our analysis, we focused on the lower one, which is expected to be more subject to stress.

The Wear Index was calculated *via* image analysis. We took a series of pictures of the surface of the diamond wheels and analysed these by an image analysis software. The software has been specifically developed for this project from the working team of the University of Parma. We used a Dino-Lite Digital Microscope (model AD7013MT) to take the pictures, with a 50x zoom. Also in this case, data acquisitions were performed twice a day during the measurement campaign, each time taking about 100 photos on different (random) areas of the diamond wheel. An example of these pictures is proposed in Figure 3.

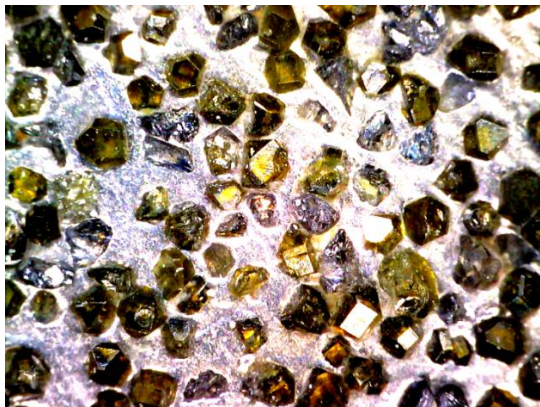


Figure 3 - Picture of the diamond wheel surface taken with digital microscope.

The software adopted is able to scan the colours of the pictures and to distinguish the diamonds from the metal surface. Therefore, it allowed to find out the size distribution of the diamonds at various time steps, as well as the diamond coverage of the wheels surface.

The KPI2 was then determined taking in consideration the average percentage amount of wheels surface covered with diamonds.

3. RESULTS AND DISCUSSION

3.1. Debranning yield over time

Figure 4 shows results for the Debranning Ratio. In this figure, the curves reflect the different power absorption levels, with both the traditional and diamond wheels. To be more precise, the red curves depict the performance of the silicon carbide wheels, while the blue ones those of the diamond wheels.

Typically, the useful life of traditional silicon carbide grinding wheels is indicated by the supplier and can be estimated in approximately 12 months, with some variations that may depend on the work load. In our experimental campaign, the traditional wheels needed to be replaced after about 14 months from the installation due to excessive wear, which led to the formation of deep cracks. This is why the relative curves span from 0 to 14 months.

Conversely, diamond wheels were still functioning after 26 months, and were replaced after 28 months (May 2016).

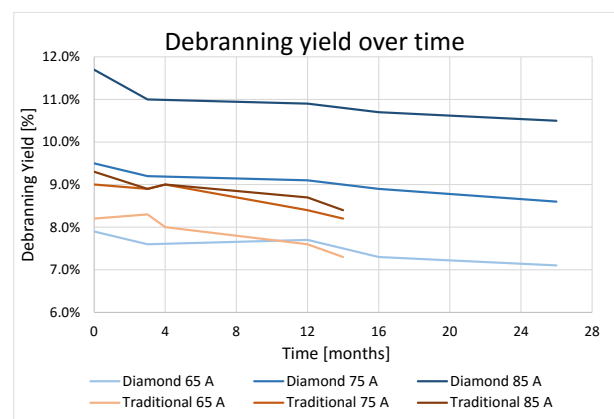


Figure 4 - Debranning ratio at different power absorption levels of the machine with traditional and diamond wheels.

Analyzing the results, it is easy to see that, no matter the device used, the debranning effectiveness immediately starts decreasing, with an almost constant rate during all life-cycle. During their life-cycle, both the silicon carbide and the diamond wheels suffered from a relative decline in the debranning yield of about 10%, reflecting the limit below which the wheat is likely to not be treated sufficiently. At this stage, the wheels need to be replaced. Figure 4 highlights some additional key points:

- At the lowest power absorption level the curves are all quite close. The traditional grindstone package has a higher initial Debranning Ratio, which however falls faster than the one of diamond wheels;
- The curves at 75 A absorption are slightly more distant, with diamond wheels showing a better performance. Also in this case the traditional package curve decrease more rapidly;

- At the highest power absorption rate, the distance between the two performances is instead very high. The diamond grinders index increase proportionally to the increase in power, while traditional wheels seem to reach a maximum effectiveness that could no longer be improved. This is probably due to the higher surface roughness of diamond wheels.

As previously mentioned, the general worsening of the performance in time is due to the surface deterioration of the wheels. Traditional grinding wheels wear out in an evident manner, with mineral material losses and changing of the wheel profile. The wear of diamond wheel is less noticeable, as there are no macroscopic damages, but nonetheless it causes loss of abrasiveness of the devices. KPI2 aims to quantify this latter point.

3.2. Diamond coverage over time

The second KPI was calculated *via* image analysis, and took into account the percentage amount of wheels surface covered with diamonds. Obviously, such a percentage will decrease in time, as a result of the progressive wear and detachment of diamonds. The decline of debranning yield can be right attributed to this phenomenon.

Experimental tests allowed us to derive the empirical curve shown in Figure 5. **L'origine riferimento non è stata trovata.** that represents the wear of diamond wheels over time. The five measurement points are highlighted in the figure. Starting from these data, a mathematical law was extrapolated.

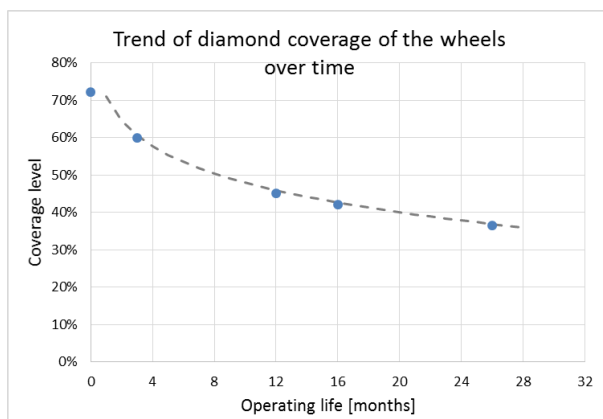


Figure 5 - Wear curve of the diamond wheels, representing the percentage of the wheel surface covered with diamonds over time.

The trend of the diamond coverage percentage in time follows an exponential law. On new wheels diamonds cover near 72% of the surface. In the first months of usage, the index reduction is higher: after 4 months the coverage level reaches 57%. Afterwards, the curve flattens progressively and after 12 months the reduction trend is almost linear. At the end of the useful life the index dropped to 36%. This means that the coverage has more than halved during the life of the grindstone package.

It emerged that the diamond coverage reduction can be caused by three main factors, i.e.:

- diamonds detachment from the metal layer;
- diamonds size reduction due to progressive erosion;
- diamonds breakage due to the frequent impacts.

3.3. Life-cycle model for the diamond debranning wheels

On the basis of the two KPIs computed, we were able to develop a life-cycle model of the diamond wheels. Such a model correlates the normalized debranning yield and the diamond coverage indicator.

To get comparable values for the various power absorption levels, the Debranning Ratio was normalized with respect to the maximum obtainable yield at a given power absorption level, which of course is always reached at the beginning of the life of the grinding wheels. Therefore, the debranning effectiveness of a grindstone package is always maximum (100%) with new wheels and decreases progressively.

After that, by means of a fitting procedure, we derived a mathematical model that correlates the normalized Debranning Ratio and the Wear Index. It is the life-cycle model of a grindstone package with diamond wheels, and represents the evolution of its operating performances with respect to its deterioration (see Figure 6). Such a model is not directly dependent on the time, meaning that it allows knowing the operating point of a grinding wheel simply by evaluating the wear, or even to predict the level of wear of a grinding wheel from the analysis of its debranning yield.

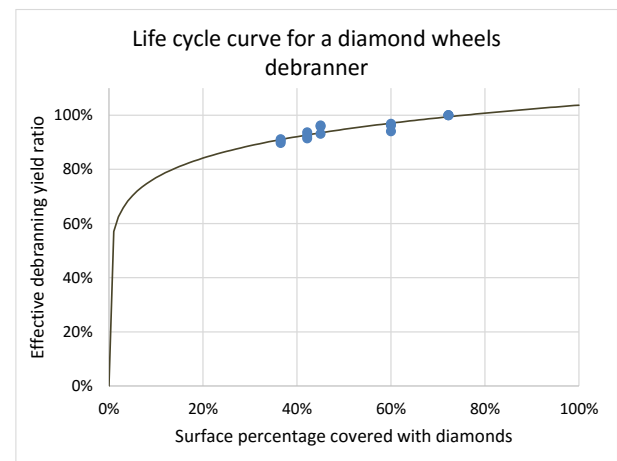


Figure 6 - Correlation between debranning yield and diamond residual coverage.

The graph in Figure 7 represents a detail of the life-cycle curve, at the higher level of Debranning Ratio. The red dotted lines represent the normalized yield limits: 100% is the new wheels condition while 90% is the limit acceptable effectiveness to have a compliant process. All the blue points are the various combination of yield and wear registered during the measurement campaign at every energy absorption level of the machine. The

continuous line represents the life-cycle model of the diamond wheels.

The mathematical equation chosen to represent the relationships between the two KPIs is a power law, shown below:

$$f(x) = ax^k \quad (1)$$

Where: $a = 1.037$
 $k = 0.130$

This equation shows a good fit with the sampling data ($R^2 = 0.834$), so the model seems to describe the samples with a good level of approximation.

When the coverage percentage reaches 0, the wheels have no action on the kernels. Then, it quickly rises up and it reaches an almost asymptotic trend at high levels of coverage.

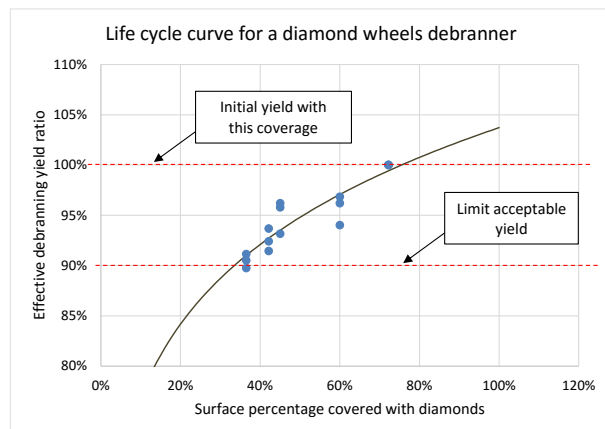


Figure 7 - Correlation between debranning yield and diamond residual coverage (detail of the curve).

With a coverage level higher than the one of the new wheels (72%), the model assumes a higher debranning yield, above 100%. However, the yield increase is modest, meaning that the abrasiveness of the devices does not significantly increase over the current coverage level. If reaching an ideal 100% coverage, the maximum yield would be only 3.7% greater than the current one.

4. CONCLUSIONS

The aim of the present work was to develop a life-cycle model for an innovative diamond grindstone wheels for wheat debranning. On the basis of the data collected through an extensive experimental campaign, we derived a mathematical model able to correctly describe the deterioration suffered by the grinding wheels during their useful life. The model allowed to obtain some important technical and economic conclusions on the diamond wheels compared to the traditional ones.

Traditional silicon carbide wheels, as previously mentioned, have an average useful life of about 1 year, which can vary as a function of the processed product. Moreover, their time to fail has a very relevant variability.

Innovative diamond wheels, instead, have a useful life of 26 to 30 months, with a much more controllable wear process, resulting in higher reliability. The data collected show a slower decrease of the debranning yield over time using diamond wheels compared to the traditional ones. The developed model shows good accuracy in predicting the relationship between the two fundamental parameters that characterize the debranning process. By means of a simple analysis of the diamond wheel surface, the model allows to understand at what point in its life cycle it is, and what level of yield would be expected.

Future developments of this work might include the economic analysis of the two different solutions: as the investment required to build the innovative wheels is higher, it is essential to determine a payback point for this technology. Such a payback would be useful to identify the minimum duration of the diamond wheels that makes them preferable to the traditional ones from an economic point of view.

REFERENCES

- Bass, E.J., 1988. Wheat flour milling. In Pomeranz, Y. (ed.), *Wheat: chemistry and technology* (3rd ed.). St. Paul, MN: American Association of Cereal Chemists, 1–68.
- Dexter, J.E. and Sarkar, A.K., 1993. FLUOR | Roller Milling Operations. *Encyclopedia of Food Science, Food Technology and Nutrition*. Academic Press, New York, 1993.
- Dexter, J.E. and Sarkar, A.K., 2004. Wheat - Dry Milling. In: Wrigley, C., Corke, H. and Walker, C., *Encyclopedia of Grain Science*. Oxford: Elsevier.
- Dexter, J.E., Martin, D.G., Sadaranganey, G.T., Michaelides, J., Mathieson, N., Tkac, J.J., and Marchylo, B.A., 1994. Preprocessing – Effects on durum-wheat milling and spaghetti-making quality. *Cereal Chemistry*, 71(1), 10-16.
- Dexter, J.E., & Wood, P.J., 1996. Recent applications of debranning of wheat before milling. *Trends in Food Science & Technology*, 7, 35–41.
- Fellers, D.A., Mossman, A.P., Johnston, P.H., & Wheeler, E.L., 1976. Mechanical debranning of whole-kernel wheat. III Composition, cooking characteristics and storage stability. *Cereal Chemistry*, 53(3), 308–317.
- Hemery, Y., Rouan, X., Lullien-Pellerin, V., Barron, C., Abecassis, J., 2007. Dry processes to develop wheat fractions and products with enhanced nutritional quality. *Journal of Cereal Science*, 46, 247-327.
- MacMasters, M.M, Bradbury, D., & Hinton, J.J.C., 1964. Microscopic structure and composition of the wheat kernel. In Hlynka, I. (Ed.), *Wheat: Chemistry and technology* (3rd ed.). St. Paul, MN: American Association of Cereal Chemists, 55–110.
- McGee, B.C. (1995). The Peritec process and its application to durum wheat milling. *Association of Operators and Millers Bulletin*, 6521–6528.
- Mousia, Z., Edherly, S., Pandiella, S.S., Webb, C., 2004. Effect of wheat pearling on flour quality. *Food Research International*, 37, 449-459.

Sekon, K.S., Singh, N., & Singh, R.P., 1992. Studies on the improvement of quality of wheat Infected with karnal bunt. I. Milling, rheological and baking properties. *Cereal Chemistry*, 69(1), 50–54.

Wilson, E., 2000. Debranning wheat: Debranning offers opportunities for adding value to wheat milling. *World-Grain.com*, 10/01/2000.

AUTHORS BIOGRAPHY

Davide Marchini is a scholarship holder in Industrial Engineering at the University of Parma (Department of Engineering and Architecture. He got a master degree in Mechanical Engineering for the Food Industry in 2011. His research interests are in the field of food processing and plant design. He presented his works in many international conferences, including two Modelling and Applied Simulation (MAS) International Conference editions (2013 & 2014). In 2013 his work titled “*Advanced design of industrial mixers for fluid foods using computational fluid dynamics*” was awarded as the best paper of MAS 2013 conference.

Eleonora Bottani is Associate professor of Industrial Logistics at the Department of Industrial Engineering of the University of Parma. She graduated (with distinction) in Industrial Engineering and Management in 2002, and got her Ph.D. in Industrial Engineering in 2006, both at the University of Parma. Her research interests are in the field of logistics and supply chain management. She is the coordinator of a national project, called ESCALATE (Economic and environmental Sustainability of Supply Chain and Logistics with Advanced Technologies) related to supply chain sustainability. She is author (or co-author) of approx. 120 scientific papers, referee for more than 60 international scientific journals, editorial board member of five scientific journals, Associate Editor for one of those journals, and Editor-in-chief of a scientific journal.

Roberto Montanari is Full professor of Mechanical Plants at the University of Parma. He graduated (with distinction) in 1999 in Mechanical Engineering at the University of Parma. His research activities mainly concern equipment maintenance, power plants, food plants, logistics, supply chain management, supply chain modelling and simulation, inventory management. He has published his research in approx. 70 papers, which appear in qualified international journals and conferences. He acts as a referee for several scientific journals, is editorial board member of 2 international scientific journals and editor of a scientific journal.

Giorgia Tagliavini is a Research Assistant at the Department of Industrial Engineering at the University of Parma, where she graduated in Mechanical Engineering in March 2015. Her research activities focus mainly on CFD simulation and process modeling of Industrial and Food Engineering processes.

Simona Digiuni is a postdoctoral fellow at the Department of Industrial Engineering of the University of Parma, Italy. She graduated in Agricultural Biotechnology in 2002 from the University of Milano. After obtaining a PhD in Natural Sciences from the University of Cologne in Germany, she moved to US at the Genome Center at UC Davis. Her research continued focusing on plant biomechanics at the ENS of Lyon. During her career, she collaborated with mathematicians, bioinformaticians, physicists and engineers to work on a multidisciplinary approach to plant research.



CFD SIMULATION OF A CO-ROTATING TWIN-SCREW EXTRUDER: VALIDATION OF A RHEOLOGICAL MODEL FOR A STARCH-BASED DOUGH FOR SNACK FOOD

Giorgia Tagliavini^(a), Federico Solari^(b), Roberto Montanari^(c)

^(a) CIPACK Interdepartmental Center, University of Parma – Parco Area delle Scienze, 43124 Parma (Italy)

^{(b), (c)} Department of Industrial Engineering, University of Parma – Parco Area delle Scienze, 43124 Parma (Italy)

^(a)giorgia.tagliavini@unipr.it, ^(b)federico.solari@unipr.it, ^(c)roberto.montanari@unipr.it

ABSTRACT

The extrusion of starch-based products has been a matter of interest, especially for the pasta and snack food production. In recent years, twin-screw extruders for snack food were studied from both structural and fluid dynamics viewpoints.

This project started from the rheological characterization of a starch-based dough (corn 34wt%, tapioca 32wt%), comparing viscosity values acquired in laboratory with different theoretical models found in literature.

A CFD simulation recreating the simple case of a fluid flow between two parallel plates was carried out in order to validate the former comparison. After the rheological characterization was completed, the second phase of this work covered a 3D CFD simulation of the first part of the twin-screw extruder (feeding zone).

The objective was to find a suitable model for describing the dough rheological behavior and the operating conditions of a co-rotating intermeshing twin-screw extruder.

Once the model would be design, it would allow to investigate several working conditions and different screws geometries of the machine, predicting the evolution of the product rheological properties.

Keywords: twin-screw extruders, starch-based dough, computational fluid-dynamics, rheological model

1. INTRODUCTION

In the food industry, the extrusion of starch-based doughs has been widely studied.

One of these doughs main features is the non-Newtonian behavior, which is characterized by changes in the rheological properties depending on the undergoing process (Pessini, 2001). These rheological changes are affected by temperature, shear stress and shear rate (Lagarrigue & Alvarez, 2001), moisture content (Rao et al., 1997) and other occurring substances inside the dough (Xei et al., 2009; Jamilah et al., 2009).

All these factors are thus crucial in terms of obtaining the desired product.

Extrusion is a technique employed for quite some time especially in the food industry. It consists in the conveying of high viscosity fluids by increasing the pressure from the hopper towards the extruder die. Extruders can be divided in three key zones: a feeding zone, a plasticization zone and a metering zone (as shown in Figure 1).

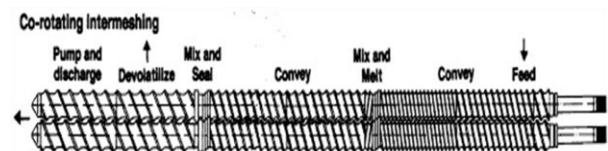


Figure 1: Simplified scheme of a co-rotating intermeshing twin-screw extruder (modified from: <http://plastictechnologies.blogspot.de>).

The extruder may also be a single- or twin-screw: in the latter, the two parallel screws can co-rotate or counter-rotate, according to the pressure needed (Messori 2005). A co-rotating twin-screw extruder provides a more accurate regulation on the process and a higher range of shear stresses (and of shear rate as a result).

In the food industry the main goal is to achieve a smooth and homogeneous products, reason why twin-screw extruders are preferred over single-screw ones.

Nevertheless, inside twin-screw extruders, it is more complicated to evaluate the fluid dynamics behavior and the share rate distributions. For this reason, fluid dynamics simulations are essential especially in the design phase.

In the last decade, twin-screw extruders for snack food were studied from both structural (with finite element method) and fluid-dynamics (with CFD simulations) perspectives (Yamsaengsung et al., 2010; Fabbri et al., 2012; Cubeddu et al., 2014; Bertrand et al., 2003).

Computational fluid dynamics (CFD) has been gaining highlights in recent years for predicting fluid dynamic behavior for a wide range of industrial processes.

The objective of this work is the rheological characterization of a starch dough for snack food and the design of a CFD model with ANSYS FLUENT 17.0 of a twin-screw extruder first section (feeding zone).

2. MATERIALS AND METHODS

2.1. Data collection

The first step of this work started with laboratory measurements, collecting the viscosity data of the product at known shear rates.

The instrumentation used for the data collection consisted in a Brookfield Engineering RST Controlled Stress Rheometer (RST-CC Coaxial Cylinder model). The rheometer and the spindle technical specifications are listed in Table 1 and Table 2.

Table 1: RST-CC rheometer technical specifications.

Viscosity Range [Pa·s]	0.00005 – 5.41M
Speed [rpm]	0.01 – 1.3K
Max. Torque [mNm]	100
Torque Res. [μNm]	0.15

Table 2: CCT-25 spindle technical specifications.

Viscosity Range [Pa·s]	0.002 – 177K
Shear Rate [s ⁻¹]	0.013 – 1.67K
Max. Shear Stress [Pa]	2.28K
Sample Volume [mL]	16.8

The viscosity values and the associated shear rates collected during the laboratory campaign are shown in Table 3.

Table 3: Collected data from laboratory tests.

Shear Rate [s ⁻¹]	Viscosity [Pa·s]
4.5	0.171
7.47	0.167
12.51	0.158
20.88	0.137
40.77	0.115
58.05	0.104

2.2. Rheological models

The next step was the rheological characterization of the starch (corn 34wt%, tapioca 32wt%) dough.

As mentioned before, one of this doughs main features is the non-Newtonian behavior, which implies changes in the rheological properties, depending on the extrusion conditions.

For Newtonian fluids, the shear stress is described by Equation 1, as a function of the rate-of-deformation tensor $\overline{\overline{D}}$:

$$\overline{\overline{\tau}} = \mu \overline{\overline{D}} \quad (1)$$

where μ is the viscosity, which is independent of $\overline{\overline{D}}$. $\overline{\overline{D}}$ is defined by Equation 2 as:

$$\overline{\overline{D}} = \left(\frac{\partial u_j}{\partial x_i} + \frac{\partial u_i}{\partial x_j} \right) \quad (2)$$

where u and x are the velocity and the coordinate respectively.

The situation is different when it comes to non-Newtonian fluids. In this case, there is a dependence between the viscosity η (non-Newtonian viscosity) and the rate-of-deformation tensor $\overline{\overline{D}}$ (Equation 3):

$$\overline{\overline{\tau}} = \eta(\overline{\overline{D}}) \overline{\overline{D}} \quad (3)$$

In relation to this study case, the viscosity η depends only on the shear rate $\dot{\gamma}$, which is related to the tensor $\overline{\overline{D}}$ according to the following equation:

$$\dot{\gamma} = \sqrt{\frac{1}{2} \overline{\overline{D}} : \overline{\overline{D}}} \quad (4)$$

For simplification purposes, the temperature effects on viscosity were omitted at this first stages.

The related terms will, therefore, not be shown in the following equations.

An extensive bibliographic research revealed that the most commonly used models for describing starch-based fluids are the non-Newtonian Power Law, the Carreau and the Cross model (Emin & Schuchmann, 2012).

The governing equations of the models mentioned above are described below, in accordance with the formulation presented in the ANSYS FLUENT *Theory Guide* (Ansys, Inc., 2009).

2.2.1. Power Law for non-Newtonian Viscosity

A non-Newtonian flow is modeled with Equation 5, according to the power law for the non-Newtonian viscosity:

$$\eta = K \dot{\gamma}^{n-1} \quad (5)$$

where K is the consistency index, n is the power law index, a measure of the average viscosity of the fluid and a measure of the fluid deviation from Newtonian behavior respectively, which determines the fluid class:

- $n = 1 \rightarrow$ Newtonian fluid;
- $n > 1 \rightarrow$ shear-thickening (dilatant fluid);
- $n < 1 \rightarrow$ shear-thinning (pseudo-plastic).

2.2.2. The Carreau Model for pseudo-plastics

The power law model described in Equation 5 results in a fluid viscosity that varies with shear rate.

The Carreau model attempts to describe a wide range of fluids thanks to a curve-fit, which synthesizes functions for both Newtonian and shear-thinning non-Newtonian laws. In the Carreau model, the viscosity is:

$$\eta = \eta_{\infty} + (\eta_0 - \eta_{\infty}) [1 + \dot{\gamma}^2 \lambda^2]^{(n-1)/2} \quad (6)$$

where the parameters n , λ , η_0 and η_{∞} depend upon the fluid. λ is the time constant, n is the power law index, η_0 and η_{∞} are respectively the zero- and the infinite- shear viscosities. The viscosity is limited by η_0 for $\dot{\gamma} \rightarrow 0$ and by η_{∞} for $\dot{\gamma} \rightarrow \infty$.

2.2.3. The Cross Model

The Cross model for viscosity is:

$$\eta = \frac{\eta_0}{1 + (\lambda \dot{\gamma})^{1-n}} \quad (7).$$

η_0 is the zero-shear viscosity, λ is the natural time (i.e., inverse of the shear rate at which the fluid changes from Newtonian to power-law behavior) and n is the power law index.

2.3. Data processing and analysis

The data were processed with Microsoft Office Excel 2013.

The experimental viscosities were used to derive the coefficients of the rheological models by minimizing the mean squared error between the experimental results and those obtained using Equations 5, 6 and 7.

Then the coefficient of determination R^2 was estimated. This was a fundamental step for the continuation of the study, since the coefficients values are required by the CFD simulation software for the fluid characterization. The results are shown in Tables 4 and 5 and Figure 3.

Table 4: Viscosity values.

Viscosity [Pa·s]			
Lab tests	Power Law	Carreau	Cross
0.171	0.179	0.172	0.173
0.167	0.163	0.166	0.165
0.158	0.148	0.155	0.154
0.137	0.134	0.139	0.140
0.115	0.118	0.115	0.116
0.104	0.110	0.103	0.102

Table 5: Coefficients and R^2 values.

	Power Law	Carreau	Cross
K	0.239		
n	0.809	0.635	0.129
λ		0.083	0.014
η_0		0.176	0.189
η_{∞}		0.011	
R^2	0.936	0.997	0.991

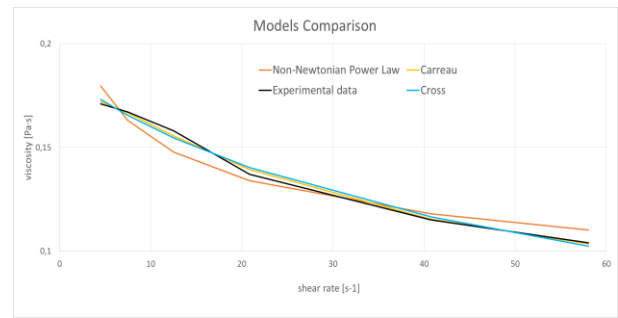


Figure 2: Models comparison from the Microsoft Office Excel elaboration.

3. CFD SIMULATION FOR RHEOLOGICAL MODELS VALIDATION

A CFD simulation was helpful to identify the most suitable rheological model among the ones mentioned previously. A 2D geometry was implemented in ANSYS FLUENT, recreating the simple case of a fluid flow between two fixed, parallel plates.

Figure 3 shows a detail of the 2D fluid domain used in the simulation.



Figure 3: 2D computational domain with inlet velocity.

The length, in particular, was extended at 5 m to get a fully-developed flow inside the duct.

The domain sizes are presented in Table 6, while Table 7 lists the mesh specification.

Table 6: Domain sizes.

	Size [m]
Height (D)	0.1
Length (L)	5

The duct was decomposed with ANSYS MESHING, according to the Finite Element Method.

Table 7 lists the mesh specifications.

Table 7: Mesh specifications.

Element Type	Quadrilaterals
Num. Elements	5240
Num. Nodes	5523
Min. Size	0.0025 m
Max. Size	0.498 m
Max. Face Size	0.249 m
Wall Edge Sizing	Num. of division: 250
Inlet/Outlet Edge Sizing	Num. of division: 20

Three different simulations (one for each rheological model) was carried out in ANSYS FLUENT 17.0 with stationary operating conditions.

The inlet velocity was fixed at 2.5 m/s and the atmospheric pressure was set at the outlet.

For the fluid characterization, the software requires the coefficients of the chosen model and the density. The models' coefficients and a density of 588.94 kg/m^3 were implemented in the simulator.

The fluid flow was set as laminar, due to the high viscosity of the product.

3.1. Results

The aim of this phase was finding the model that best fits the experimental data.

First the viscosity values were observed with the contour using CFD-Post software.

The results are shown in Figures 4 and 5.

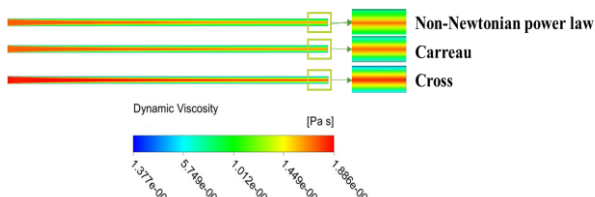


Figure 4: Dynamic viscosity contour comparison between rheological models.

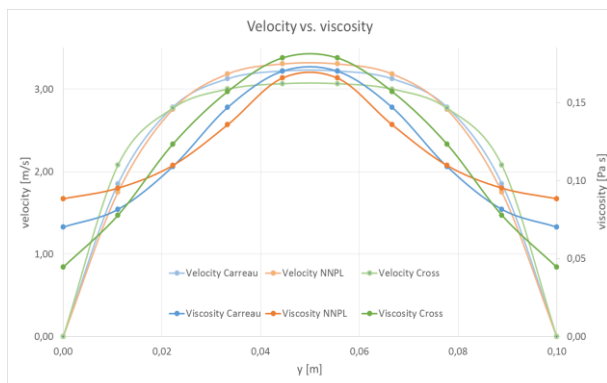


Figure 5: Comparative graph with velocity and viscosity values for different rheological model, depending upon duct height.

The profiles shown in Figure 5 are dependent upon the domain height and reveal how well each model reproduce the fluid behavior in terms of velocity and viscosity.

Afterwards, the viscosity values were plotted as a function of the shear rate together with the experimental data. The shear rate was solved taking the derivative of the velocity in ∂y .

This approach allows to see which model implemented in the software would be more accurate.

Finally, the viscosities were put together in the same graph as a function of $\partial v/\partial y \text{ [s}^{-1}\text{]}$.

Figure 6 illustrates the results.

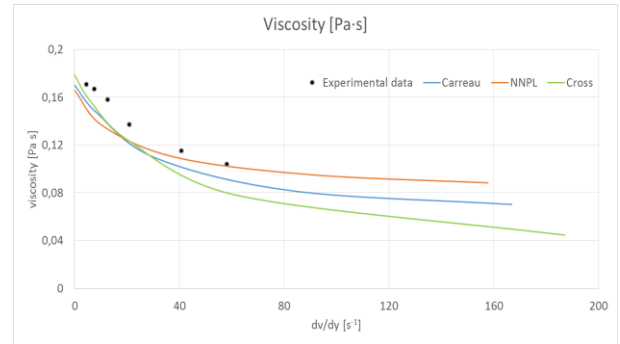


Figure 6: Comparison between the viscosity simulation and experimental data as a function of shear rate.

The values reveal that the most suitable model was the Carreau one.

The non-Newtonian Power Law marks the experimental data quite well, while the Cross model was the less appropriate.

4. CFD SIMULATION OF THE TWIN-SCREW EXTRUDER

The second phase of the study began with 3D modeling of the twin-screw extruder (feeding zone section).

The geometry reproduced the layout of the extruder's first section of the pilot plant, on which the experimental tests will be carried out to collect a further amount of data for future validation.

Figure 7 shows the size of the model and Figure 8 depicts the 3D geometry.

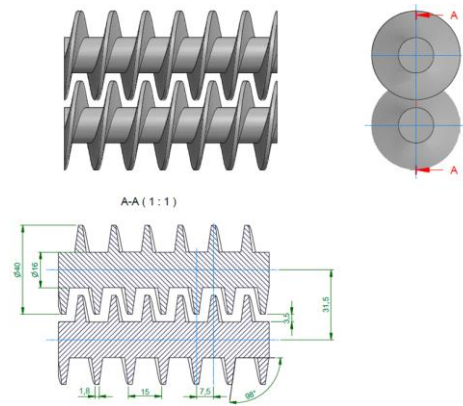


Figure 7: Extruder sizes in (m).



Figure 8: 3D geometry of the twin-screw extruder implemented in ANSYS FLUENT 17.0.

The designed geometry defining the computational fluid volume was decomposed with ANSYS MESHING, according to the Finite Element Method.

Special attention was paid to the creation of the mesh, in order to have accurate information about fluid dynamic behavior in near-wall regions and in leakage areas. Actually, there are narrow gaps between the screws and between the screw threads and the barrel. Hence, an inflated mesh is required in those areas to prevent the lack of details during the calculation.

Furthermore, a dedicated mesh was generated for the boundary layer in connection with the solid parts (barrel and screws walls).

Table 8 and Figure 9 show the mesh structure and specifications.

Table 8: Extruder mesh specifications.

Element type	Volume: tetrahedrons Boundary: quadrilaterals
Num. Elements	2721599
Num. Nodes	9259878
Min. Size	$8 \cdot 10^{-5}$ m
Max. Size	$1 \cdot 10^{-3}$ m
Max. Face Size	$1 \cdot 10^{-3}$ m
Inflation (boundary layer)	Total thickness Num. of layers: 4 Max thickness: $1 \cdot 10^{-4}$ m
Threads sizing	$2 \cdot 10^{-4}$ m
Screw sizing	$6 \cdot 10^{-4}$ m
Barrel sizing	$8 \cdot 10^{-4}$ m
Edge sizing	$4 \cdot 10^{-4}$ m

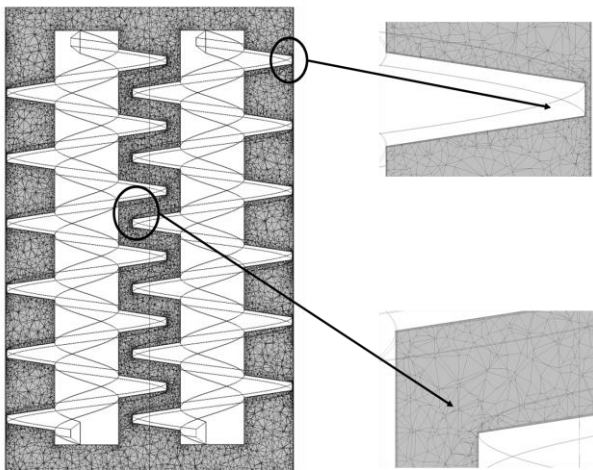


Figure 9: Mesh structure with details of near-wall region and leakage areas.

The simulation was carried out in a transient state to stress the influence of the screw rotation on the flow behavior. The fluid parameters are those used in the 2D simulation, i.e. the Carreau model and the laminar flow regime.

The atmospheric pressure was set at the inlet, so that the fluid flow would be influenced solely by the screw rotation. A sharp restriction at the outlet cross-section (not shown in Figure 8) was imposed to reproduce the pressure drop caused by the machine consecutive sectors.

To impose the angular velocity of 370 rpm a UDF in C language was created and compiled inside ANSYS FLUENT.

To recreate the screws rotation the dynamic mesh option was chosen. This method allows to subdivide the mesh motion zones, remeshing zones and static zones. The remeshing zone, precisely, are the areas where the mesh is rebuilt following the solid parts rotation step by step during the calculation.

In the present case, before starting to create the dynamic mesh zones, the fluid domain was split into several parts. Specifically, the boundary layers related to the screws and the barrel walls was separated from the rest of the fluid domain.

In this way the fluid volume was divided into 4 regions. The areas created by the dynamic mesh are illustrated in Table 9.

The term “*rigid body*” specifies the moving zones, “*deforming*” the zones affected by the remeshing process and “*stationary*” the fixed zones, not subjected to remeshing.

Table 9: Dynamic mesh zones.

Screws	Rigid body
Screws boundary layer	Rigid body
Barrel wall	Stationary
Barrel wall boundary layer	Stationary
Inlet	Stationary
Inlet boundary layer	Stationary
Outlet	Stationary
Outlet boundary layer	Stationary
Extruder interior	Deforming

Therefore, the dynamic mesh allows the various boundary layers to move together with its corresponding wall, so as to facilitate the remeshing operation and confine it to tetrahedral elements, which are easier to manage.

The simulation time was chosen in accordance with the real dough’s residence time inside the machine.

4.1. Results

Once the simulations ended, velocity and viscosity values were observed.

The velocity vectors (Figure 10) show how the product is conveyed only by the screws’ rotation. This agrees with the real case and with the boundary conditions entered in the software.

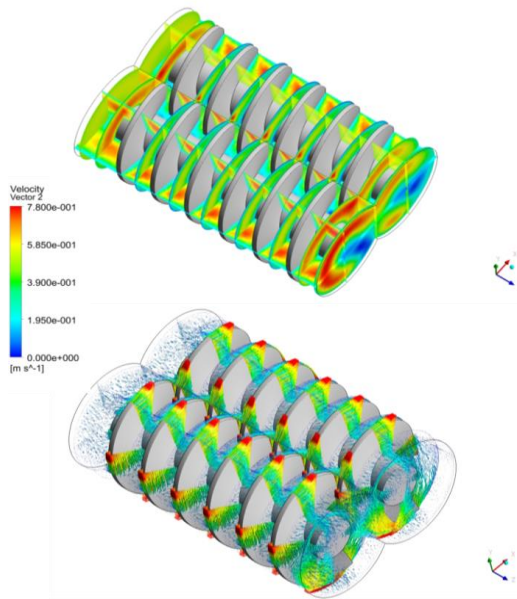


Figure 10: Velocity module and vectors. The fluid flows along the z-positive direction.

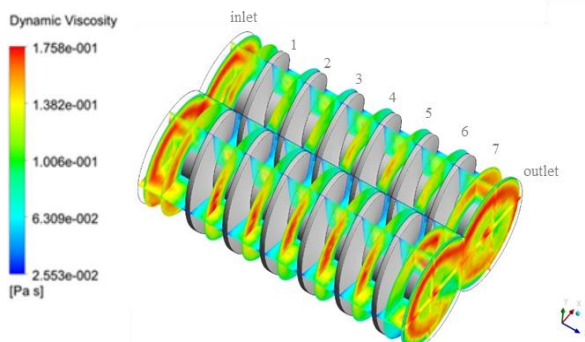


Figure 11: Viscosity contour.

Observing values of the dynamic viscosity in Figure 11, it is evident how they agree with the ones found in Table 4, for the laboratory results.

In Figure 11 the sampling sections are shown, from which the viscosity values were calculated as reported in the graph in Figure 12.

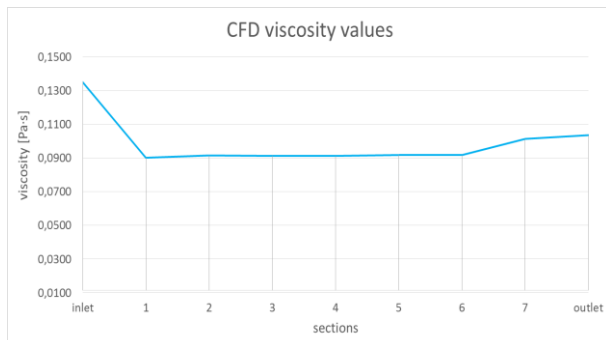


Figure 12: Viscosity values as function of the sampling sections.

5. CONCLUSIONS

This work has both the objective to find a rheological model for a corn and tapioca dough used for snack food and design a 3D computational model, which could recreate the operating conditions of a co-rotating twin-screw extruder.

A set of viscosity values was obtained experimentally at specific shear rates.

The experimental data were then compared with the theoretical viscosity from non-Newtonian Power Law, Carreau and Cross models, which equations are often used for describing non-Newtonian fluid behavior.

To find which model was the most suitable, a simple 2D geometry of two parallel flat planes was created. Three simulations were carried out with this geometry and it turned out that the Carreau model was the one that best reproduced the trend of the experimental values.

Furthermore, the operating condition of the twin-screw extruder were simulated using the Carreau model for describing the flow behavior.

The viscosity values from this simulation were plotted as a function of chosen sampling sections.

The next step of this project will be the CFD model validation thanks to an experimental campaign on a scaled pilot plant, which is now under construction. This campaign will contemplate the viscosity evaluation in each sampling section identified during the computational analysis.

Once the validation will be done, the CFD model could be used for studying different screws geometries to find which configuration provides the best results in terms of product quality.

ACKNOWLEDGMENTS

This work is partly supported by “POR-FESR 2014-2020, Emilia-Romagna Region, Asse 1: Ricerca e Innovazione - Bando per progetti di ricerca industriale strategica rivolti agli ambiti prioritari della Strategia di Specializzazione Intelligente - Progetto: Nuovi paradigmi per la progettazione, costruzione ed il funzionamento di macchine e impianti per l'industria alimentare”.

REFERENCES

- Ansys, Inc, (2009), Ansys Fluent Theory Guide. Chapter 8, Paragraph 4.5.
- Bertrand, F., Thibault, F., Delamare, L., & Tanguy, P. A. (2003). Adaptive finite element simulations of fluid flow in twin-screw extruders. *Computers & Chemical*, 27, 491–500.
- Cubeddu, A., Rauh, C., & Delgado, A. (2014). 3D Thermo-Fluid Dynamic Simulations of High-Speed-Extruded Starch Based Products. *Open Journal of Fluid Dynamics*, 04(01), 103–114.
- Emin, M. a., & Schuchmann, H. P. (2012). Analysis of the dispersive mixing efficiency in a twin-screw extrusion processing of starch based matrix. *Journal of Food Engineering*, 115(1), 132–143.

- Fabbri, A., Angioloni, A., Di Stefano, A., Fava, E., Guarnieri, A., & Lorenzini, G. (2012). Preliminary Investigation of Pasta Extrusion Process: Rheological Characterization of Semolina Dough. *Journal of Agricultural Engineering*, 38(2), 21–24.
- Jamilah, B., Mohamed, A., Abbas, K. a., Abdul Rahman, R., Karim, R., & Hashim, D. M. (2009). Protein-starch interaction and their effect on thermal and rheological characteristics of a food system: A review. *Journal of Food, Agriculture and Environment*, 7(2), 169–174.
- Lagarrigue, S., & Alvarez, G. (2001). The rheology of starch dispersions at high temperatures and high shear rates: A review. *Journal of Food Engineering*, 50(4), 189–202.
- Messori, M. (2005). *Tecnologie di Trasformazione dei Materiali Polimerici: Estrusione ed applicazione dell'estrusione. Stampaggio ad iniezione Soffiaggio di corpi cavi*, 8(I).
- Peressini, D. (2001). Evaluation methods of dough rheological properties. *Tecnica Molitoria*.
- Rao, M. A., Okechukwu, P. E., Da Silva, P. M. S., & Oliveira, J. C. (1997). Rheological behavior of heated starch dispersions in excess water: role of starch granule. *Carbohydrate Polymers*, 33(4), 273–283.
- Xie, F., Yu, L., Su, B., Liu, P., Wang, J., Liu, H., & Chen, L. (2009). Rheological properties of starches with different amylose/amylopectin ratios. *Journal of Cereal Science*, 49(3), 371–377.
- Yamsaengsung, R., Noomuang, C., Law, H., Law, B., Law, B., Law, C., Extruder, a S. S. (2010). Finite Element Modeling for the Design of a Single-Screw Extruder for Starch-Based Snack Products. *Engineering*, III, 8–11.

Roberto MONTANARI is a Full professor of Mechanical Plants at the University of Parma. He graduated (with distinction) in 1999 in Mechanical Engineering at the University of Parma. His research activities mainly concern equipment maintenance, power plants, food plants, logistics, supply chain management, supply chain modelling and simulation, inventory management. He has published his research in approx. 70 papers, which appear in qualified international journals and conferences. He acts, as a referee, for several scientific journals, is editorial board member of two international scientific journals and editor of a scientific journal.

AUTHORS BIOGRAPHY

Giorgia TAGLIAVINI is a Research Assistant at the Department of Industrial Engineering at the University of Parma, where she graduated in Mechanical Engineering in March 2015. Her research activities focus mainly on CFD simulation and process modeling of Industrial and Food Engineering processes.

Federico SOLARI is a PhD in Industrial Engineering at the University of Parma, from where he got a Master degree in Food Industry Mechanical Engineering, discussing a thesis related to the design of a plant for the volatile compounds extraction. He achieved his PhD with a thesis entitled “Advanced approach to the design of industrial plants by means of computational fluid dynamics”. He attended several conferences related to food process, modelling and simulation. He published several papers on the same topics on international journal and conferences.

MODELLING AND SIMULATION OF NITROGEN INJECTION IN VEGETABLE OLIVE OIL

Filippo Ferrari^(a), Simone Spanu^(b), Giuseppe Vignali^(c)

^{(a), (c)} Department of Industrial Engineering, University of Parma, Parco Area delle Scienze 181/A, 43124 Parma (Italy)

^(b) CERIT Center, University of Parma, Parco Area delle Scienze 181/A, 43124 Parma (Italy)

^(a) filippo.ferrari5@studenti.unipr.it, ^(b) simone.spanu@nemo.unipr.it, ^(c) giuseppe.vignali@unipr.it

ABSTRACT

The aim of this work is to analyze, by means of a CFD analysis, the injection of gaseous Nitrogen (N_2) in vegetable oil.

This process, called sparging, is important to enhance oil shelf-life, because it allows to separate by stripping the Oxygen (O_2) dissolved in the product. In fact, when the tank filling begins, N_2 bubbles start to rise towards the free surface of the product, dragging along with themselves part of the dissolved O_2 . In this way the probability of initiation of oxidative reactions is reduced and, consequently, is reduced also the possibility of oil degradation.

The final goal of this work is to compare different sparger configurations and observe how they influence the stripping process during the tank filling phase.

The various configurations have been compared in terms of O_2 residual inside the tank at the end of the filling phase. The simulations still need to be experimentally validated.

Keywords: CFD, Vegetable Oil, Modified Atmosphere, Gas Flushing

1. INTRODUCTION

In the vegetable oils sector, keeping under control the aging process of the product is of particular importance to, because it can significantly influence the final quality of the sale unit. In fact, during aging, vegetable oils are subject to a process of degradation due to fats rancidity. This phenomenon affects the organoleptic characteristics of the product, but not its hygienic stability, as the vegetable oils have a very low water activity (a_w) and are hardly subject to microbial growth (Gunstone, 2011). For these reasons, no aseptic conditions must be maintained and only a clean filling technology is required. For the same reasons and due to the low resistance to the high temperatures, hot-filling technology is not admitted (Manfredi and Vignali, 2015)

One of the process phases that contributes more to the product degradation is storage. In this case, fats rancidity is mainly due to four factors (Choe and Min, 2006):

1. exposure to high conservation temperature (usually the maximum storage temperature is

- of 25°C, except for palm oil, which tends to solidify at room temperature (Shahidi, 2005));
2. exposure to light: low wavelength radiation (and thus high energy radiation) increase the probability of fat rancidity;
3. time: higher is the storage period higher will be the probability of fats rancidity;
4. exposure to Oxygen (O_2), since rancidity is due to the formation of free radicals and to the absorption of O_2 by fatty acids, especially unsaturated ones.

The first three factors are easily controlled: to avoid exposure to light and to high temperature is sufficient to keep the product in thermo-stated stainless steel tanks, while to avoid an excessively long storage period is sufficient a proper management of the oil purchasing process.

In order to minimize exposure to O_2 , instead, three main techniques are adopted: minimization of tank head space, blanketing and sparging.

In the first case, when oil level has decreased under a certain limit, the product is moved to a lower-capacity tank, in order to keep head space minimized, and so on until stock exhaustion. When blanketing is applied, instead, the tank head space is filled with gaseous Nitrogen (N_2), or with a different inert gas, so to avoid the contact between oil and atmospheric O_2 during the entire period of storage. Finally, sparging process consists in injecting gaseous N_2 in the vegetable oil stream, thus, in this case, N_2 is directly mixed to the product. The goal of this treatment is to supersaturate vegetable oil with N_2 . In this way, when the product starts to fill the tank, the previously injected gas is released through the oil free surface, pushing out the air and occupying the tank headspace. In some cases, blanketing and sparging are adopted simultaneously, saturating the tank with N_2 before the beginning of the tank filling phase, so to avoid the contact between oil and O_2 also during filling (Shahidi, 2005).

Compared to blanketing, sparging process has more advantages. When, during the tank filling phase, N_2 bubbles start to rise towards the free surface, they drag along with themselves part of the O_2 dissolved in the product (Masella et al., 2010). This contributes in reducing the vegetable oil alteration since, usually, there

can be a maximum of 36 mg/l of dissolved O₂ in the product (Parenti et al., 2007.).

As already proposed in other food sectors, in the case the process is hardly visible and experimental tests do not give sufficient information, a Computational Fluid Dynamics (CFD) approach can be used. As already shown in other works using multiphase flows (Spanu and Vignali, in press; Mosna and Vignali, 2015; Bottani et al, 2014), the advantages of using CFD are consistent and very affordable.

Based on these premises, the aim of this work is to adopt Computational Fluid Dynamics (CFD) to assess the efficacy of the N₂ sparging process in removing the O₂ dissolved in the oil. In particular, some different geometrical configuration of the duct in which is inserted the sparger will be analyzed, to check how a different geometry can influence the distribution of N₂ within the vegetable oil flow and, consequently, the removal of dissolved O₂.

2. MATERIALS AND METHODS

The sparging process that has been taken into account relies on a sparger (realized by *Mott Corp.*[®]) made of sintered stainless steel, with a porosity of about 70% and a nominal pore diameter of 40 μm.

2.1. Equipment

The way adopted to place the sparger inside the pipeline in which the vegetable oil flows is shown in Figure 1.

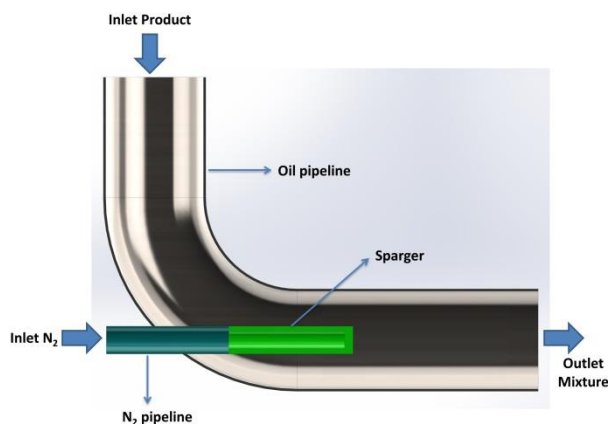


Figure 1: sparger's position inside vegetable oil pipeline

As can be noticed from Figure 1, the sparger is elbow mounted, in order to avoid the creation of a dead leg along the piping, from which could arise cleanability issues. The pipeline where vegetable oil flows is realized with commercial pipes having a nominal diameter of 80 mm (DN80, according to DIN standards), while the pipeline which carries gaseous N₂ to the sparger is realized with commercial pipes having a nominal diameter of 20 mm (DN20, according to DIN standards).

As previously explained, different geometrical configurations of the oil pipeline have been analyzed, in order to assess if a different geometry can influence N₂

distribution inside oil flow, and thus the removal of dissolved O₂. In particular, four configurations have been compared:

1. a configuration where the sparger is followed by a straight DN80 pipe;
2. a configuration where the sparger is followed by a Venturi-like pipe, with the Venturi throat having a diameter of 30 mm and the outlet section having a diameter of 50 mm;
3. a configurations where the sparger is followed by a Venturi-like pipe having some protuberances in the Venturi throat, to enhance the turbulence and, thus, the mixing between the gas and the vegetable oil (also in this case the diameter of the Venturi throat is equal to 30 mm and the diameter of the outlet section is equal to 50 mm);
4. a configuration where the sparger is followed by a Venturi-like pipe having some protuberances in the Venturi throat, but with the outlet section having a diameter equal to 80 mm.

The first configuration represents the standard system used in companies that adopt the sparging technology to preserve vegetable oil from deterioration.

In each one of the four analyzed configurations the distance between the top of the sparger and the outlet section is equal to 460 mm. The four configurations are highlighted in Figure 2.

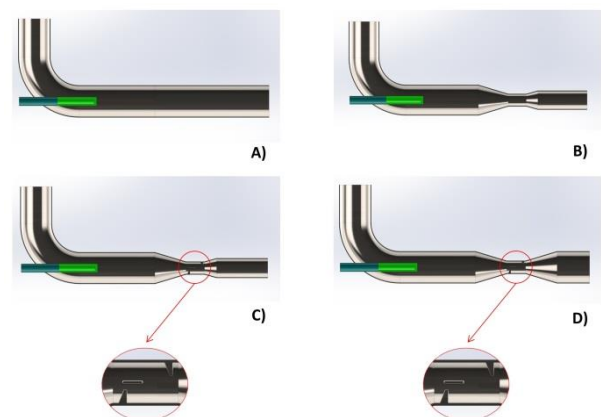


Figure 2: A) first configuration, B) second configuration, C) third configuration, D) fourth configuration

The tank considered in the simulation of the filling phase, instead, is a small capacity tank of 150 liters, made of stainless steel.

In particular, two version of the tank are adopted: in the first version the tank inlet section has a diameter of 80 mm (which will be coupled with sparging systems having a DN80 outlet), while in the second version it has a diameter of 50 mm (which will be coupled with sparging systems having a DN50 outlet). Connected to the inlet section there is a small-length pipe which

addresses the in-flow of vegetable oil towards the bottom of the tank. On the top of both versions, instead, there is a gas outlet, which allows the escape of the gas that accumulates above oil.

The following Figure 3 shows the two configurations of the tank adopted in the simulations.

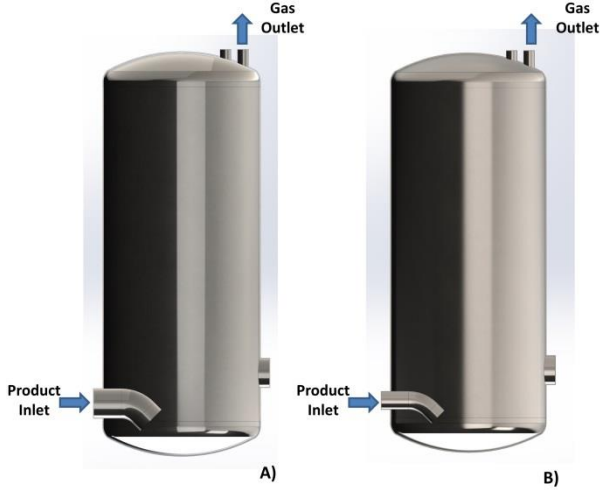


Figure 3: A) tank with DN80 inlet, B) tank with DN50 inlet

2.2. CFD Modelling

Considering the co-presence of a liquid phase (vegetable oil) and of two gaseous substances (N_2 and O_2) in this case a multi-phase simulation has to be set up.

Consequently, to set up the physics and solve the calculation, Ansys CFX version 16.1 has been used, because this software allows to simulate multi-phase flows. In fact, a 3D multi-phase simulation has been set up, considering a mixture of vegetable oil, N_2 and O_2 .

In particular, in both simulations (sparger simulations and tank filling simulations) the “Homogeneous Model” has been adopted, in the first case because the fluids share the same velocity field, since the gases are entrained by the oil stream, and, in the second case, because it allows a better modeling of the free surface inside the tank, according to Ansys CFX Reference Guide.

In a multi-phase simulation, with the “Homogeneous Model” activated, the continuity equation becomes:

$$\frac{(r_\alpha \cdot \rho_\alpha)}{\partial t} + \nabla \cdot (r_\alpha \cdot \rho_\alpha \cdot \mathbf{U}) = S_{MS_\alpha} + \sum_{\beta=1}^{N_p} \Gamma_{\alpha\beta} \quad (1)$$

where:

- ρ_α is the density of phase α ;
- r_α is the volume fraction of phase α ;
- \mathbf{U} is the vector of velocity $U_{x,y,z}$, which is the same for all of the considered phases;
- S_{MS_α} describes user specified mass sources;
- $\Gamma_{\alpha\beta}$ is the mass flow rate per unit volume from phase β to phase α . This terms only occurs if

interphase mass transfer takes place, so in this case is equal to 0.

Instead, for the “Homogeneous Model”, the momentum equation is given by:

$$\frac{(\rho \cdot \mathbf{U})}{\partial t} + \nabla \cdot (\rho \mathbf{U} \otimes \mathbf{U} - \mu (\nabla \mathbf{U} + (\nabla \mathbf{U})^T)) = S_M - \nabla p \quad (2)$$

where:

- $\rho = \sum_{\alpha=1}^{N_p} r_\alpha \rho_\alpha$ is the phase-averaged density;
- $\mu = \sum_{\alpha=1}^{N_p} r_\alpha \rho_\alpha$ is the phase-averaged dynamic viscosity;
- S_M is a term that describes a user specified momentum source.

Furthermore, is present a constraint which specifies that the volume fractions must sum up to unity in every instant and in every point of the fluid domain, meaning that the following equation:

$$\sum_{\alpha=1}^{N_p} r_\alpha = 1 \quad (3)$$

has to be always respected.

With regard to energy exchanges, it has been considered that the analyzed processes are carried out at room temperature, with a negligible heat transfer between the fluid domain and the outside environment. Consequently, the isothermal model with a fixed temperature of 25°C has been set up.

Moreover, in the case of the tank filling simulations, to achieve a better modeling of the oil free surface, the “Standard Free Surface Model” has been adopted. In this case, if there are just two phases, the following equations is used for interfacial area density:

$$A_{\alpha\beta} = |\nabla r_\alpha| \quad (4)$$

Finally, for both cases (sparger simulations and tank filling simulations) the $k-\varepsilon$ turbulence model has been adopted, because it is suitable both for fluid flow inside in Venturi-like pipes (Guerra et al., 2012) and both for tank problems (Godderidge et al., 2009). The $k-\varepsilon$ model is a two equations eddy viscosity turbulence model which is widely used to solve a large number of industrial problems (Blazek, 2015). The equation governing the $k-\varepsilon$ model can be found in Ferziger and Peric (2002).

2.2.1. Mesh setting for the fluid domain

The fluid domains have been obtained starting from the 3D CAD models of the four sparger configurations and from the 3D CAD models of the two tank configurations by means of the CAD software SolidWorks (version 2014). Instead, the discretization of the fluid domains has been performed using the software Ansys Meshing version 16.1.

The grids were initially set by creating a uniform subdivision, and then thickened in the critical areas of the fluid domains.

In particular, considering the sparger configurations, a finer mesh was used near the inlets, near the outlet, near the walls and in the Venturi throat.

At the end of the operation, the unstructured grids obtained for the sparging simulations had, on average, a total of 680,000 nodes and 3,730,000 tetrahedrons each.

Figure 4 shows a section of the obtained volume meshes. In particular, Figure 4 A) shows the mesh for the first sparger configuration, Figure 4 B) shows a close-up of the mesh in the Venturi throat and Figure 4 C) shows a close-up of the mesh in the Venturi throat when the protuberances are present.

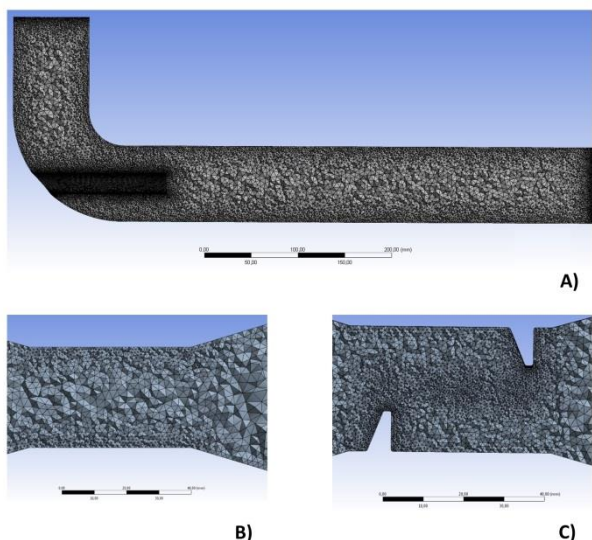


Figure 4: A) section of the volume mesh for first sparger configuration, B) close-up of the volume mesh in the Venturi throat, C) close-up of the volume mesh in the Venturi throat with protuberances

Also for the two tank configurations an unstructured grid has been adopted. Figure 5 shows a section of the volume mesh for both of the analyzed configurations.

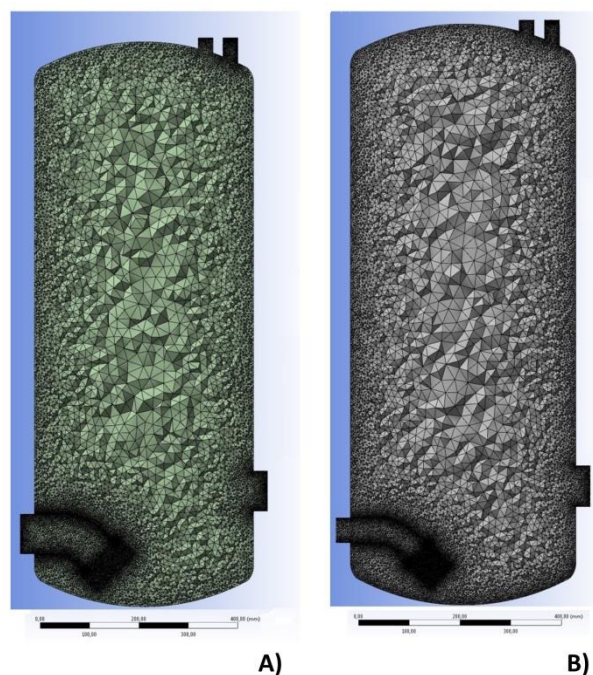


Figure 5: A) volume mesh for tank with DN80 inlet, B) volume mesh for tank with DN50 inlet

As can be noticed from Figure 5, in this case a finer mesh was adopted in correspondence of the gas outlet and in correspondence of the point where oil flows exits the inlet tube and enters the tank, which are the areas where the velocity gradients are expected to be higher.

An unstructured grid with about 1,000,000 nodes and 5,600,000 tetrahedrons was obtained for both tank configurations.

2.2.2. Simulation setting

Settings for sparger simulations

A 3D multi-phase simulation has been set up considering the fluid domain as composed by oil, N_2 and O_2 .

N_2 and O_2 were considered as ideal gases and the values of the thermo-physical properties adopted for their characterization were the ones present by default in Ansys CFX materials database. Furthermore, since vegetable oil is not present in Ansys CFX materials library, it has been created using the settings showed in Table 1. In particular, the values adopted to define the thermo-physical properties of this substance are referred to Olive Oil characteristics at 25°C and atmospheric pressure.

Table 1: Olive Oil settings

Olive Oil Settings	
Thermodynamic State	Liquid
Density	$916 \frac{\text{kg}}{\text{m}^3}$
Molar Mass	$276.72 \frac{\text{g}}{\text{mol}}$
Specific Heat Capacity	$2090 \frac{\text{J}}{\text{kg K}}$
Specific Heat Type	Constant Pressure
Reference Temperature	25 °C
Reference Pressure	1 atm
Dynamic Viscosity	0.08 Pa·s
Thermal Conductivity	$0.169 \frac{\text{W}}{\text{m K}}$

Obviously, Olive Oil is not a pure substance but a mixture of chemical compounds (mostly fatty acids), so it is not possible to define in an exact way the molar mass for this element. Consequently, it has been obtained by calculating the weighted average of the molar masses of the oil main components.

Figure 6 shows the boundary conditions adopted for this set of simulations.

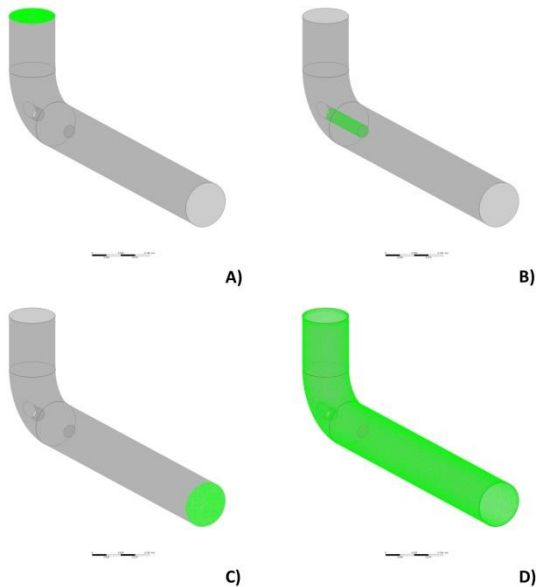


Figure 6: boundaries for sparging simulation: A) product inlet, B) N₂ inlet, C) outlet, D) wall

From Figure 6 B) can be noticed that the sparger has not been modeled as a porous domain but that the sparger's external walls have simply been set as a N₂ inlet. This has been done because we were not interested in modeling the N₂ pressure loss through the sparger but only the achievable distribution of N₂ inside the oil stream. However, only the 70% of the inlet surface was considered as emanating N₂, and the generated gas bubbles have been considered with a diameter of 40 μm, in order to take account of the porosity and the average diameter of the sparger's pores.

The values set on the boundary conditions previously described are shown in Table 2.

Table 2: boundary and initial conditions for original case

Boundary Conditions	
Product inlet	Mass Flow-Rate = 1.273 kg/s Oil volume fraction = 97.3 % O ₂ volume fraction = 2.7 % N ₂ volume fraction = 0
N ₂ inlet	Mass Flow-Rate = 4.0e-4 kg/s Oil volume fraction = 0 O ₂ volume fraction = 0 N ₂ volume fraction = 100 %
Outlet	Relative pressure = 0,718
Wall	No Slip Wall Adiabatic
Initial Conditions	
Domain Composition	Oil volume fraction = 97.3 % O ₂ volume fraction = 2.7 % N ₂ Volume fraction = 0
Velocity	0 m/s
T	25°C
p	1 bar

From the previous Table it can be noticed that, on the product inlet and in the initial domain composition, has been set an O₂ volume fraction equal to 2.7%. This has been done to consider that there could be a maximum of 36 mg/l of dissolved O₂ in vegetable oil (Parenti et al., 2007.). Instead, N₂ flow rate has been calculated considering that are necessary about 0.34 m³ of N₂ in order to supersaturate 1 m³ of oil, as reported by O'Brien (2008).

The outlet pressure, instead, was chosen considering that on the outlet section there must be an adequate counter pressure to make sparging process effective.

The analysis was stationary, because product flow and N₂ flow have considered not time dependent.

Obviously the simulation and boundary conditions settings were the same for all of the analyzed sparger configurations.

Settings for tank filling simulations

Also in this case a 3D multi-phase simulation has been set up considering the fluid domain as composed by oil, N₂ and O₂.

As previously explained N₂ and O₂ were considered as ideal gases, while oil thermo-physical properties were created considering Olive Oil characteristics at 25°C and atmospheric pressure.

The boundary conditions adopted for these simulations are shown in Figure 7.

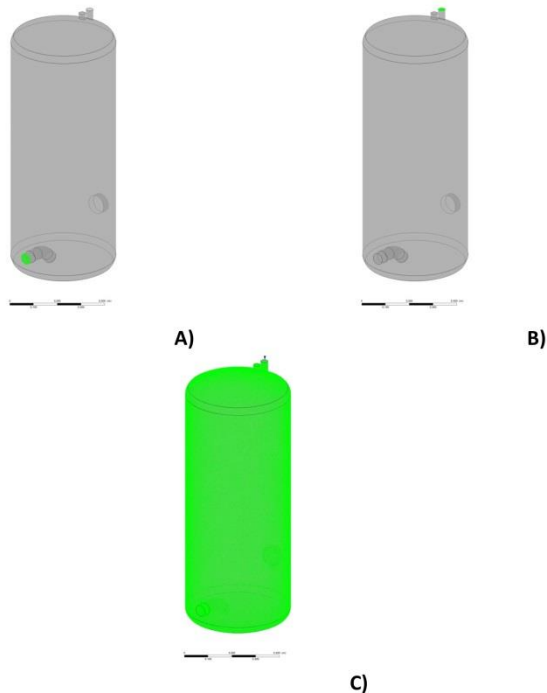


Figure 7: boundaries for tank filling simulation: A) tank inlet, B) tank gas outlet, C) wall

In this case on the tank inlet will be imported the results obtained on the outlet section at the end of the sparging process simulation. In particular will be imported the volume fractions and the flow velocity.

On the gas outlet atmospheric pressure, a N_2 volume fraction equal to 78.5% and a O_2 volume fraction equal to 21.5%, in order to reproduce air presence. Moreover, also in this case on the domain walls was set a no-slip adiabatic condition.

Finally, in this case, the analysis was carried out in transient mode, because to model the increase of product quantity inside the tank is necessary to consider the passing of time. In particular a total time of 110 s has been simulated, with a time-step of 0.05 s. The results were registered every 2.5 s. At 90 s the product in-flow has been interrupted, so to allow, in the last 20 s of the simulation, the diffusion of gas dissolved in vegetable oil through the product free surface. The time instant in which to stop the product in-flow has been chosen keeping in mind that 90 s is the time considered necessary, considering the flow rate, to have in the tank a product quantity such that the head space is equal to about the 20% of the volume of the tank itself. This has been done in accordance with a practical rule which says that the head space should be between 10% and 30% of the volume.

The conditions of the fluid domain at the beginning of the simulation are shown in Table 3.

Table 3: Tank filling simulation initial conditions

Initial Conditions	
Domain Composition	Oil volume fraction = 15% N_2 volume fraction = 85% O_2 volume fraction = 0
Velocity	0 m/s
T	25°C
p	1.7 bar

From Table 3 can be noticed that at the beginning of the simulation the tank is considered already partially filled with oil, which accumulates on its bottom, while the head space is filled with N_2 . Consequently in analyzed case sparging and blanketing are applied simultaneously, to avoid the contact between the product and atmospheric O_2 during filling. An absolute pressure of 1.7 bar, instead, has been selected because it is the expected average absolute pressure on the outlet section on spargers configuration, considering the setting adopted for these analyses.

3. RESULTS AND DISCUSSION

3.1. CFD simulation of the sparging process

The first analyses that were performed have been the ones involving the four different configurations adopted for the sparging process. The simulations converged after about 500 iterations.

In this case the main analyzed result was the N_2 distribution on the outlet section of the systems. These results are summarized in Figure 8, which shows N_2 volume fraction for each one of the four analyzed configurations.

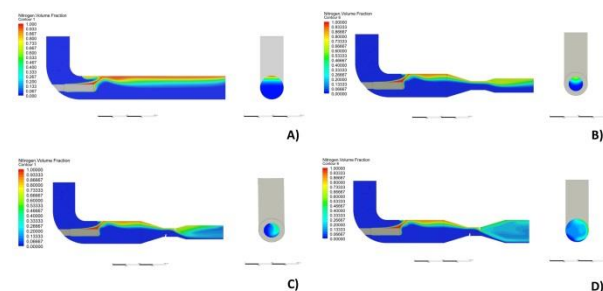


Figure 8: N_2 distribution inside sparging system: A) N_2 volume fraction in first configurations, B) N_2 volume fraction in second configuration C) N_2 volume fraction in third configuration, D) N_2 volume fraction in fourth configuration

It can be noticed that, in the first configuration (Figure 8 A), gaseous N_2 tends to stratify above vegetable oil and, consequently, N_2 distribution on the outlet section is not homogeneous. Also the second configuration (Figure 8 B)) is affected by this problem, although to a slightly smaller extent, thanks to the introduction of the Venturi. On the contrary, in the third and in the fourth configuration (Figure 8 C) and D)), the protuberances placed in the Venturi throat allow to achieve a better mixing between N_2 and the product in

the final part of the pipeline, thus obtaining a more homogeneous N₂ distribution on the outlet section.

Also a quantitative analysis of these results was performed, which is highlighted in Figure 9.

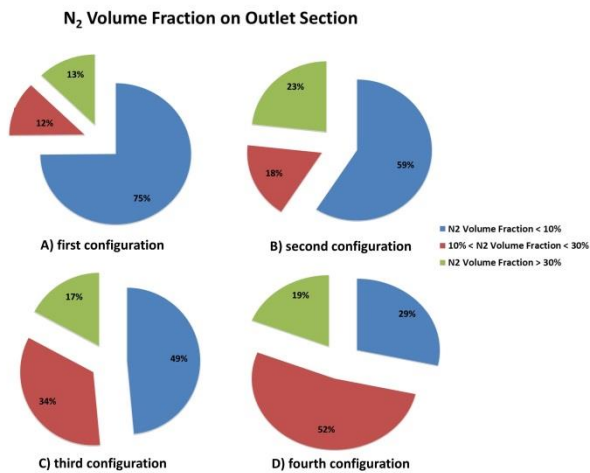


Figure 9: N₂ distribution on the outlet section of the sparging systems

As can be observed from the previous Figure, in the third and in the fourth configuration, the percentage of the outlet section area where N₂ volume fraction is lower than 10% is considerably lower than in the first two configurations. Consequently, we can say that the introduced changes improve the mixing between N₂ and the product. Then, the simulations of the tank filling phase will highlight if the realized changes have an impact also on the amount of the dissolved O₂ that can be removed.

Other analyzed results are the average absolute pressure and the average velocity on the outlet section, which are shown in Table 4.

Table 4: Average absolute pressure and average velocity on outlet section

Variables	Configurations			
	Conf. 1	Conf. 2	Conf. 3	Conf. 4
Average Absolute Pressure	1.73 bar	1.73 bar	1.73 bar	1.73 bar
Average Velocity	0.36 m/s	0.87 m/s	0.93 m/s	0.69 m/s

It may be noticed that the average absolute pressure on the outlet section is 1.73 bar, which confirms the correctness of the settings regarding the initial pressure for the simulations of the tank filling phase.

3.2. CFD simulations of tank filling

In this section are presented the results of the simulations of the tank filling phase. In particular three simulations have been carried out:

- 1) tank filling starting from the results obtained at end of the analysis of the first sparger configuration;
- 2) tank filling starting from the results obtained at the end of the analysis of the third sparger configuration;
- 3) tank filling starting from the results obtained at the end of the analysis of the fourth sparger configuration.

To carry out the simulations the results obtained on the spargers outlet section in terms of velocities and volume fractions were imported on tank inlet. A coupling between the second sparger configuration and the tank was not analyzed, because the N₂ distribution on the outlet section of the sparging system was deemed too similar to that obtainable with the first analyzed system.

In this case, the main analyzed result is evolution in time of the O₂ residual in oil. The graph in Figure 10 compares the O₂ residual for the three simulated configurations.

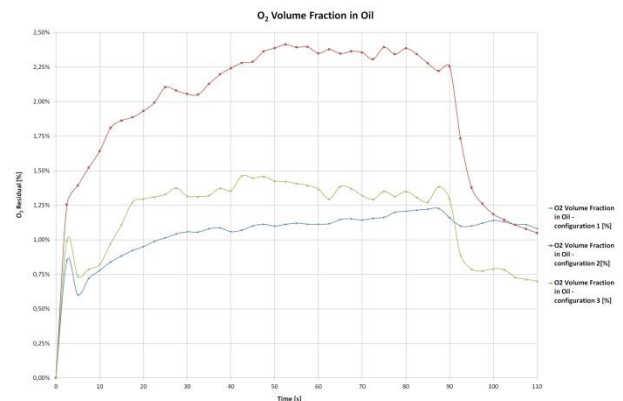


Figure 10: O₂ residual in oil for the three tank filling simulations

First of all, it can be noticed that, for all of the three analyzed configurations, O₂ residual in oil increases for the first 90 s, then, when the filling is stopped, the injected N₂ starts to spread through the product free surface, dragging O₂ along with itself and thus causing a rapid decrease of the residual, as expected. This trend is more pronounced for the second and the third configurations than in the first one.

It can be observed that the first configuration allows to reach a final O₂ residual in oil equal to 1.08%, starting from an initial average volume fraction of O₂ in oil, on the inlet section, equal to 2.4%. Moreover, in this case O₂ residual in oil during filling never reaches a value higher than 1.23% (at 87.5 s). This value is lower than the O₂ volume fraction on inlet section, consequently, in this case, seems that N₂ is pushing O₂ towards the outlet section also during the filling phase.

This phenomenon is confirmed also for the third analyzed configuration. In this case, the final O₂

residual is equal to 0.7% (also in this case starting from an initial average volume fraction of O₂ in oil, on the inlet section, equal to 2.4%) while, the maximum value reached by O₂ volume fraction in oil during filling, is equal to 1.46%.

Instead, in the second configuration, the final O₂ residual in oil is equal to 1.04%, starting from a O₂ volume fraction on inlet of 2.4%. Moreover, the maximum value reached by O₂ volume fraction in oil during filling, is equal to 2.4%, showing how, in this case, injected N₂ is less effective in eliminating dissolved O₂ during filling. This could be related to the higher average velocity on tank inlet which, excluding the different N₂ distribution in oil stream, is the main difference between this configuration and the other two.

3.3. Discussion

The results described in section 3.2 are summarized in the following Table 5.

Table 5: O₂ residual after tank filling

	O ₂ residual after tank filling			
	O ₂ volume fraction on inlet	Max O ₂ volume fraction in Oil during filling	Final O ₂ residual in Oil	% decrease of dissolved O ₂
Sim. 1	2.40 %	1.23 %	1.08 %	55 %
Sim. 2	2.40 %	2.40 %	1.04 %	57 %
Sim. 3	2.40 %	1.46 %	0.70 %	71 %

Comparing the residuals highlighted in Table 5 we can say that simulation 2 (coupling between tank and third sparger configuration) and simulation 3 (coupling between tank and fourth sparger configuration) show better results than simulation 1. In particular, the best case seems to be simulation 3, which allows to reduce the amount of dissolved O₂ by 71%. Consequently, we can say that the sparging configuration and the N₂ distribution inside the oil stream have an important influence on the removal process of dissolved O₂.

Two points instead should be discussed: the trend in the decrease of O₂ volume fraction in oil when the filling stops (at 90 s) and the maximum O₂ volume fraction that is reached in oil during filling.

With respect to the first point, from Figure 10 can be seen that, when the filling stops, in simulation 2 and simulation 3 there is a drop in the amount of O₂ dissolved in oil. Instead, this does not happen in simulation 1, which shows only a small decrease. A possible explanation is in the amount of N₂ in the oil inside the tank. If we compare N₂ volume fraction in the tank at 92.5 s we can see that in the first simulation it is considerably lower than in the last two analyzed configurations, as highlighted in Figure 11. Consequently, also the quantity of O₂ pushed towards the outlet section is lower and thus, in simulation 1, is lower the drop in O₂ concentration.

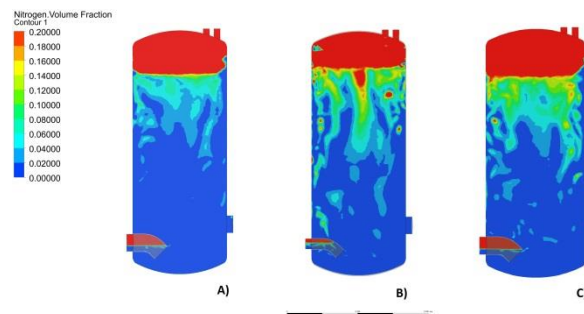


Figure 11: N₂ volume fraction in tank at 92.5 s: A) first tank simulation, B) second tank simulation, C) third tank simulation

Instead, considering the second point, again from Figure 10 it can be observed that, in simulation 2, during filling, the maximum concentration of O₂ that is reached in the bulk of oil is equal to 2.4%, while, in other simulations, is considerably lower (never higher than 1.46%). This means that, somehow, in the second case N₂ cannot separate O₂ also during filling and that its action becomes significant only when the filling is stopped. This may be related to the higher fluid velocity. In this case, in fact, tank inlet has a DN50 section and, consequently, the average fluid velocity over the inlet is higher, as highlighted in in Table 4. This could lead to a very chaotic filling, which instead of favoring N₂ action partially hinders it. However, of fundamental importance will be a subsequent experimental phase, which will allow not only to test the model and modify it if necessary, but also to verify in laboratory the origin of these two behaviors.

4. CONCLUSIONS

The sparging process of vegetable oil with gaseous N₂ (or with another inert gas) is one of the most adopted techniques to preserve vegetable oil from spoilage. This technique consist in inject the inert gas directly in the oil stream by means of a porous sparger. Subsequently, the injected gas, during tank filling operation, diffuses trough the free surface on the product, and saturates tank head-space, preventing the contact between oil and atmospheric O₂, which is the major spoilage agent. In some cases sparging is used coupled with blanketing, which consists in saturating the tank inner volume with N₂, in order to create an inert environment. In this case sparging main goal is to separate the O₂ dissolved in the product, which could be present in quantity of 36 mg/l. In this case, when gaseous starts to diffuse through product's free surface, it drags along with itself parts of the dissolved O₂.

The objective of this work was to simulate various sparger configurations and the subsequent tank filling operation, to assess if the sparger geometry could affect the N₂ distribution inside the oil stream and, consequently, the O₂ removal process. In particular four different configurations were modeled:

1. a configuration where the sparger is followed by a straight DN80 pipe;
2. a configuration where the sparger is followed by a Venturi-like pipe, with the Venturi throat having a diameter of 30 mm and the outlet section having a diameter of 50 mm;
3. a configurations where the sparger is followed by a Venturi-like pipe having some protuberances in the Venturi throat, to enhance the turbulence and, thus, the mixing between the gas and the vegetable oil (also in this case the diameter of the Venturi throat is equal to 30 mm and the diameter of the outlet section is equal to 50 mm);
4. a configuration where the sparger is followed by a Venturi-like pipe having some protuberances in the Venturi throat, but with the outlet section having a diameter equal to 80 mm.

The first configuration represents the standard system used in companies that adopt the sparging technology to preserve vegetable oil from deterioration.

Configurations 3 and 4 allowed to obtain a more homogeneous N₂ distribution on the system outlet section and, consequently, they were coupled with the tank, to evaluate also the filling operation and the effectiveness of the O₂ removal process, in order to compare them with the original configuration.

At the end of these sets of simulations, has been verified that both configurations are more effective in removing the dissolved O₂ than the original one. In particular, the fourth sparger configuration was identified as the best case, since it allows to remove the 71% of the dissolved O₂, compared to the 55% obtained with the original configuration. This work, consequently, proved that the sparging system geometry and that the N₂ distribution inside the oil stream are very important to obtain an effective removal of dissolved O₂. In particular, simulations have shown that, with changes having a limited cost, is possible to increase the effectiveness of the removal process by 77%.

Points to be addressed are the trend in the O₂ residual in oil when the filling stops, which is different when adopting the original sparging system, and the fact that in one case there is a small accumulation of O₂ in the tank during filling.

Future researches should focus on the execution of an experimental phase, in order to validate the simulations described in this paper and to observe, in a laboratory, the origin of the two described unexpected behaviors.

Moreover, simulations of the described systems in a vertical position should be carried out, since, frequently, the adopted sparging solution is used also in this way.

REFERENCES

- ANSYS CFX-solver modeling guide, release 16.1. ANSYS, Inc. Southpointe 2600 ANSYS Drive, 2015.
- ANSYS CFX-solver theory guide, release 16.1. ANSYS, Inc. Southpointe 2600 ANSYS Drive, 2015.
- Blazek, J., 2015. Computational fluid dynamics: principles and applications. Butterworth-Heinemann.
- Bottani E, Ferretti G, Manfredi M, Vignali G. Modeling and thermo-fluid dynamic simulation of a fresh pasta pasteurization process. *International Journal of Food Engineering*, 9:327–39.
- Choe, E., Min, D. B., 2006. Mechanisms and factors for edible oil oxidation. *Comprehensive reviews in food science and food safety*, 5(4), 169-186.
- Ferziger JH, Peric M., 2002. Computational methods for fluid dynamics. Axel-Springer Verlag.
- Godderidge, B., Turnock, S., Tan, M., Earl, C., 2009. An investigation of multiphase CFD modelling of a lateral sloshing tank. *Computers & Fluids*,38(2), 183-193.
- Guerra, V. G., Béttega, R., Gonçalves, J. A., Coury, J. R., 2012. Pressure drop and liquid distribution in a venturi scrubber: experimental data and CFD simulation. *Industrial & Engineering Chemistry Research*, 51(23), 8049-8060.
- Gunstone, F. (Ed.), 2011. Vegetable oils in food technology: composition, properties and uses. John Wiley & Sons.
- Manfredi, M., Vignali, G. 2015 Comparative Life Cycle Assessment of hot filling and aseptic packaging systems used for beverages. *Journal of Food Engineering*, 147, pp. 39-48.
- Masella, P., Parenti, A., Spugnoli, P., Calamai, L., 2010. Nitrogen stripping to remove dissolved oxygen from extra virgin olive oil. *European Journal of Lipid Science and Technology*, 112(12), 1389-1392.
- Mosna, D., Vignali, G. 2015. Three-dimensional cfd simulation of a "steam water spray" retort process for food vegetable products. *International Journal of Food Engineering*, 11 (6), pp. 715-729.
- O'brien, R. D., 2008. Fats and oils: formulating and processing for applications. CRC press.
- Parenti, A., Spugnoli, P., Masella, P., & Calamai, L., 2007. Influence of the extraction process on dissolved oxygen in olive oil. *European journal of lipid science and technology*, 109(12), 1180-1185.
- Shahidi, F., 2005. *Bailey's Industrial Oil and Fat Products*, 6 Volume Set (Vol. 1).
- Shahidi, F., 2005. *Bailey's Industrial Oil and Fat Products*, 6 Volume Set (Vol. 5).
- Spanu, S., Vignali, G. 2015. CFD analysis of coffee packaging in capsules using gas flushing modified atmosphere packaging. *International Food Operations and Processing Simulation Workshop, FoodOPS 2015*, pp. 1-8.

Spanu, S., Vignali, G., in press. Modelling and Multi-objective Optimisation of the VHP Pouch Packaging Sterilisation Process. International Journal of Food Engineering, DOI: 10.1515/ijfe-2015-0061

AUTHORS BIOGRAPHY

Filippo FERRARI is a recent graduate at the University of Parma. After taking the bachelor degree in engineering management in February 2014, in July 2016 he has achieved a master degree in Mechanical Engineering for the Food Industry at the same University. His main fields of interest concern food process modelling and simulation.

Simone SPANU is a scholarship holder at CERIT research center at the University of Parma. In March 2014 he has achieved a master degree in Mechanical Engineering for the Food Industry at the same university. His main fields of research concern food process modelling and simulation, with a particular focus on the CFD simulation for the advanced design of food and beverage processing plants.

Giuseppe VIGNALI is an Associate Professor at University of Parma. He graduated in 2004 in Mechanical Engineering at the University of Parma. In 2009, he received his PhD in Industrial Engineering at the same university, related to the analysis and optimization of food processes. Since August 2007, he worked as a Lecturer at the Department of Industrial Engineering of the University of Parma. His research activities concern food processing and packaging issues and safety/security of industrial plant. Results of his studies related to the above topics have been published in more than 70 scientific papers, some of which appear both in national and international journals, as well in national and international conferences.

JOINING SIMULATION AND SITUATION AWARENESS FOR AN ITALIAN PRODUCTION SYSTEM

Massimo De Falco^(a), Vincenzo Loia^(b), Luigi Rarità^(c), Stefania Tomasiello^(d)

^{(a), (b)} Dipartimento di Scienze Aziendali – Management & Information Systems,
University of Salerno, Via Giovanni Paolo II, 132, 84084, Fisciano (SA), Italy
^{(c), (d)} CO.RI.SA, CONSORZIO di RICERCA Sistemi ad Agenti,
University of Salerno, Via Giovanni Paolo II, 132, 84084, Fisciano (SA), Italy

^(a)mdefalco@unisa.it, ^(b)loia@unisa.it, ^(c)lrarita@unisa.it, ^(d)stomasiello@unisa.it

ABSTRACT

The paper focuses on simulation results for a real supply network, dealing with tomatoes production, which is widespread in Southern Italy. The dynamics of the system is studied via differential equations, that involve either parts on arcs or queues that consider the exceeding goods. Two different numerical schemes are compared to test the approximation degrees, and then used for simulations. Through a procedure of Situation Awareness, a possible choice of the input flow to the supply network is analyzed. The obtained results prove that using Situation Awareness allows, at least for the real system in consideration, good compromises in order to modulate production queues.

Keywords: supply networks, Situation Awareness, differential equations, tomatoes production

1. INTRODUCTION

Italian economy, as well as the wealth of each Italian region, depends on various phenomena that are also connected to the distribution/production of different goods. As the intention is an increment of prestige at international and national levels, a careful attention is always devoted to the analysis of some marketing strategies that foresee the exporting of cultivated goods. Hence, big efforts aim to guarantee a suitable treatment of products via supply networks, by which producers and consumers are both satisfied. Such a situation is highly studied in Campania, an Italian region where production and distribution of tomatoes represent a serious issue. Indeed, the primary key factor is the production, as its possible delays have consequent negative impacts on the delivery in the foreseen times.

The aim of this paper is to focus on supply networks for tomatoes, also considering environment factors that always establish a hard constraint in terms of input flows to production systems. In particular, supply networks are modelled using a fluid-dynamic model, based on Partial and Ordinary Differential Equations (PDEs, ODEs). Input flows to such networks are chosen by an approach of Situation Awareness (Endsley 1995, Endsley 2015, Wickens 2008), applied

to the tomatoes production. The advantages are evident: on one hand, the fluid-dynamic model allows focusing on time-space dynamics of goods; on the other hand, Situation Awareness establishes, considering environment parameters, possible correct inputs to the production systems in order to avoid unsuitable situations, such as remainders of goods to process.

Supply networks and their behaviors have been studied by different mathematical models, see for instance Daganzo 2003, Helbing 2005, Kleijnen 2003, Longo 2008 and Wang 2010. Some approaches are discrete and based on dynamics of individual parts; others are continuous and deal with differential equations (see, for example, Cascone 2008 and Manzo 2012 for applications to road networks). The first work in this direction is by Armbruster, Degond and Ringhofer (Armbruster 2006), who used a limit procedure to obtain a conservation law (Bressan 2000a, Bressan 2000b and Dafermos 1999), which refers to densities of parts. Other papers have been introduced to focus on further phenomena of supply systems (Armbruster 2007, Armbruster 2003). In our case, we consider the model proposed in Göttlich 2005 and Göttlich 2006, where conservation laws for densities of parts and queues for each supplier are analyzed. Considering various discretizations for PDEs (examples are in Canic 2015, De Falco 2016 and Leveque 2002), two different numerical schemes are analyzed for the fluid-dynamic model: an Upwind-Euler approach (precisely, Upwind method for PDEs and Euler scheme for ODEs), with different space meshes and a fixed time grid mesh to overcome problems of not rational ratios for lengths of suppliers (details are in Cutolo 2011); a Differential Quadrature (DQ) approach, firstly introduced in Bellman 1971 and considered as higher order Finite Differences (FDs), see Shu 2000, Shvartsman 2016, Tomasiello 2013. DQ based methods have found many applications in science and engineering (De Rosa 1998, De Rosa 2007, De Rosa 2016, Fantuzzi 2016, Kamarian 2016, Tomasiello 2007, Tornabene 2016, Tornabene 2015a, Tornabene 2015b), because of the improved computational efficiency.

As there is the exigency of controlling the production processes and hence the input flows to the supply networks, Situation Awareness is necessary. As for Endsley's opinion (Endsley 1995), Situation Awareness deals with "the perception of the elements in the environment within a volume of time and space, the comprehension of their meaning, and the projection of their status in the near future". Such a model deals with three different levels, useful to plan decisions on input flows of supply systems: perception, by which elements of the environment are perceived; comprehension, that considers which data from the environment are useful for the goals to achieve; projection, which is the capability of projecting the recognized elements in the future. Great advantages of Situation Awareness are simply obtained focusing on the characteristics of the three levels, useful to take decisions for particular domains. An example is in D'Aniello 2016, where the authors discuss a possible Decision Support System for smart commerce environment.

Finally, simulations are made: first, the Upwind-Euler method and the Differential Quadrature approach are compared, showing that they have similar characteristics in terms of numerical approximations and computational times. Then, starting from the numerical results, a real example of supply system for tomatoes production is considered. In this case, input flows are chosen in two different cases: decisions planned by the leadership of a little business company in Campania region (Italy); decisions obtained by a model of Situation Awareness, considering real environment data. It is proven that Situation Awareness is useful to accelerate the system dynamics, in terms of emptying of queues in some parts of the system.

The outline of the paper is the following. Section 2 presents Situation Awareness within the context of tomatoes production. Section 3 considers the mathematical model for supply networks. Section 4 deals with numerical methods for the proposed model: Upwind-Euler with different space meshes for different suppliers; Differential Quadrature rules. Finally, Section 5 contains the simulation results: first, numerical errors for the described numerical approaches are considered; then, the case study of a supply network for tomatoes is presented. Conclusions end the paper in Section 6.

2. SITUATION AWARENESS FOR TOMATOES PRODUCTION

In this section, we discuss a possible application of Situation Awareness using the Endsley's model (Endsley 1995), that is contextualized to processes for tomatoes production within a real little business company in Campania region (Italy). The overall approach is in Figure 1.

In detail, the *environments* consist of conditions by which high quality tomatoes depend, namely: presence of wind, humidity for arable fields and weather. In such a framework, a *situation* describes a state for a good growth of tomatoes and has three different phases:

- *Perception*: environment data are obtained and kept.
- *Comprehension*: data of the previous step are elaborated. This operation represents a serious issue, as combinations of parameters for tomatoes growth imply possible forecasts on the quality of goods. In this work, the comprehension step is made by analysing time series.
- *Projection*: results of the second phase are used to plan possible future decisions. The effect of this phase is to define a Decision Support System (DSS).

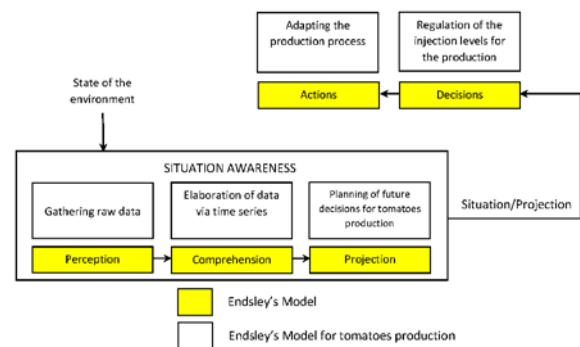


Figure 1: Situation-aware Decision-making process

The DSS, not described in detail here, represents a support for the leadership of the business company. The DSS has rules, based on Fuzzy Logic, that allow to understand possible correct levels of injection to the production networks.

3. A MODEL FOR SUPPLY NETWORKS

In this section, we present an ODE-PDE model for supply networks (see Göttlich 2006), based on the analysis of Armbruster 2006 and described for supply chains in Göttlich 2005. The model considers: a conservation laws formulation for density of parts over the suppliers; time - dependent queues for the transition of parts among suppliers; distribution coefficients which indicate how the outgoing flows from a given node distribute over suppliers which are downstream.

A supply network is a directed graph with a set of arcs J and a set of vertices V .

Each arc $j \in J$ is parameterized by a real interval $[a_j, b_j]$, represents a supplier (possibly having infinite endpoints) and is considered: incoming if $b_j < +\infty$; outgoing if $a_j > -\infty$. For each outgoing arc $j \in J$, there exists a queue.

Each vertex $v \in V$ is connected to a set of incoming arcs $Inc(v) \subset J$ and a set of outgoing arcs $Out(v) \subset J$.

There are distributions coefficients $(\alpha_{v,j})_{j \in Out(v)}$ such that $\alpha_{v,j} \in]0,1[$ and $\sum_{j \in Out(v)} \alpha_{j,v} = 1 \quad \forall v \in V$.

Notice that the coefficient $\alpha_{v,j}$ indicates the percentage of flux outgoing from v and directed to the supplier j .

For each arc $j \in J$, indicate by: $\mu_j > 0$ the maximum processing capacity; $L_j > 0$ the length; $T_j > 0$ the processing time; $v_j := L_j/T_j$ the processing velocity; $\rho_j(t, x) \in [0, \rho_j^{\max}]$ the density of parts at point x and time t ; $f_j(\rho_j(t, x)) := \min\{\mu_j, v_j \rho_j(t, x)\}$ the flux function.

Considering that parts over each arc $j \in J$ are processed with velocity v_j and with a maximal flux μ_j , the phenomenon is defined by the conservation law:

$$\partial_t \rho_j(t, x) + \partial_x f_j(\rho_j(t, x)) = 0, \quad \forall x \in [a_j, b_j], \quad t > 0, \quad (1)$$

$$\rho_j(0, x) = \rho_{j,0}(x) \geq 0, \quad \rho_j(t, a_j) = \frac{f_{j,inc}(t)}{v_j}, \quad (2)$$

where $\rho_{j,0}$ and the inflow, $f_{j,inc}(t)$, have to be assigned.

If, for some vertex $v \in V$, we get that arc $j \in Out(v)$, we have a time dependent queue, $q_j(t)$, that obeys this equation:

$$\frac{d}{dt} q_j(t) = \alpha_{v,j} \sum_{k \in Inc(v)} f_k(\rho_k(b_k, t)) - f_{j,inc}(t). \quad (3)$$

For each arc $j \in J$, we assume that:

$$f_{j,inc}(t) := \begin{cases} \varphi_j(t), & \text{if } a_j = -\infty, \\ \min \left\{ \alpha_{v,j} \sum_{k \in Inc(v)} f_k(\rho_k(b_k, t)), \mu_j \right\}, & \text{if } q_j(t) = 0, \\ \mu_j, & \text{if } q_j(t) > 0. \end{cases} \quad (4)$$

where $\varphi_j(t)$ is an assigned input profile on the left boundary $\{(a_j, t) : t \geq 0\}$.

The following holds:

Lemma 1. Consider a solution to (1), (2), (3) and (4), given by $\rho_j(t, x)$ and $q_j(t)$. Then, $\rho_j(t, x) \geq 0$, $q_j(t) \geq 0$ for every $j \in J$, $t \geq 0$ and x .

Proof. As $\alpha_{j,v} > 0$, the inflows (4) are positive and the fluxes f_j vanish at 0, the density ρ_j is always positive by the comparison principle of conservation

laws. Equations (3) and (4) ensure that $q'(t) > 0$ when $q(t) = 0$, hence the conclusion follows.

Remark 2. Lemma 1 also holds for supply chains, considering $\alpha_{j,v} = 1$.

4. NUMERICAL SCHEMES

We deal with some numerical schemes for the model of Section 3, in order to define approximations of densities and queues. Two possible alternatives are considered:

- UE scheme: Upwind method for the PDE (1) and explicit Euler for the ODE (3) in case of different space meshes, see further details in Cutolo 2011.
- DQ scheme: Differential Quadrature rules (e.g. see Tomasiello 2007, Tomasiello 2013).

4.1. UE Schemes

In this Section we introduce the Upwind-Euler method with different space meshes for different suppliers. This is useful either when L_j have not rational ratios or when computational complexity reductions are needed, see Cutolo 2011.

For each arc $j \in J$, define a numerical grid in $[0, L_j] \times [0, T]$ with points $(x_i, t^n)_j$, $i = 0, \dots, N_j$, $n = 0, \dots, \eta_j$, where: N_j is the number of segments into which the j -th supplier is divided; η_j is the number of segments into which $[0, T]$ is divided.

Then, we indicate by: ${}^j \rho_i^n$ the value assumed by the approximated density at the point $(x_i, t^n)_j$; q_j^n the value of the approximate queue buffer occupancy at time t^n .

For each supplier $j \in J$, set a fixed time grid mesh Δt and different spaces grid meshes $\Delta x_j = v_j \Delta t$. Then, grid points are $(x_i, t^n)_j = (i \Delta x_j, n \Delta t)$, $i = 0, \dots, N_j$, $n = 0, \dots, \eta_j$. The Upwind scheme for the parts density of arc j reads as:

$${}^j \rho_i^{n+1} = {}^j \rho_i^n - \frac{\Delta t}{\Delta x_j} v_j ({}^j \rho_i^n - {}^j \rho_{i-1}^n), \quad j \in J, \quad (5)$$

$i = 0, \dots, N_j$, $n = 0, \dots, \eta_j$. Notice that, as

$$\Delta t = \min \left\{ \frac{\Delta x_j}{v_j} : j \in J \right\},$$

the CFL condition (see Leveque 2002) is automatically satisfied.

For queues, if $a_j < -\infty$, the explicit Euler method gives:

$$q_j^{n+1} = q_j^n + \Delta t \left[\alpha_{v,j} \sum_{k \in Inc(v)} f_k({}^k \rho_{N_k}^n) - f_{j,inc}^n \right], \quad (6)$$

$n = 0, \dots, \eta_j$, where:

$$f_{j,inc}^n = \begin{cases} \min \left\{ \alpha_{v,j} \sum_{k \in Inc(v)} f_k(\rho_{N_k}^n), \mu_j \right\}, & q_j^n(t) = 0, \\ \mu_j, & q_j^n(t) > 0. \end{cases} \quad (7)$$

As we need ${}^j \rho_j^n \geq 0$, $q_j^n \geq 0 \quad \forall n \geq 0, j \in J$, $i = 1, \dots, N_j$, the following numerical correction for $f_{j,inc}^n$ is provided:

$$f_{j,inc}^n = \frac{\Delta t' \mu_j + (\Delta t - \Delta t') \alpha_{v,j} \sum_{k \in Inc(v)} f_k(\rho_{N_k}^n)}{\Delta t}, \quad (8)$$

where:

$$\Delta t' := \frac{q_j^n}{\mu_j - \alpha_{v,j} \sum_{k \in Inc(v)} f_k(\rho_{N_k}^n)}. \quad (9)$$

Finally, if $a_j = -\infty$, suitable boundary data are needed, using ghost cells and the expression of inflows given by $\varphi_j(t)$, see equation (4).

4.2. DQ Scheme

The numerical scheme is defined through DQ rules (Bellman 1971), applied to approximate the derivatives of the equations.

In what follows, first we consider a short overview of DQ rules. Then, a suitable scheme for the model of Section 3 is provided.

4.2.1. Differential Quadrature rules: an overview

Consider a continuous function $u(x)$ in the interval $I = [0, L]$, whose a fixed and arbitrary partition is $0 = x_1 < x_2 < \dots < x_M = L$. The DQ rules allow to approximate the r -th order derivative of $u(x)$ by a weighted sum of the functional values at the grid points $u_j = u(x_j)$ as:

$$\frac{d^r}{dx^r} = \sum_{j=1}^M A_{ij}^{(r)} u_j, \quad i = 1, \dots, M. \quad (10)$$

The weighting coefficients are computed as follows, see Shu 2000: with regard to the first-order derivative weighting coefficients, we get:

$$A_{ij}^{(1)} = \frac{\prod_{p=1, p \neq i}^M (x_i - x_p)}{(x_i - x_j) \prod_{p=1, p \neq i}^M (x_i - x_p)}, \quad i, j = 1, 2, \dots, M, j \neq i; \quad (11)$$

with regard to the higher-order derivative weighting coefficients ($2 \leq r \leq M-1$), we have:

$$A_{ij}^{(r)} = r \left[A_{ii}^{(r-1)} A_{ij}^{(1)} - \frac{A_{ij}^{(r-1)}}{(x_i - x_j)} \right], \quad i, j = 1, 2, \dots, M, j \neq i; \quad (12)$$

on the other hand, for $i = j$ ($1 \leq r \leq M-1$):

$$A_{ii}^{(r)} = - \sum_{p=1, p \neq i}^M A_{ip}^{(r)}, \quad i = 1, 2, \dots, M. \quad (13)$$

As for the partition, it can be uniform or not. An usual choice for non-uniform partitions is given by the Gauss-Chebyshev-Lobatto (GCL) distribution:

$$x_i = \frac{1}{2} \left[1 - \cos \frac{(i-1)\pi}{(M-1)} \right], \quad i = 1, 2, \dots, M. \quad (14)$$

The approximate solution, which is obtained by applying the DQ rules, is in general written as (Tomasiello 2007):

$$\bar{u}(x) = \mathbf{V}(x)^T \mathbf{d}, \quad (15)$$

where $\mathbf{d}^T = (u_1, \dots, u_M)$, while $\mathbf{V}(x)$ is the shape functions vector of which the j -th element is:

$$V_j(x) = \delta_{1j} + \sum_{r=1}^{M-1} A_{ik}^{(r)} \frac{x^r}{r!}, \quad (16)$$

being δ_{1j} the well-known Kronecker operator. Notice that equation (15) (with equation (16)) expresses an $M-1$ terms Taylor expansion around $x=0$. So, the residual is $O(x^M)$ (see also Shu 2000).

4.2.2. The discretized equations

Let us consider equation (1). By applying DQ rules to the spatial derivative, we get for the j -th arc:

$$\partial_t \rho_j(t, x_i) + \sum_{k=1}^{M_j} A_{ik}^{(1)} f_j(\rho_j(t, x_k)) = 0, \quad i = 1, \dots, M_j. \quad (17)$$

By discretizing with respect to the time simply by conventional FDs, as in the UE scheme, we finally obtain:

$${}^j \rho_i^{n+1} = {}^j \rho_i^n - \Delta t \sum_{k=1}^{M_j} A_{ik}^{(1)} f_j(\rho_j(t_n, x_k)) = 0, \quad (18)$$

$i = 1, \dots, M_j$, $n = 0, \dots, \eta_j$. For the queues, we apply the Euler scheme as described in Section 4.1.

As one can notice, the main difference with the UE scheme is in the fact that in the DQ scheme we have M_j (in general not equally spaced) grid points over the spatial axis instead of N_j intervals with length Δx_j .

5. SIMULATIONS

This section is devoted to the presentation of simulation results for the dynamics of queues and parts on supply networks. In particular, after considering a short case study to analyze the goodness of approximations for different numerical approaches, the attention is focused on a supply network to simulate a typical process for the tomatoes treatment.

5.1.1. Test 1 – Comparison between UE and DQ schemes

In what follows, we consider a supply chain with $N = 6$ suppliers, whose parameters (lengths, processing times and maximal fluxes) are in Table 1.

Table 1: Parameters of the supply chains

Supplier j	L_j	T_j	μ_j
1	1	1	40
2	0.5	1	35
3	1.5	3	30
4	2	4	15
5	0.5	1	10
6	0.5	1	5

For the simulation results, we assume:

- Empty suppliers and queues at $t = 0$.
- Total simulation time $T = 350$.
- Inflow $\varphi(t)$ for the first supplier defined as:

$$\varphi(t) := \begin{cases} 15, & 0 \leq t \leq 20, \\ 5 + \frac{t}{2}, & 20 < t \leq 50, \\ 60 - \frac{3}{5}t, & 50 < t \leq 100, \\ 0, & 100 < t \leq T. \end{cases} \quad (19)$$

Using the UE scheme with $\Delta t = 0.0125$ and $\Delta x_j = v_j \Delta t$, $j = 1, \dots, 6$, we have the queue buffer occupancies in Figure 2. Notice that the various queues decrease with slow velocities as $\mu_2 > \mu_3 > \mu_4 > \mu_5 > \mu_6$. Although the processing

velocities v_j , $j = 2, \dots, 6$, are the same, q_6 is the highest queue.

The same test is made by the DQ scheme, using $M = 6$ CGL grid points on each arc. Figure 3 shows the behaviour of the queue buffer occupancy $q_4(t)$. Evident similar numerical approximations are obtained.

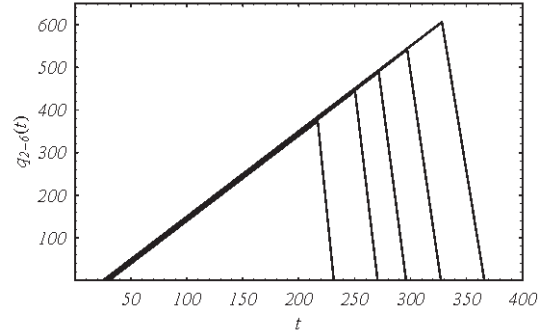


Figure 2: Queues $q_j(t)$, $j = 2, \dots, 5$; $q_2(t)$ is the first on the left; $q_3(t)$ is the second on the left, and so on

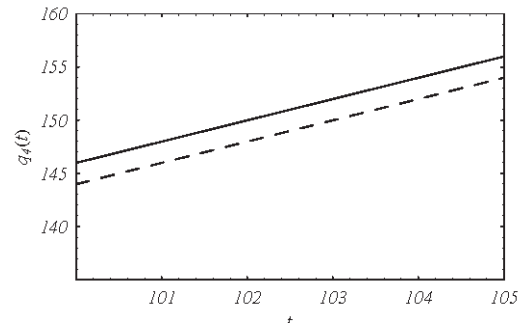


Figure 3: Numerical approximation of $q_4(t)$ via different numerical methods: UE scheme (continuous line); DQ scheme (dashed line)

Further remarks about the convergence errors (see Cutolo 2011 and De Falco 2016) are useful to compare the numerical methods, see Table 2.

Table 2: Errors for UE and DQ schemes

Δt	Errors for UE	Errors for DQ
0.00625	0.01175	0.01554
0.0125	0.02512	0.02812
0.025	0.07822	0.08212

From the obtained results, we get that the considered schemes have similar characteristics as for goodness of approximation.

5.1.2. Test 2 – Simulation of a process for treating tomatoes

We analyze some simulation results of a real supply network, that deals with tomatoes, see Figure 4. The network is used inside a little business company in Campania region (Italy) and, following the interpretation given in Göttlich 2006, each arc is either a conveyor belt or a machine.

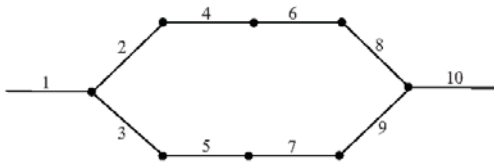


Figure 4: Supply network for tomatoes

In this case, the roles of each arc are described as follows. Arc 1 is a conveyor belt that transports tomatoes. According to a distribution coefficient 0.5, tomatoes are equally distributed to arcs 2 and 3, conveyor belts useful to discriminate goods for the production of peeled and diced tomatoes, respectively. Arcs 4 and 5 are machines with the same function, namely: peeling and skins separations for tomatoes. Arcs 6 and 7 work for a suitable selection of the processed tomatoes. Arcs 8 and 9 consider the closure of containers for tomatoes. Finally, arc 10 is useful for palletizing operations.

The supply network is simulated by the UE scheme with $\Delta t = 0.00625$ and the following parameters for the arcs: $L_i = T_i = 1$, $i = 1, \dots, 10$; $\mu_1 = 500$; $\mu_{10} = 15$; $\mu_j = 34 - 2j$, $j = 2, \dots, 9$; $\rho_i(0, x) = 0$, $i = 1, \dots, 10$; $q_i(0) = 0$, $i = 2, \dots, 10$; total simulation time $\bar{T} = 400$; input profile for arc 1 given by:

$$\varphi(t) = \begin{cases} t, & 0 \leq t \leq 70, \\ 70, & 70 < t \leq 80, \\ 80, & 80 < t \leq 150, \\ 0, & t > 150. \end{cases} \quad (20)$$

Function (20) is chosen considering the real cases of production inside the business company in discussion, namely: tomatoes are injected inside the system following, first, a linear increasing profile (hard injection); then, constant ones; finally, a decreasing one (light injection).

In Figures 5–7, queues are depicted. Notice that $q_2(t)$ is smoother than other queues as arc 2 receives directly goods from arc 1. Slopes of queues $q_j(t)$, $j = 3, \dots, 9$, are quite different from the one of $q_{10}(t)$, due to the values of μ_j , $j = 1, \dots, 10$. Moreover, although (20) is zero $\forall t > 150$, queues dynamics is very slow. This is confirmed by $q_{10}(t)$ that vanishes at a time instant, which is about 390, much higher than 150.

In Figure 8, we have the density of arc 3 for various instants of time. Unlike the behaviour of queues, arcs become full in a short time, i. e. arc 3 at $t = 40$ already reaches the maximal density (coincident with μ_3 as $v_3 = 1$).

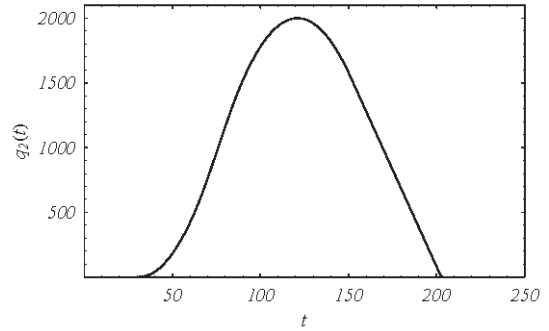


Figure 5: Behaviour of $q_2(t)$

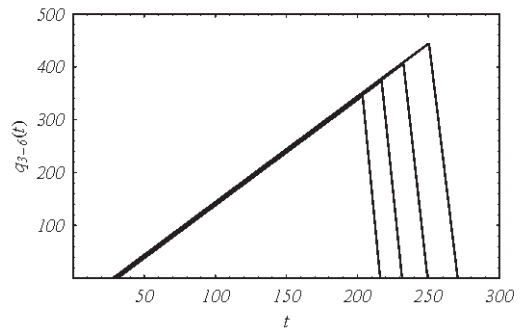


Figure 6: Dynamics of queues $q_j(t)$, $j = 3, \dots, 6$; $q_3(t)$ is the first on the left; $q_4(t)$ is the second on the left, and so on

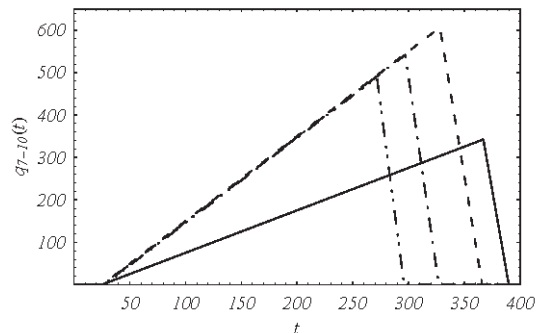


Figure 7: Queues $q_j(t)$, $j = 7, \dots, 10$; $q_7(t)$: dot dot dashed line; $q_8(t)$: dot dashed line; $q_9(t)$: dashed line; $q_{10}(t)$: continuous line

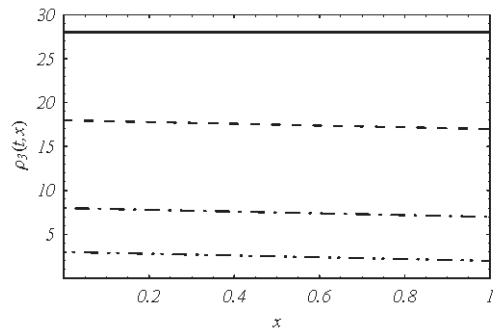


Figure 8: Density $\rho_3(t, x)$ for different time instants; $t = 5$ (dot dot dashed line); $t = 10$ (dot dashed line); $t = 20$ (dashed line); $t = 40$ (continuous line)

Notice that the presence of queues is principally due to $\varphi(t)$, v_j and μ_j , $j=1,\dots,10$. In general, as it is not possible to redesign the system in terms of lengths, processing times and maximal fluxes, the levels of $\varphi(t)$ determine the dynamics of the overall supply network. A possible optimization of supply systems modelled by a fluid-dynamic approach is nowadays still under investigation, especially in terms of criteria for a correct choice of $\varphi(t)$ in order to erase queues.

In our case, using an approach based on Situation Awareness, the aim is to establish an alternative choice for $\varphi(t)$. From environment data and using the procedure described in Section 1, we get that $\tilde{\varphi}(t)$, the new choice of $\varphi(t)$, foresees only constant levels, namely:

$$\tilde{\varphi}(t) = \begin{cases} 30, & 0 \leq t < 45, \\ 80, & 45 \leq t \leq 90, \\ 50, & 90 < t \leq 150, \\ 10, & t > 150. \end{cases} \quad (21)$$

Decisions for (21) are due to typical Italian weather conditions in months useful for tomatoes, from May to September. Assuming that the time t is expressed in days, a Situation Awareness procedure suggests to have constant levels of injections, that obey the following criteria: a light injection from May 1st to June 15th (about 45 days); a high profile from June 15 to July 30th; a medium injection from August 1st to September 30th; a low profile from September 30th.

Indeed, performances due to $\varphi(t)$ and $\tilde{\varphi}(t)$ are evaluated via the cost functional:

$$J := \frac{1}{10} \sum_{i=1}^{10} \left(\int_0^{\bar{r}} q_i(t) dt \right), \quad (22)$$

that measures the average area due to queues inside the supply system. As queues are strictly dependent on the input profiles, different values occur for the choices $\varphi(t)$ and $\tilde{\varphi}(t)$. We get that:

$$J(\varphi(t)) = 149889, \quad J(\tilde{\varphi}(t)) = 112742. \quad (23)$$

As expected, the adoption of a new profile is not suitable to erase queues in the overall system. Indeed, choosing $\tilde{\varphi}(t)$ allows only to decrease the contribution of queues. This last aspect is still under investigation.

6. CONCLUSIONS

Focusing on the model for supply systems proposed in Göttlich 2005 and Göttlich 2006, a real case of production network for tomatoes has been studied.

First, two numerical approaches have been proposed, proving that different schemes produce the same orders of approximation.

Then, using a procedure based on Situation Awareness, the simulations have showed that input profiles are able to modulate production queues, but not to erase them completely.

Further studies, based on Situation Awareness and Fuzzy Logic for the comprehension and the projection phases, are going to be developed in order to obtain robust optimization criteria for the performances of supply networks.

REFERENCES

- Armbruster D., Degond P., Ringhofer C., 2006. A model for the dynamics of large queueing networks and supply chains. *SIAM Journal on Applied Mathematics*, 66, 896–920.
- Armbruster D., Degond P., Ringhofer C., 2007. Kinetic and fluid models for supply chains supporting policy attributes. *Bulletin of the Institute of Mathematics Academia Sinica (N.S.)*, 2, 433–460.
- Armbruster D., Marthaler D., Ringhofer C., 2003. Kinetic and fluid model hierarchies for supply chains. *Multiscale Modeling and Simulation*, 2, 43–61.
- Bellman R., Casti J., 1971. Differential quadrature and long-term integration. *Journal of Mathematical Analysis and Applications*, 34, 235–238.
- Bressan A., 2000. *Hyperbolic Systems of Conservation Laws - The One - dimensional Cauchy Problem*. Oxford Univ. Press, Oxford.
- Bressan A., Crasta G., Piccoli B., 2000. Well-posedness of the Cauchy problem for $n \times n$ systems of conservation laws. *Memoirs of the American Mathematical Society*, 146 (694), viii+134.
- Canic S., Piccoli B., Qiu J., Ren T., 2015. Runge-Kutta Discontinuous Galerking Method for Traffic Flow Model on Networks. *Journal of Scientific Computing*, 63 (1), 233–255.
- Cascone A., D'Apice C., Piccoli B., Rarità L., 2008. Circulation of car traffic in congested urban areas. *Communications in Mathematical Sciences*, 6 (3), 765–784.
- Cutolo A., Piccoli B., Rarità L., 2011. An Upwind-Euler scheme for an ODE-PDE model of supply chains. *SIAM Journal on Scientific Computing*, 33 (4), 1669–1688.
- Dafermos C., 1999. *Hyperbolic Conservation Laws in Continuum Physics*. Springer Verlag.
- D'Aniello G., Gaeta A., Gaeta M., Lepore M., Orciuoli F., Troisi O., 2016. A new DSS based on situation awareness for smart commerce environment. *Journal of Ambient Intelligence and Humanized Computing*, 7 (1), 47–61.

- Daganzo C., 2003. *A Theory of Supply Chains*. Springer Verlag, New York, Berlin, Heidelberg.
- De Falco M., Gaeta M., Loia V., Rarità L., Tomasiello S., 2016. Differential Quadrature-based numerical solutions of a fluid dynamic model for supply chains. *Communications in Mathematical Sciences*, 14 (5), 1467–1476.
- De Rosa M. A., Franciosi C., 1998. On natural boundary conditions and DQM. *Mechanics Research Communications*, 25 (3), 279–286.
- De Rosa M. A., Lippiello M., 2007. Non-classical boundary conditions and DQM for double beams. *Mechanics Research Communications*, 34 (7-8), 538–544.
- De Rosa M. A., Lippiello M., 2016. Nonlocal frequency analysis of embedded single-walled carbon nanotube using the Differential Quadrature Method. *Composite Part B*, 84, 41–51.
- Endsley M. R., 1995. Toward a theory of situation awareness in dynamic systems. *Human Factors The Journal of the Human Factors and Ergonomic Society*, 37 (1), 32–64.
- Endsley, M. R., 2015. Situation awareness misconceptions and misunderstandings. *Journal of Cognitive Engineering and Decision Making*, 9 (1), 4–32.
- Fantuzzi N., Dimitri R., Tornabene F., 2016. A SFEM-Based Evaluation of Mode-I Stress Intensity Factor in Composite Structures. *Composite Structures*, 145 (1), 162–185.
- Helbing D., Lämmer S., 2005. Supply and production networks: from the bullwhip effect to business cycles. In *Networks of Interacting Machines: Production Organization in Complex Industrial Systems and Biological Cells*, D. Armbruster, A. S. Mikhailov, and K. Kaneko eds.. World Scientific, Singapore, 33–66.
- Kamarian S., Salim M., Dimitri R., Tornabene F., 2016. Free Vibration Analysis of Conical Shells Reinforced with Agglomerated Carbon Nanotubes. *International Journal of Mechanical Sciences*, 108-109 (1), 157–165.
- Göttlich S., Herty M., Klar A., 2005. Network models for supply chains. *Communications in Mathematical Sciences*, 3, 545–559.
- Göttlich S., Herty M., Klar A., 2006. Modelling and optimization of Supply Chains on Complex Networks. *Communications in Mathematical Sciences*, 4, 315–330.
- Kleijnen J.P.C., Smits M.T., 2003. Performance metrics in supply chain management. *Journal of the Operational Research Society*, 54 (5), 507–514.
- Leveque R. J., 2002. *Finite Volume Methods for Hyperbolic Problems*. Cambridge University Press, Cambridge.
- Longo F., Ören T., 2008. Supply chain vulnerability and resilience: A state of the art overview. *Proceedings of 20th European Modeling & Simulation Symposium*, pp. 527–533, September 17-19, Campora S. Giovanni (CS, Italy)
- Manzo R., Piccoli B., Rarità L., 2012. Optimal distribution of traffic flows at junctions in emergency cases. *European Journal on Applied Mathematics*, 23 (4), 515–535.
- Shu C., 2000. *Differential Quadrature and its Application in Engineering*. Springer Verlag, London.
- Shvartsman B., Majak J., 2016. Numerical method for stability analysis of functionally graded beams on elastic foundation. *Applied Mathematical Modelling*, 40 (5, 6), 3713–3719.
- Tomasiello S., 2007. A generalization of the IDQ method and a DQ based method to approximate non-smooth solutions. *Journal of Sound and Vibration*, 301, 374–390.
- Tomasiello S., 2013. DQ based methods: Theory and application to engineering. In *Handbook of Research on Computational Science and Engineering: Theory and Practice*, Publisher: IGI Global, Editors: J. Leng and W. Sharrock, 316–346.
- Tornabene F., Dimitri R., Viola E., 2016. Transient Dynamic Response of Generally-Shaped Arches Based on a GDQ-Time-Stepping Method. *International Journal of Mechanical Sciences*, 114, 277–314.
- Tornabene F., Fantuzzi N., Baccocchi M., Dimitri R., 2015. Free Vibrations of Composite Oval and Elliptic Cylinders by the Generalized Differential Quadrature Method. *Thin-Walled Structures*, 97 (1), 114–129.
- Tornabene F., Fantuzzi N., Baccocchi M., Dimitri R., 2015. Dynamic Analysis of Thick and Thin Elliptic Shell Structures Made of Laminated Composite Materials. *Composite Structures*, 133 (1), 278–299.
- Wang W., Fu W-P., 2010. Review of research on modeling and simulation for dynamics and complexity of supply chain systems. *Journal of System Simulation*, 22 (2), 271–279.
- Wickens C. D., 2008. Situation awareness: Review of Mica Endsley’s 1995 articles on situation awareness theory and measurement. *Human Factors*, 50 (3), 397-403.

AUTHORS BIOGRAPHY

MASSIMO DE FALCO received the master’s degree in Aeronautical Engineering from the University of Naples, Italy, in 1991 and the Ph.D. degree in Industrial Plants from the same university in 1994. He has held various research and consulting projects for leading national and international companies. He currently joins the Department of Management and Innovation Systems at the University of Salerno. His current research interests include analysis and management of industrial plants.

His email address is mdefalco@unisa.it.

VINCENZO LOIA received the master's degree in Computer Science from the University of Salerno, Italy, in 1984 and the Ph.D. degree in Computer Science from the University of Paris VI, France, in 1989. He is currently the head of the Department of Management and Innovation Systems at the University of Salerno. His current research interests include merging soft computing and agent technology to design technologically complex environments, with particular interest in Web Intelligence applications. He holds several roles in the IEEE Society. His e-mail address is loia@unisa.it.

LUIGI RARITÁ was born in Salerno, Italy, in 1981. He graduated cum laude in Electronic Engineering in 2004, with a thesis on mathematical models for telecommunication networks, in particular tandem queueing networks with negative customers and blocking. He obtained PhD in Information Engineering in 2008 at the University of Salerno discussing a thesis about control problems for flows on networks. He is actually a research assistant at CO.RI.SA., University of Salerno, Italy. His scientific interests are about numerical schemes and optimization techniques for fluid –dynamic models, energy systems modelling and queueing theory. His e-mail address is lrarita@unisa.it.

STEFANIA TOMASIELLO, Ph.D. in computer science (University of Salerno, Italy), is currently a senior researcher and project manager at CO.RI.SA. (Research Consortium on Agent Systems), University of Salerno, Italy. She was an adjunct professor of Fundamentals of Computer Science, Human-Computer Interaction, Computational Methods and Finite Element Analysis at the University of Basilicata, Italy. She is an expert evaluator (ex-ante and ex-post) of research projects joining academia and industry for the Italian Ministry of Economic Development and the Italian Ministry of University and Research. Her research interests lie in scientific and soft computing, fuzzy mathematics. She is member of the editorial board of International Journal of System Assurance Engineering and Management (Springer). Her e-mail address is stomasiello@unisa.it.

PETRI NET MODEL OF A PRODUCTION PROCESS FOR AGARICUS BISPORUS MYCELIUM

Latorre-Biel JI ^(a), Jiménez-Macías E ^(b), Pérez de la Parte M ^(c), Leiva-Lázaro FJ ^(d),
Martínez-Cámara E ^(e), Blanco-Fernández J ^(f)

^(a) Public University of Navarre, Tudela, Navarre, Spain
^(b,d,e) University of La Rioja, Logroño, Spain

^(a) juanignacio.latorre@unavarra.es, ^(b) emilio.jimenez@unirioja.es, ^(c) mercedes.perez@unirioja.es,
^(d) francisco.leiva@unirioja.es, ^(e) mercedes.perez@unirioja.es, ^(f) julio.blanco@unirioja.es

ABSTRACT

The development of a Petri net model in food industry is the topic of this document. In particular, the production of mycelium seeds of common mushroom (*Agaricus Bisporus*) is addressed. This product constitutes an essential first step in the cultivation of common mushroom. The model covers all the stages in the manufacturing of mycelium, detailing shared resources, conflicts, duration of tasks, as well as the amount of stored raw materials. As a consequence, the Petri net model is appropriate for decision making support by means of simulation and what-if analysis or optimization. The model is also suitable for structural analysis. Applying this model, it may be possible to improve the knowledge of the behavior of the production facility, as well as to identify bottlenecks, deadlocks, to quantify the number of common resources required, and to find out optimal or quasi-optimal assignment of resources to the different production tasks.

Keywords: Petri nets, *Agaricus Bisporus*, food industry, mycelium, decision support, simulation, model.

1. INTRODUCTION

The development of accurate models of production facilities may lead to the improvement of the expected results. In fact, the model of a system can be used as a practical tool for widening the knowledge of the system itself and its behavior. Furthermore, several techniques can be applied for structural analysis and performance evaluation with the purpose of quantifying the results expected from the system under a particular configuration (Latorre et al. 2013b).

As a consequence, developing a model of a production system may be a useful step for guaranteeing its sustainability and success (Recalde et al. 2004). Regarding the objectives of the production facility described in the model, the concept of success would be defined following different approaches, such as financial, social, or environmental criteria.

In particular, food production processes experience strong competition in a world-wide market. Continuous improvement and appropriate decision making are very

convenient items for the survival of the involved companies.

Many processes in food industry can be described as discrete event systems. Furthermore, Petri nets constitute a modelling formalism suitable for describing discrete event systems showing parallelism, concurrence, synchronization, and resource sharing (Silva 1993), (David and Alla 2010).

Several authors have already described Petri net models of production systems belonging to the food industry. See for example Guan et al. (2010), Latorre et al. (2015), Latorre et al. (2014), Latorre et al. (2013a), Latorre et al. (2012), Léger et al. (2011), Melberg and Davidrajah (2009), or Shikanai et al. (2008).

Leiva et al. (2015a) addresses the analysis of the environmental impact of the *Agaricus bisporus* mycelium production, describing a production process for this product. Moreover, Leiva et al. (2015b) addresses the complete process of cultivation of the mushroom. However, as far as the authors of this document know, there is not any Petri net model of a facility for producing mycelium seeds reported in the literature.

In this paper, a Petri net model of a facility for the production of mycelium seeds of the common mushroom is described. The model that is detailed in this document has been developed as a result of a tradeoff between level of detail and size, since the computational cost of simulating a Petri net model is proportional to the its size.

Next section is devoted to the description of the production facility and the production process of mycelium seeds, while section 3 introduces briefly the modelling formalism. Section 4 details the Petri net model of the system and the following two sections focus on the conclusions and the bibliographical references respectively.

2. PRODUCTION PROCESS

In the present paper, the production process of an essential raw material for the cultivation and production of common mushroom is discussed. In particular, a Petri net model of the production process of mycelium seeds of *Agaricus Bisporus* is developed.

Common mushroom is one of the most successful mushroom consumed throughout the world, due to both its appreciated gastronomical and pharmacological properties.

Mycelium is the mass of hyphae and constitutes the vegetative body of a mushroom. In order for the mycelium to reproduce and form fruiting bodies, it is necessary that two compatible monokaryotic mycelia join and form a dikaryotic mycelium.

The three main stages in the mycelium production process, which are considered in the Petri net model developed in the present paper are:

a) Preparation of the growth medium for the mycelium.

At this stage, sorghum, wheat, rye seeds, or other appropriate products are selected as growth medium for the mycelium.

These products are processed for improving the growth performance of mycelium.

b) Creation of the inoculum.

A first phase of this stage starts with the cultivation of the mycelium in Petri dishes, under artificial culture medium in a lab.

c) Preparation of the mycelium seed packages.

The mushroom mycelium, inoculated in grains, is incubated at an optimal temperature. When the incubation finishes, the seeds are kept at low temperature and mixed with a compost preparation to produce seed packages in the culture.

3. MODELLING FORMALISM

Petri nets constitute a modeling paradigm particularly gifted for describing discrete event systems showing a complex behavior, such as parallelism, concurrence, synchronization, or competition for shared resources.

Following Silva (1993) it is possible to define a Petri net in the following way:

Definition 1. A marked Petri net or net system R is a couple $\langle N, M_0 \rangle$, where

i) N is a Petri net, i.e. a four tuple $\langle P, T, Pre, Post \rangle$, such that P and T are disjoint and finite sets of places and transitions respectively, $Pre: P \times T \rightarrow \mathbf{N}$, and $Post: P \times T \rightarrow \mathbf{N}$.

ii) M_0 is an initial marking, i.e. an application of P on the set \mathbf{N} of non-negative integers.

□

The model to be presented in this paper is timed. This means that the duration of some production tasks are integrated in the model of the system. In particular it will be considered a T-timed Petri net, where time will be added to the transitions of the Petri net model.

According to David and Alla (2010), it is possible to state the following definition:

Definition 2. A T-timed Petri net is a pair $\langle R, Tempo \rangle$ such that:

R is a marked Petri net;

Time is a function from the set T of transitions to the set of positive or zero rational numbers. $Tempo(T_j) = d_j =$ timing associated with T_j .

□

The evolution rules of a Petri net is modified, when introducing time. In the case of a T-timed Petri net, an enabled transition T_j does not become necessarily fireable, since an additional necessary condition implies that a time $Tempo(T_j) = d_j$ should elapse after enabling.

Two additional items are worth to be mentioned at this point. There may be transitions with a 0 time associated, called immediate transitions. For example, if T_k is an immediate transition, then $Tempo(T_k) = d_k = 0$, meaning that, when enabled, it becomes also fireable. Furthermore, a conflict may lead to indeterminism in the firing of the transitions involved, since the firing of some of them implies the disabling of the others.

In this document immediate transitions are represented by thin bars, while timed transitions (delay time greater than zero) are drawn by means of rectangles.

4. DEVELOPMENT OF THE MODEL

The model of the production facility has been developed following a bottom-up approach. This methodology consists in developing a detailed model of every subsystem and linking them by means of certain places or transitions.

The main subsystems of the production system are three:

a) Facility for the preparation of the growth medium of the mycelium.

This stage of the production process consists of the preparation of the bags of rye, sorghum, or wheat, which will be inoculated by the mycelium.

The model for this subsystem has been represented in Figure 1.

b) Facility for the creation of the mother culture and mother spawn.

This stage is focused on the creation of the culture medium for the mycelium and its inoculation in the growth medium developed in the previous subsystem.

The model for this subsystem is represented in Figure 2.

c) Facility for the creation of the final spawn or mycelium seed packages.

In this stage of the production process, the mycelium is inoculated in the growth medium and is left to sprout until the mycelium has completely colonized it. The resulting product is packaged and stored until its expedition to the customers, which use to be composters creating compost from the seed packages.

The model for this subsystem, in conjunction with the previous one, has been depicted in Figure 2.

4.1. Subsystem 1: preparation of the growth medium

The model of this facility, see Figure 1, consists of 39 places and 28 transitions. Some of the transitions are timed, represented by rectangles and the rest of them are immediate transitions, depicted by thin bars.

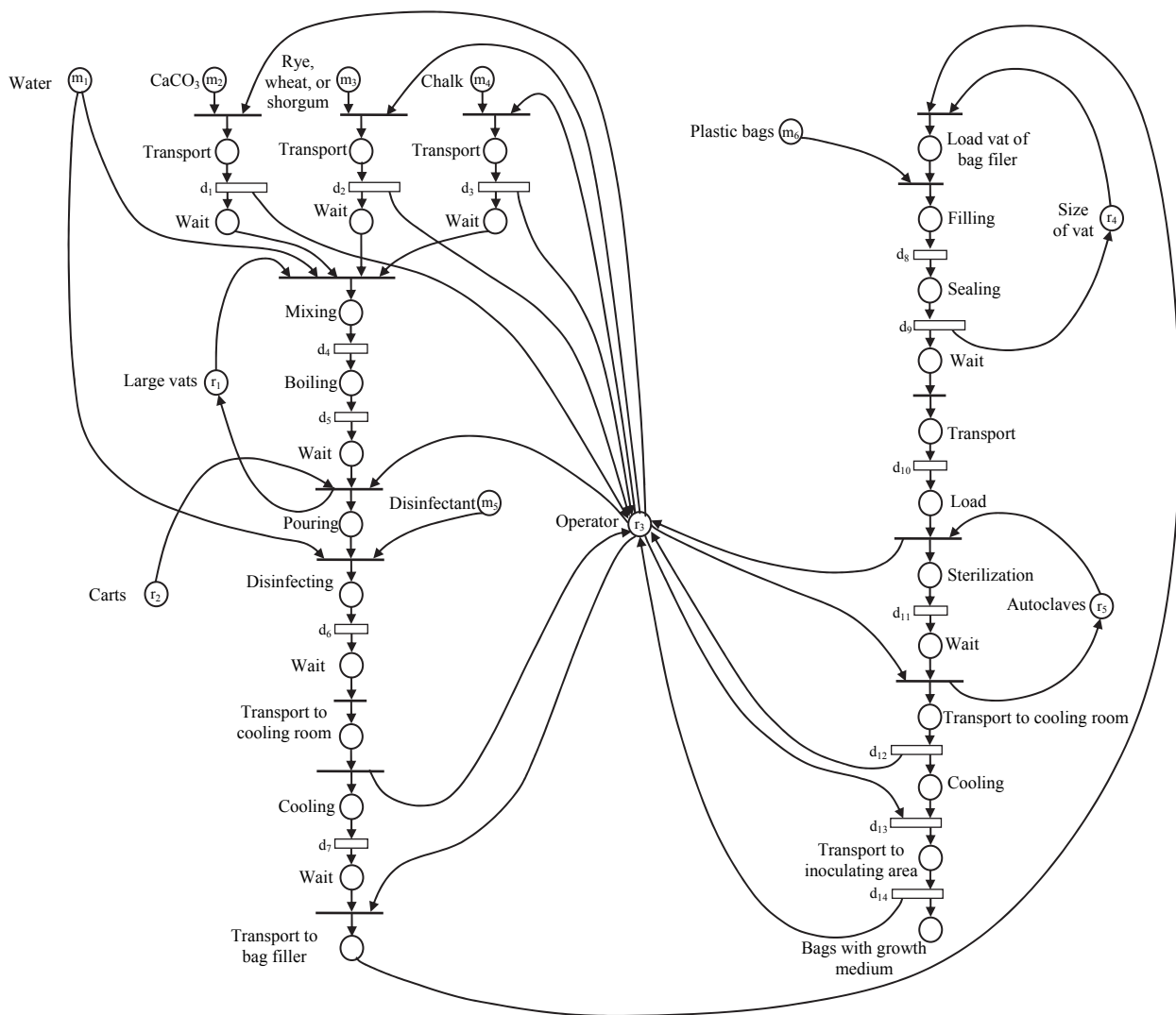


Figure 1. Model of the facility for the preparation of the growth medium of the mycelium.

This model has been depicted in two columns that represent two sequential stages in the production process.

The first step represents the raw materials supply, followed by the stage of mixing and boiling the raw materials. Next, the operation of disinfection begins, to remove pathogen microorganisms, which might reduce drastically the efficiency of the production process.

The following stage is the cooling process, followed by the filling of plastic bags with the growth medium.

The last steps are a sterilization phase in autoclaves, another cooling process and the transport to the inoculating area, which leads to a place labelled “Bags with grow medium”, which is a link place to the model represented in Figure 2. In fact, this same place has also been drawn in the model representing the creation of the mycelium seed packages.

Analogously, there are another three places that are shared by both models. One of them is labelled “Carts”, and represent the transportation means used in most of the conveying tasks of materials in the production

process. This resource is used in this subsystem and released in subsystem 3, after the storage of the final product. Another shared place is labelled “operator” and represents a shared resource, the operators, who can devote their time to different tasks. The last shared place is labelled “plastic bags” and represents the bags used to contain the growth medium for the mycelium.

This model presents several freedom degrees, which can be implemented as fixed numbers, stochastic values, or controllable parameters, also called decision variables, depending on the conditions of the real facility that has been modelled.

Some of these freedom degrees are represented by means of the initial marking of certain places. Others are associated to the conflicts that arise in the evolution of the Petri net model. It has not been included in this model, but it is even possible to introduce structural parameters, as the weight of certain arcs, to represent, for example, the size of the conveying lot of product or raw materials at certain stages of the process.

The freedom degrees associated to the initial marking of certain places have been classified into two categories:

- a) Raw materials, represented by the letter “m” inside the places.
- b) Shared resources, represented by the letter “r” inside the places.

The main difference between the elements of both categories is that raw materials are consumed and resources are used and released for additional uses. The subsequent wear of the resources, as a consequence of their reiterated usage, has not been considered in this model, but it may be added easily.

The list of raw materials in this system 1 is the following:

m₁: water

m₂: calcium carbonate

m₃: rye, wheat or sorghum

m₄: chalk

All these first four raw materials are direct components of the growth medium for the mycelium.

m₅: disinfectant for disinfecting the growth medium

m₆: plastic bags for sealing inside the growth medium, prior to the sterilization and cooling processes.

Moreover, the list of shared resources in this same subsystem are:

r₁: large vats for mixing and boiling the raw materials

r₂: carts for conveying the semifinished and finished products

r₃: operator developing any general task in the production process

r₄: size in kg of the vat in the filling and sealing machine for the production of growth medium bags

r₅: autoclaves for the sterilization of the growth medium bags.

Other parameters of the model for this first subsystem are the delay times associated to the timed transitions: **d₁** to **d₁₄**.

Many of these timed transitions are related to conveying operations, such as **d₁**, **d₂**, **d₃**, **d₁₀**, **d₁₂**, and **d₁₄**

Other timed transitions are related to production operations, such as mixing, boiling, disinfecting, cooling, filling, sealing, or sterilization in autoclaves.

Additional freedom degrees are the conflicts of the net, i.e. the places with more than one output arc to transitions with the same associated delay, when the marking of the place is not able to fire all the output transitions simultaneously. In this case there is a conflict in the place “Operator”.

This conflict is associated to the need of defining a managing strategy for the assignment of the available operators to the different tasks that may arise along the production cycle.

There is a structural conflict in the place “Water” but if there is not any shortage in the water supply, it is not expected that this structural conflict becomes an actual conflict. In other words, if there is enough water, it is not necessary to choose in which production operation should be used. All the operations can receive all the water they request.

Finally, it might be possible to add structural parameters in the Petri net model of this subsystem as freedom degrees, defining, for example, the lot size in certain transport operations or in the processing tasks of certain machines. These lot sizes would be limited by the capacity of the carts or machines. However, simulating the results under different capacities for the industrial equipment, some conclusions could be raised on the decisions to acquire and install these elements.

4.2. Subsystems 2 and 3: preparation of the mycelium seed packages

The model of these two subsystems has been represented in Figure 2 and is composed of 47 places and 35 transitions.

The different steps of the production process are performed in different stages of the facility, represented sequentially in the Petri net model, depicted in two columns. The first step is the creation of the culture medium for the mother culture and it is performed in the lab, by specialized technicians. This step is followed by a sterilization of this medium and the inoculation of the mycelium. This mycelium grows in Petri dishes and later on in rye bags, starting a first stage in sprouting chambers. The obtained mycelium is inoculated again twice in rye bags, followed by growth in sprouting chambers to maximize the production results and a final storage precedes the expedition to the customer. A final place labelled “sold” inventory the mycelium seed packages sold to the customers.

These subsystems present several freedom degrees, which constitute one of the interesting potential of the model presented in this paper. These freedom degrees allow the application of different methodologies, such as what-if analysis or optimization to check different configurations of the model that lead to the best achievement of the objectives of the company exploiting the production facility.

The freedom degrees belong to the following categories:

- 1) Initial marking:
 - a. Raw materials (**m₅** to **m₁₀**)
 - b. Resources (**r₂**, **r₃**, and **r₇** to **r₁₀**)
- 2) Delay associated to timed transitions (**d₁₅** to **d₃₄**)
- 3) Actual conflicts

More in detail, the raw materials not detailed in the previous section are the following:

m₇: malt extract

m₈: Glucose and agar. They are in fact two different raw materials and could be represented by independent parameters associated to different places.

m₉: Peptone

The previous raw materials are the basis for the culture medium for the mother culture, which is completed with **m₁₀**.

m₁₀: mycelium

Analogously, the resources not explained in the previous section are the following ones:

r₆: technician for laboratory operations

- r_7 : Petri dishes for the mother culture
- r_8 : plastic containers for a culture first sprouting stage.
- r_9 : size of the sprouting chambers, measured in carts filled with product
- r_{10} : inoculating machines

The delays associated to timed transitions can be controllable parameters or not, depending on the possibility for them to change as a result of a decision. For example, if it is possible to change the layout of the production system, modifying the time required for

certain transport operations, the associated parameter d_i can be considered a controllable parameter.

Many time delays are associated to transport operations, such as d_{20} , d_{22} , d_{24} , d_{26} , d_{28} , d_{30} , and d_{32} .

Other delays associated to timed transitions are associated to operations, such as mixing the raw materials, disinfecting the culture medium, inoculating the mycelium, growing and sprouting, filling and sealing, as well as the last operations of storage and expedition.

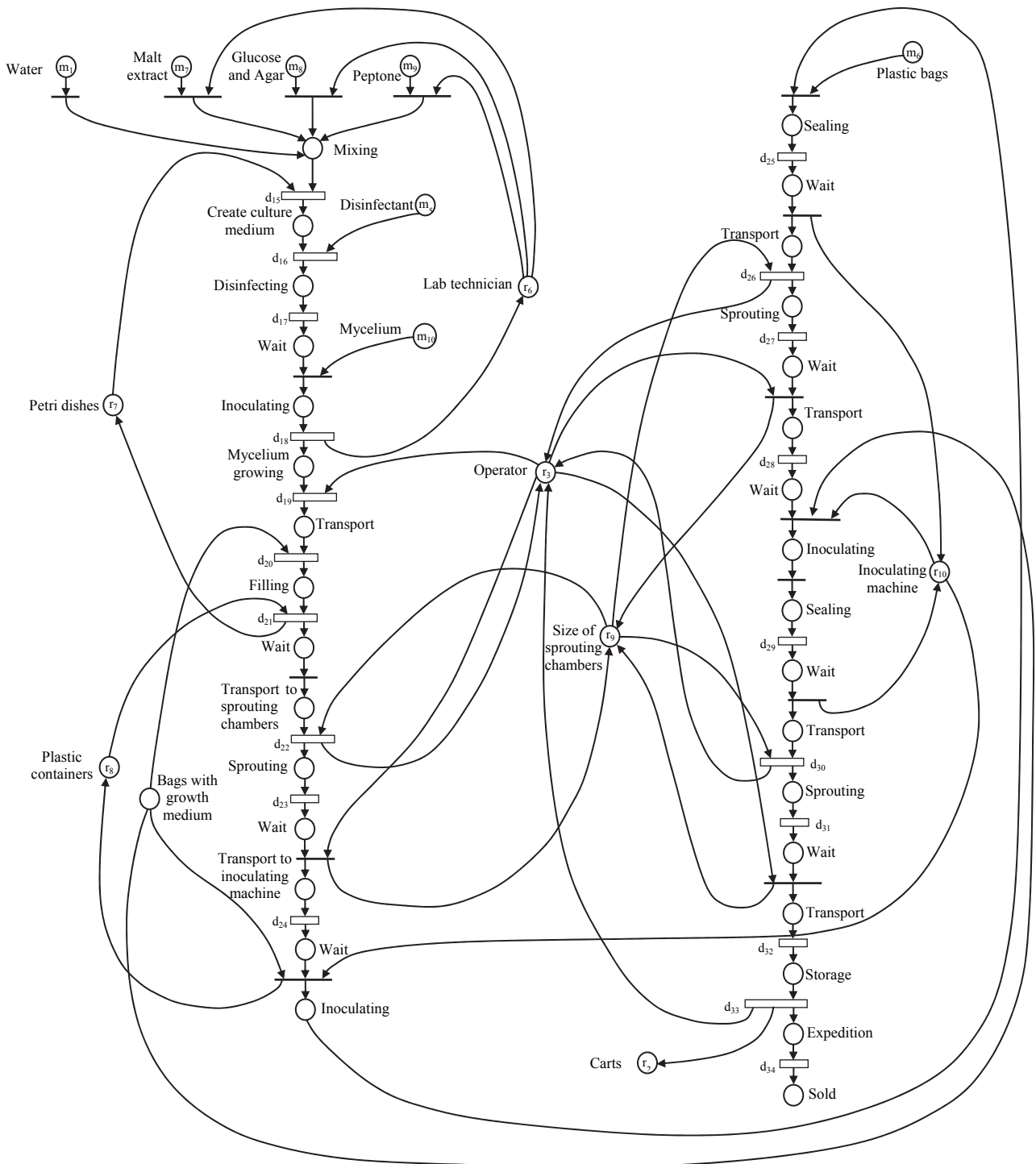


Figure 2. Model of the facility for the preparation of the mycelium seed packages.

Finally, the freedom degrees associated to conflicts of the Petri nets are the following ones:

- a) Place labeled “Lab technician”. The actual conflict requires dealing with the priorities of the output transitions, in order to determine the optimal sequence of mixing the raw materials to elaborate the culture medium.
- b) Place labeled “Operator”. Already mentioned in the previous section.
- c) Place labeled “Bags with growth medium”. This place is a link place with the model of subsystem 1. If there are enough bags for all the requests there will not be any actual conflict. Otherwise, it will be convenient to decide the best strategy for assigning this resource to the different production operations.
- d) Place labeled “Size of sprouting chambers”. If there is enough place in the sprouting chambers for all the production needs, there will not be any actual conflict. Otherwise, it is necessary to find the optimal assignment of this resource to the production requests.
- e) Place labeled “Inoculating machine”. Similar to the previous ones.

5. CONCLUSIONS

A model of a production facility of mycelium seed packages of *Agaricus bisporus* has been presented in this document. A T-timed Petri net has been chosen as modeling formalism to represent the facility (seen as a discrete event system) due to its suitability to naturally describe the particularities of such a facility. As a result, a Petri net model with 82 places and 63 transitions is described and depicted in detail in two figures. This model explicitly includes a quantitative representation of different freedom degrees of the facility. Each one of them can be specified as fixed numbers, controllable parameters, or stochastic values, depending on the real facility in a particular application. This model contains 20 parameters in the initial marking of the net, representing amounts of raw materials and resources, 34 parameters in the delay associated to a same number of timed transitions, and 5 structural conflicts. All the freedom degrees require a particular configuration for operating the production facility and the model allows testing different configurations and simulating the evolution of the system to quantify the performance of every solution. Furthermore, the model itself can be used to improve the knowledge of the real system, performing structural analysis, and identifying bottlenecks and deadlocks; thus, being a practical tool for decision making support.

REFERENCES

David, R. and Alla, H. 2010. Discrete, Continuous, and Hybrid Petri Nets. Springer.

Guan, S., Nakamura, M., and Shikanai, T. 2010. Hybrid Petri Nets and Metaheuristic Approach to Farm Work Scheduling. In Aized, T. (Ed.) *Advances in PN Theory and Applications*. Chapter 8. Sciyo.

Latorre, J.I., Jiménez, E., Blanco, J., Sáenz, J.C. 2015. Decision Support System, Based on The Paradigm of the Petri Nets, for the Design and Operation of a Dairy Plant. *International Journal of Food Engineering*, 11(6): 767-776.

Latorre, J.I., Jiménez, E., Blanco, J., Sáenz, J.C. 2014. Optimal Design of an Olive Oil Mill by Means of the Simulation of a Petri Net Model. *International Journal of Food Engineering*, 10(4): 573-582.

Latorre, J.I., Jiménez, E., Blanco, J., Sáenz, J.C. 2013. Integrated Methodology for Efficient Decision Support in the Rioja Wine Production Sector. *Int. Journal of Food Engineering*, 9(3): 267-278.

Latorre, J.I., Jiménez, E., Pérez, M., 2013. Petri nets with exclusive entities for decision making. *International Journal of Simulation and Process Modeling*, 8(1): 66 - 73.

Latorre, J.I., Jiménez, E., Blanco, J., Sáenz, J.C. 2012. Decision making in the Rioja wine production sector. In *Proceedings of the 24nd European Modelling and Simulation Symposium (EMSS 12)*. Vienna, Austria, pp. 452-457.

Léger, B., Naud, O., Gouache, D., 2011. Specifying a strategy for deciding tactical adjustment of crop protection using CPN tools. *Congress of the European Federation for Information Technology in Agriculture, Food and Environment Efitia 2011*.

Leiva, F.J., Saenz-Díez, J.C., Martínez E., Jiménez E., Blanco J. 2015. “Environmental impact of *Agaricus bisporus* mycelium production”. *Agricultural Systems* 138 (2015) 38–45.

Leiva-Lázaro, F.J., Blanco-Fernández, J., Martínez-Cámara, E., Latorre-Biel, J.I., Jiménez-Macías, E. “Mushroom cultivation process, *agaricus bisporus* variety: comparison between traditional and climate controlled cultivation and identification of environmental impacts of the production processes”. *Proc. of the Int. Workshop on Simulation for Energy, Sustainable Development & Environment 2015*. Bruzzone et al. Eds.

Melberg, R., Davidrajah, R. 2009. Modeling Atlantic salmon fish farming industry. In *Proceedings of the IEEE International Conference on Industrial Technology. ICIT 2009*. Pages 1-6.

Recalde, L.; Silva, M.; Ezpeleta, J.; and Teruel, E. 2004. Petri Nets and Manufacturing Systems: An Examples-Driven Tour. In Desel, J.; Reisig, W.; and Rozenberg, G. (Eds.), *Lectures on Concurrency and Petri Nets: Advances in Petri Nets*, LNCS / Springer-Verlag. 3098: 742-788.

Shikanai, T.; Nakamura, M.; Guan S.; Tamaki, M. 2008. Supporting system for management of agricultural corporation of sugarcane farming in Okinawa Islands. *World conference on agricultural information and IT, IAALD AFITA WCCA 2008*, Tokyo University of Agriculture, Tokyo, Japan, 24 - 27, pp. 1101-110.

Silva, M. 1993. Introducing Petri nets. In *Practice of Petri Nets in Manufacturing*, Di Cesare, F., (editor), pp. 1-62. Ed. Chapman&Hall.

PETRI NET MODELLING AND OPERATIONAL OPTIMIZATION OF A FACILITY FOR THE PREPARATION, CULTIVATION AND PRODUCTION OF COMMON MUSHROOM (AGARICUS BISPORUS)

Latorre-Biel JI ^(a), Jiménez-Macías E ^(b), Pérez de la Parte M ^(c), Leiva-Lázaro FJ ^(d),
Martínez-Cámara E ^(e), Blanco-Fernández J ^(f)

^(a) Public University of Navarre, Tudela, Navarre, Spain
^(b,d,e) University of La Rioja, Logroño, Spain

^(a) juanignacio.latorre@unavarra.es, ^(b) emilio.jimenez@unirioja.es, ^(c) mercedes.perez@unirioja.es,
^(d) francisco.leiva@unirioja.es, ^(e) mercedes.perez@unirioja.es, ^(f) julio.blanco@unirioja.es

ABSTRACT

A Petri net model of a facility for cultivating common mushroom (*Agaricus Bisporus*) is presented and implemented in the development of a decision support system for the operation of the facility. The formalism of the compound Petri net has been chosen for its ability for including parameters in the incidence matrices of the model. The decision support system is based in the solution of an optimization problem by means of a metaheuristics combined con simulations of the model of the system. The implementation of the system may lead to an improvement in the performance of the facility, while reducing the required resources, the produced wastes and the costs involved in the procurement of raw materials.

Keywords: Petri nets, farming company, decision support system, optimization, modelling, simulation, *Agaricus Bisporus*, common mushroom.

1. INTRODUCTION

Simulation and simulation-based optimization constitute nowadays approaches that find many applications in decision support systems (Longo et al. 2014), (Latorre et al. 2011), and (Latorre et al. 2010).

Decision support systems applied to companies that face a globalized competence has been proven to be very successful. They ease the hard task of making decisions that may affect the profitability of a company, which can be the difference between the success and the failure.

Petri net based modelling for decision making in food industry has been addressed by diverse authors. As examples, it can be considered the sector of wine production (Cicirelli et al. 2010), (Latorre et al. 2013), and (Latorre et al. 2012), sugarcane cultivation and harvesting (Guan et al. 2010), (Shinakai et al. 2008), olive oil extraction (Latorre et al. 2014), salmon fish farming (Melberg and Davidrajuh, 2009), dairy products manufacturing (Latorre et al. 2015), or wheat crop protection (Leger et al. 2010).

The world commercialization of common mushrooms (*Agaricus bisporus*) reaches every year a few million

tons produced by around 70 countries (Leiva et al. 2015a). However, production of common mushroom (*Agaricus bisporus*) has not received so much attention by the research community than other agricultural sectors. An overview of the process, from the point of view of sustainability and life cycle assessment can be found in Leiva et al. (2016), Leiva et al. (2015a), and Leiva et al. (2015b).

This fact, together with the need of developing tools for the efficient decision support of farmers and producers of mushrooms has motivated the present research.

In this paper, a description of the development of a decision support system for the optimal management of a facility for composting and producing mushrooms is presented.

This system is based in obtaining a model of the system by using the formalism of the generalized Petri nets (Silva 1993) and simulating it under different configurations of the decision variables to select the configuration that better fits with the objective of the management of the company.

The rest of the paper is organized as follows. Sections 2 and 3 describe the generalities on the facilities and processes for composting and mushroom cultivation. The formalism considered to develop the model of the system, the paradigm of the Petri nets, is introduced in section 4. In sections 5 and 6 the models of the production facilities is presented and explained. Section 7 deals with the decision-making methodology that can be constructed by the integration of the model of the system, a simulation tool and an optimization algorithm. The following section presents the conclusions and future research lines, while the last section lists the bibliographical references.

2. PREPARATION OF MUSHROOM CULTIVATION: COMPOST PRODUCTION.

The process of production of compost for mushroom cultivation can be carried out by the development of the following stages (Leiva et al. 2016):

- a) Composting batch preparation. This first stage starts by soaking an amount of wheat straw and continues by homogeneously mixing the rest of raw

materials: poultry manure, gypsum, calcium carbonate, urea, and sulfate. The process ends by building up a compost pile in an appropriate place: a tunnel.

- b) Tunnel composting. This stage consists of a wind-row composting process of piles of mixture of around 3m high, 5m wide, and 100m long. The process lasts around 3 days after turning the piles to keep homogeneous the compost temperature. During the process many parameters, such as moisture content, temperature, pH, and aeration are controlled.
- c) Pasteurization. This process is carried out in a closed chamber and reduces the content of ammonia in the compost. Aeration is controlled by air recirculating and the temperature is kept in safe limits, reaching up to 60°C.
- d) Packaging. Planting packages are manufactured and stored for the cultivation of the mushroom.

3. CULTIVATION PROCESS

The second facility, whose model is presented in this paper, carries out the cultivation of common mushroom. The different stages that compose this process of cultivation are described in the following paragraphs (Leiva et al. 2015a).

- a) Preparation of the soil. This stage starts with the disinfection of the work area, where peat, water, and fungicides are mixed and placed in a container.
- b) Preparation of the growing chambers. At this stage the growing chambers are disinfected, the seed packages are placed in cages and the previously prepared soil is poured covering the seed packages. Eventually, water is added to start the following stage.
- c) Growing process. In order to favor the development of this stage fungicides and pesticides are applied. Once the fruition is completed, the product is harvested manually and placed into boxes for its expedition.

4. THE PETRI NETS PARADIGM

As it has been mentioned before, the modeling formalism considered in this document is the Petri nets. For a formal definition of the generalized Petri nets and more information about the fundamentals of this formalism it may be consulted Silva (1993).

The decision making methodology to be presented in this paper, requires the integration in the model of the system of some freedom degrees belonging to the original discrete event system. These freedom degrees, represented in the Petri net model by controllable parameters, determine a particular configuration of the model of the system. Solving a decision making problem, under this approach, consists of finding the configuration of the controllable parameters that allow the system to achieve best the goals of the discrete event system.

The controllable parameters can play different formal roles in the Petri net model of the system. In particular

they may belong to the initial marking of certain places, to the incidence matrices, the delays associated to transitions in T-timed Petri nets, or the priorities of the transitions involved in actual conflicts, just to give some examples.

5. MODEL OF THE COMPOSTING SYSTEM

The process of constructing a Petri net model of a system, in this case a facility devoted to the production of compost for the preparation of mushroom cultivation, can be carried out by means of two different approaches. Following Silva (1993), it is possible to classify the modeling approaches into two methodologies with wide application into the development of Petri net models for discrete event systems.

a) Top-bottom modelling.

This approach starts with the development of a global model with low level of detail. Its number of places and transitions is reduced.

A second step in the application of this modelling approach is the development of the subsystems expanded from the high level model. These new model, with more details, provide with a larger amount of information.

b) Bottom-up modelling.

This second approach is applied by the development of independent models for the different subsystems that compose the discrete event system of interest.

A subsequent step consists of detailing the links between the models that allow integrating them in the constitution of a complete model, with high degree of detail, describing the structure and the state of the discrete event system.

The models developed in this paper have been built up following the approach of bottom-up modelling.

The construction of the Petri net model of the composting facility has been developed with the purpose of elaborating a decision support tool that may ease the management tasks of such a facility. For this reason, the constructed models present a series of controllable parameters or decision variables, whose values will define the solution to a decision making problem.

These controllable parameters are mainly defined as the initial marking of several places of the model. Even though it has not been considered explicitly in these models, other controllable parameters can be associated to the delay times of a T-timed Petri net model. Some tasks might present a duration that can be changed depending on the equipment acquired, on the way the operations are performed, on the layout of operators and machines, etc. Hence, they may also be considered as decision variables, depending upon the type of decision problem stated.

The model of the system for producing the compost that has been developed is depicted in figure 1. Some parameters are presented in the model, which represent the freedom degrees of the model and require a decision-making process for achieving an optimal or

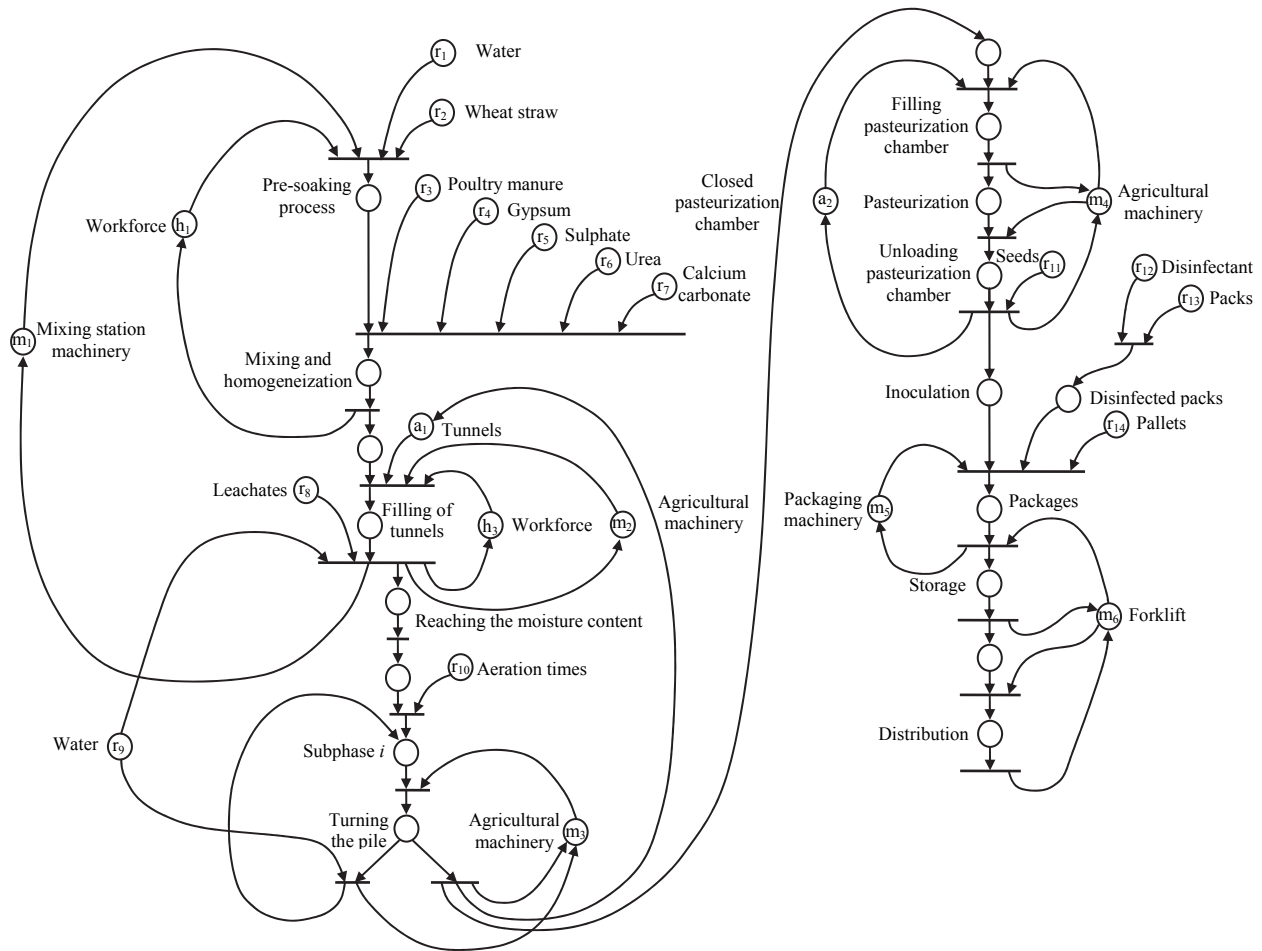


Figure 1. Model of the mushroom compost production.

quasi-optimal configuration of the system. As it has been said, some of the parameters of the model are related to the initial marking, while others are associated to the elements of the incidence matrices (structural ones).

The marking parameters are classified in four groups:

- a_i**. Production areas.
- h_i**. Human resources.
- m_i**. Production machinery, including the operators required to handle the industrial equipment.
- r_i**. Raw materials.

More in detail, where the data between brackets represent the units of the item associated with each token present in the place:

- a₁**. Tunnels (m³ of raw materials).
- a₂**. Closed pasteurization chamber (m³ of compost).
- h₁**. Operators for mixing the raw materials (person).
- h₂**. Operators for filling the tunnels (person).
- m₁**. Machinery of the mixing station (kg of wheat straw).
- m₂**. Farm tractor with implement for filling the tunnels (tractor and driver).
- m₃**. Farm tractor with implement for turning the pile of compost (tractor and driver).

- m₄**. Farm tractor with filling and unloading the pasteurization chamber (tractor and driver).
- m₅**. Packaging machinery (19 kg of compost, which conforms a package of compost inoculated with mycelium).
- m₆**. Forklift for storage and loading the trucks for distributing the compost (forklift and operator).
- r₁**. Water for the pre-soaking process (litres).
- r₂**. Wheat straw (kg).
- r₃**. Poultry manure (kg).
- r₄**. Gypsum (kg).
- r₅**. Sulphate (kg).
- r₆**. Urea (kg).
- r₇**. Calcium carbonate (kg).
- r₈**. Leachates for increasing the moisture content of the compost in the tunnel (kg).
- r₉**. Water for increasing the moisture content of the compost in the tunnel (kg).
- r₁₀**. Aeration times (times of aeration of the same duration).
- r₁₁**. Seeds of mycelium for the inoculation of the compost (g).
- r₁₂**. Disinfectant for the packages (litres).
- r₁₃**. Packages for the compost (units).
- r₁₄**. Pallets for transporting the compost packages (units).

It may be possible to incorporate structural parameters to the model of the system, in the form of weights associated to the different arcs. Since many arcs represent the flow of raw materials, as well as semifinished and finished products, some weights would represent the size of the production of conveying lot, a parameter that might have a direct impact in the yield of the production system. Despite the fact that structural controllable parameters have not been included in the model of the system, it is easy to introduce them if at a given facility it is found relevant to count on them as decision variables.

Other freedom degrees that may appear in the model are related to conflicts. In particular, structural conflicts are present in all the places with more than one output arcs. These structural conflicts are transformed into actual conflicts, real freedom degrees of the model, if the number of tokens in the place is smaller than the addition of the weights of all the output arcs. If this is the case, it is not possible to fire all the output arcs simultaneously and it might be necessary to assign priorities to the output transitions in order to solve the indeterminism that may arise in this situation.

Structural conflicts are present in the model depicted in figure 1. In particular it is possible to see the following ones:

- a) Place labeled "Water". If water is not a scarce resource, it is possible to say that it will not be necessary to choose the operation that will receive water to the detriment of other production operations. As a consequence, it is not expected that this structural conflict would be transformed into an actual conflict.
- b) Place labeled "Turning the pile". In this case, the process may be repeated several times until proceeding with the following step of the production process in the pasteurization chamber. In particular, one of the output arcs proceeds with a new turning of the pile, while the other starts the pasteurization. There is an actual conflict that should be solved with a variable priority, since a fixed one would prevent a complete process of several turnings and the subsequent pasteurization. This controllable parameter should be part of a solution for the decision problem. In particular it should be decided the number of times the pile is turned over.
- c) Place labeled "Forklift". This conveying resource may be used in different production operations. Every one of these operations would be associated to a different output arc of the place that represents this resource in idle state. At a given moment, it might happen that, the forklift is required in several operations simultaneously and then a decision must be made to solve the actual conflict. The decision on the assignment of this shared resource to the different production tasks should be a part of the solution of a decision problem stated on this system.

6. MODEL OF THE FACILITY TO PRODUCE MUSHROOMS

The model of this second system, a facility for cultivating mushrooms, has been also developed by means of a bottom-up approach. This model has been depicted in figure 2.

The decision variables of this model, may belong to several categories. Some of them have been already implemented in the model, the initial marking of some places and the actual conflicts, but others have not. However, they can be implemented easily. They are the delay times associated to certain transitions of a T-timed Petri net, and the structural parameters or weight of certain arcs.

Analogously to the model of the composting facility, the initial marking parameters can be classified into four categories: production areas (a_i), human resources (h_i), Production machinery, including the operators required to handle the industrial equipment (m_i), and raw materials (r_i).

More in detail, the following list of parameters can be stated:

- a_3 . Area for soil preparation (m^2).
- a_4 . Growing chambers (m^2).
- h_4 . Farm labourers for the manual harvesting of the mushroom fruits (persons).
- m_7 . Forklift for handling raw materials, containers, or finished mushroom packages (forklift and driver).
- m_8 . Farm tractor with implement for loading soil on containers (tractor and driver).
- m_9 . Farm tractor with implement for waste removal (tractor and driver).
- m_{10} . Machinery for packing the final product containing mushroom fruits (packages inside the machine).
- r_{15} . Disinfectant for the area for soil preparation and the growing chamber (litres).
- r_{16} . Bags of peat for soil preparation (units).
- r_{17} . Water for soil preparation and irrigation (litres).
- r_{18} . Fungicide for soil preparation (litres).
- r_{19} . Containers for transporting the prepared soil (litres).
- r_{20} . Cages for placing the inoculated compost (units).
- r_{21} . Packages that include compost and seeds (units).
- r_{22} . Insecticide for disinfecting the crop (litres).
- r_{23} . Labels for the packages of finished product (units).
- r_{24} . Boxes for the packages of finished products (units).

With regard to the category of decision variables related to the actual conflicts, a review of structural conflicts of the model can be done. Figure 2, eases the process of identifying the places associated to the structural conflicts.

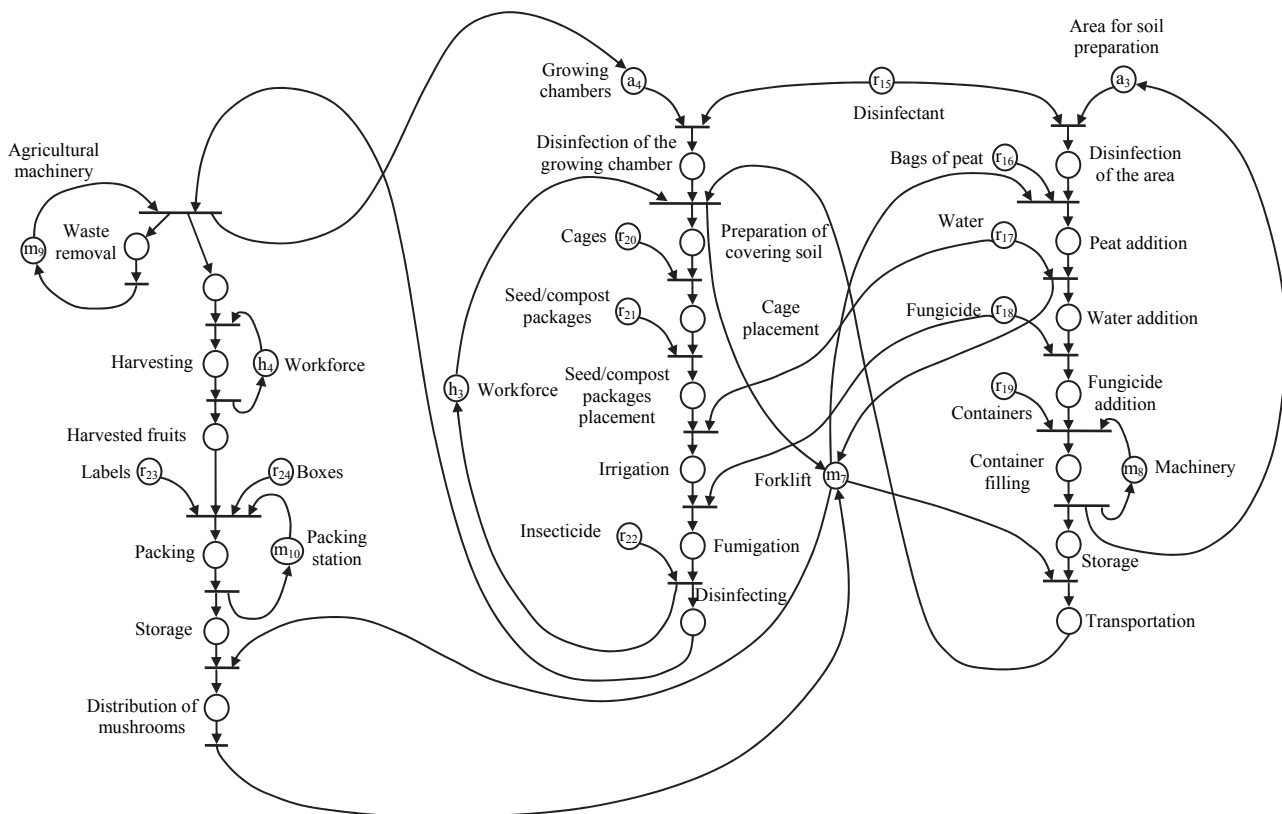


Figure 2. Model of the cultivation facility of common mushroom

As it can be seen in the model of the facility, the cultivation process of mushroom is quite sequential. However, there are some structural conflicts that can be pointed out:

- a) Place labeled “disinfectant”. This product should not be in such a restriction that it would be necessary to decide in which operation it is used and in which operation cannot be used. In food industry, it is imperative proceed with enough degree of hygiene in the production operations. For this reason, it is not convenient for this structural conflict to be transformed into an actual conflict. This fact would imply shortages in disinfectant products and it may compromise the quality and even the commercialization of the final production.
- b) Place labeled “forklift”. This place has already been explained in the previous section, since there are also this kind of shared resources, which are expensive and for that reason they are not usually overestimated. The optimal management of this kind of shared resources may have a significant impact in production yield.

7. DECISION MAKING METHODOLOGY

Once a model with freedom degrees has been constructed, as described in the previous sections, an optimization methodology can carry out in an automatic manner the search for the best configuration of the freedom degrees or, at least, for one configuration that works reasonably well if it is found in a short period of time.

The optimization problem requires a cost or objective function that quantifies the consecution of the objectives of the system from certain parameters produced during the evolution of the system. Simulation is a convenient methodology, which allows obtaining these performance parameters.

The statement of this optimization problem also requires a model of the system, a pool of feasible solutions or solution space and certain additional constraints.

The solving methodology should include a process to explore the solution space, since usually the exhaustive exploration would consume an amount of computer resources not available to be applied to the decision problem. An effective choice for this process consists of a metaheuristics, such as genetic algorithms, ant colony, particle swarm, or simulated annealing.

8. CONCLUSIONS

This document has presented a Petri net model of a facility for producing compost and for cultivating common mushroom.

The model includes explicitly several type of common controllable parameters and allows easily the addition of more types of freedom degrees. This is a key feature for testing different configurations and finding out the one that best leads the system to the main objectives of the system.

In addition, the description of an optimization methodology would allow to apply the mentioned model to a decision making support tool.

This tool would alleviate the complexity of making decisions related to the operation of a facility for the production of compost and cultivation of common mushroom. Making appropriate decisions can state the difference between success and failure in a competitive food global market.

REFERENCES

- Cicirelli F.D., Furfaro A. and Nigro L., 2010. A Service-Based Architecture for Dynamically Reconfigurable Workflows. *Journal of Systems and Software*, Vol. 83, n. 7, pp. 1148-1164.
- Guan, S., Nakamura, M., and Shikanai, T. 2010. Hybrid Petri Nets and Metaheuristic Approach to Farm Work Scheduling. In Aized, T. (Ed.) *Advances in Petri Net Theory and Applications*. Chapter 8. Sciyo.
- Latorre, J.I., Jiménez, E., Blanco, J., Sáenz, J.C. 2015. Decision Support System, Based on The Paradigm of the Petri Nets, for the Design and Operation of a Dairy Plant. *International Journal of Food Engineering*, 11(6): 767-776.
- Latorre, J.I., Jiménez, E., Blanco, J., Sáenz, J.C. 2014. Optimal Design of an Olive Oil Mill by Means of the Simulation of a Petri Net Model. *International Journal of Food Engineering*, 10(4): 573-582.
- Latorre, J.I., Jiménez, E., Blanco, J., Sáenz, J.C. 2013. Integrated Methodology for Efficient Decision Support in the Rioja Wine Production Sector. *International Journal of Food Engineering*.
- Latorre, J.I., Jiménez, E., Blanco, J., Sáenz, J.C. 2012. Decision making in the Rioja wine production sector. In *Proceedings of the 24th European Modelling and Simulation Symposium (EMSS 12)*. Vienna, Austria, pp. 452-457.
- Latorre, J.I., Jiménez, E., Pérez, M., 2011. Petri nets with exclusive entities for decision making. *International Journal of Simulation and Process Modeling*, Special Issue on the I3M 2011 Multiconference.
- Latorre, J.I., Jiménez, E., Pérez, M., 2010. On the Solution of Optimization Problems with Disjunctive Constraints Based on Petri Nets. In *Proceedings of the 22nd European Modelling and Simulation Symposium (EMSS 10)*. Fez, Morocco, pp. 259-264.
- Léger, B., Naud, O., Gouache, D., 2011. Specifying a strategy for deciding tactical adjustment of crop protection using CPN tools. *Congress of the European Federation for Information Technology in Agriculture, Food and the Environment Efitá 2011*. Pages 1 – 6.
- Leiva, F.J., Saenz-Díez, J.C., Martínez E., Jiménez E., Blanco J. “Environmental impact of mushroom compost production”. *Journal of the Science of Food and Agriculture*. In press. 2016
- Leiva, F.J., Saenz-Díez, J.C., Martínez E., Jiménez E., Blanco J. “Environmental impact of *Agaricus bisporus* cultivation process”. *European Journal of Agronomy*, 71: 141–148. 2015.
- Leiva-Lázaro, F.J., Blanco-Fernández, J., Martínez-Cámara, E., Latorre-Biel, J.I., Jiménez-Macías, E. “Mushroom cultivation process, *agaricus bisporus* variety: comparison between traditional and climate controlled cultivation and identification of environmental impacts of the production processes”. *Proc. of the Int. Workshop on Simulation for Energy, Sustainable Development & Environment 2015*. Bruzzone, Janosy, Longo, Zacharewicz Eds.
- Longo, F., De Bonis, F., Spadafora, F., and Nicoletti, L. 2014. Training in car terminals: A modular architecture based on distributed and interoperable simulation. *European Modeling and Simulation Symposium. EMSS 2014*. Bordeaux, France.
- Melberg, R., Davidrajuh, R. 2009. Modeling Atlantic salmon fish farming industry. In *Proceedings of the IEEE International Conference on Industrial Technology. ICIT 2009*. Pages 1-6.
- Shikanai, T.; Nakamura, M.; Guan S.; Tamaki, M. 2008. Supporting system for management of agricultural corporation of sugarcane farming in Okinawa Islands. *World conference on agricultural information and IT, IAALD AFITA WCCA 2008*, Tokyo University of Agriculture, Tokyo, Japan, 24 - 27, pp. 1101-110.
- Silva, M. 1993. Introducing Petri nets. In *Practice of Petri Nets in Manufacturing*, Di Cesare, F., (editor), pp. 1-62. Ed. Chapman&Hall.

FEASIBILITY STUDY OF AN AUGMENTED REALITY APPLICATION TO ENHANCE THE OPERATORS' SAFETY IN THE USAGE OF A FRUIT EXTRACTOR

Simone Spanu^(a), Massimo Bertolini^(b), Eleonora Bottani^(c), Giuseppe Vignali^(d), Luciano Di Donato^(e), Alessandra Ferraro^(f), Francesco Longo^(g)

^{(a),(b),(c),(d)} CERIT Centre - University of Parma, Viale delle Scienze 181/A, 43124 Parma, ITALY

^{(e),(f)} INAIL - Department of Technological Innovation, Via Roberto Ferruzzi, 38 - 000143 Rome (Italy)

^(g) Department of Mechanical, Energy and Management Engineering, University of Calabria, Ponte P. Bucci 41C, Arcavacata di Rende (CS), Italy

^(a)simone.spanu@nemo.unipr.it, ^(b)massimo.bertolini@unipr.it, ^(c)eleonora.bottani@unipr.it, ^(d)giuseppe.vignali@unipr.it, ^(e)l.didonato@inail.it, ^(f)ale.ferraro@inail.it, ^(g)f.longo@unical.it

ABSTRACT

This paper proposes a framework to carry out a feasibility study of the implementation of augmented reality (AR) systems in the manufacturing context, to enhance the safety of employees in carrying out maintenance tasks. AR systems are recognized as effective tools to help a user perform tasks and operations, by adding virtual information (such as live-video stream, pictures, or instructions) to the real-world environment. A feasibility study and its application to a real context has been carried on in collaboration with a primary manufacturer of food equipment. The targeted machine is a hot-break juice extractor, manufactured by the company; the machine is used to separate juice from fruit pieces. The operation where the AR systems is intended to be applied is a maintenance task, concerning the cleaning or substitution of the porous sieves of the machine. Such a task should be carried out at least every 12 hours of functioning of the machine. The main steps for the development of the AR solution, as well as the expected pros/cons of its implementation and usage are discussed.

Keywords: augmented reality (AR); feasibility study; employee safety; maintenance; food machinery.

1. INTRODUCTION

Traditional risk assessment techniques, used to evaluate workplace safety and security, showed in the past some limits in reducing the frequency and severity of accidents at work. This is mainly due to the unpredictability of human behavior that, in some circumstances, could lead to non-compliance of rules related to the workplace safety. In fact, it has been estimated that over the 65% of work accidents is caused by human errors (Geller, 2001).

On the basis of these considerations, behavioral based methodologies for risk assessment have been employed in some cases; however, they have not reached a wide industrial application, due to the lack of specific competences inside the company (Wirth and

Sigurdsson, 2008), the need for the support of computer-based systems and the high cost (Zhang and Fang, 2013).

A current challenge is to find a standardized method that is able to monitor industrial activities and to reduce the number of accidents, especially due to the man-machine interface. To this end, employees could be helped, during the execution of risky tasks (such as maintenance tasks), by augmented reality (AR) systems or by voice assistance systems. AR encompasses a set of technologies through which the view of the real world environment is augmented by computer-generated elements or objects. In other words, the term AR refers to a mediated reality, where sensory perception (in particular, visual perception) of the physical real-world environment is enhanced by means of computing devices. AR aims at simplifying the user's life by bringing virtual information not only to his/her immediate surroundings, but also to any indirect view of the real-world environment, such as live-video stream (Carmignani et al., 2010).

Based on these premises, a feasibility study is proposed in this paper to evaluate the profitability of implementing an AR system to help the operator in the execution of some maintenance tasks on an automatic machinery, which is part of a fruit juice processing plant. The AR application is intended to be installed on a mobile system, such as a smartphone or a tablet. The operator will capture the scene of interest with the device camera and will receive the same scene on the display; the scene captured will be augmented with information, warning and videos, which could help the employee to carry out the maintenance tasks in a correct and safe way.

The remainder of the paper is organized as follows. Section 2 provides the reference framework that can be followed for the feasibility study of AR implementation in real contexts. Section 3 details the feasibility study along with its application to a real industrial case. Section 4 discusses the main findings of the study and indicates future research steps.

2. REFERENCE FRAMEWORK

As mentioned, the targeted case study refers to the analysis of a maintenance task, which is carried out on a food machine that is part of a fruit processing line.

The machine under examination is a hot-break juice extractor, which is used to separate juice from fruit pieces. Hot-break means that the product entering the machine has been heated up to $85\div 90^{\circ}\text{C}$. There are four main components of this machine, namely: a stator, a rotor and two cylindrical sieves.

The rotor is concentric to the stator and rotates inside it. The external surface of the rotor contains some paddles, which force the fruit pieces against the sieves. Being pressed by the paddles, the fruit releases its juice, which can pass through the sieves, while the peels, the seeds and the fruit pieces are held back. The size of the holes diameter on the sieves depends on the product that has to be processed, although it is usually in the range $0.2\div 2$ mm. Moreover, the paddles located on the external surface of the rotor have a specific inclination, which allows to push the fruit residues towards the machine end section, where they are discharged, so partially avoiding the clogging of the stator. The targeted machine can process up to 100 ton/h of product. Figure 1 shows a 3D modeling of the main machine components.

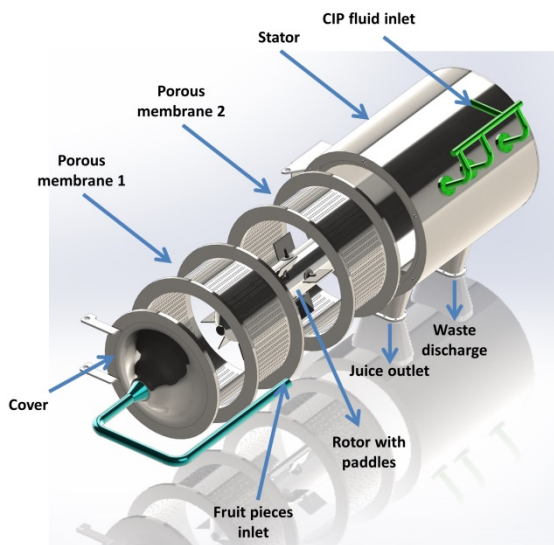


Figure 1: Main components of the juice extractor.

From Figure 1 it can be noticed that the stator is closed with a cover, through which the product to be processed is inserted, and that a pipeline located on a side of the stator carries inside its chamber some sterile water, that can be used for a gross Cleaning In Place (CIP) process.

The operation targeted to evaluate the implementation of AR systems is a maintenance task, concerning the cleaning or substitution of the sieves of the machine. This operation consists, roughly, in the following actions: (1) stopping the machine; (2)

removing the two sieves; (3) cleaning them with a water jet; (4) re-position the sieves inside the stator correctly; (5) starting again the machine. If the sieves are severely damaged or if a product change has to be carried out, the two sieves will not be cleaned; rather, they will be replaced with new ones, as the holes dimension depends on the product that has to be processed. In this case, the operator should also pick the new sieves from the warehouse and make sure that they are suitable for the type of production that will be realized once the machine is re-started.

According to the plant manufacturer, if the production line is working at full capacity, the operation described is quite frequent, being required at least every 12 hours. Changing the sieves ensures that the line efficiency is kept constant and, at the same time, should avoid an excessive wear of the paddles and of the sieves themselves, due to an accumulation of fruit residues in the stator chamber.

This operation was chosen among the whole set of maintenance tasks that can be carried out on the targeted equipment because it is relatively frequent and also because it exhibits a not negligible risk level. Indeed, before the execution of the described task, the machine is working and has to be cooled; consequently, the operator is likely to come into contact with very hot product (up to $85\div 95^{\circ}\text{C}$) and with moving parts. The manufacturer evaluated and managed these risks selecting technical and procedural measures described in the following section.

To evaluate the implementation of an AR system to help the employee in the execution of the targeted task, the following steps must be carried out:

1. collecting all the necessary data about the machine and task. Examples of these data include technical drawings of the machine or at least of the relevant components, or the detailed description of the procedure targeted for implementation (for instance, retrieved from the machine operating and maintenance manual);
2. collecting other useful information, such as photos of the equipment or of part of it, photos of the tools required to carry out the targeted operation, etc. Videos of the operation carried out by a skilled worker could also be useful to reproduce the correct execution of the task;
3. organizing the acquired information and data by means of tags or similar categorization tools. Such a classification is expected to make it easier for the AR system to search and display the proper information, for instance in response to an employee query;
4. developing the AR application. This step reflects the software implementation of the AR solution, embodying all the data collected before;
5. analyzing (or estimating) the expected cost and benefits.

In the continuation of the paper, we will address almost all the above points, along with their implementation in the targeted context. The only exception is step 4, i.e. the development of the AR application, since it deserves to be described in full detail and thus will be object of a further work.

3. FEASIBILITY STUDY

We now detail the steps briefly described at the end of the previous section.

3.1. Step 1: Analysis of the procedure for sieves cleaning/substitution

A summary of the steps to be followed to carry out the targeted maintenance task, according to the maintenance and operating manual of the juice extractor, has been proposed in section 2. It is, nonetheless, useful to depict them in the form of a diagram, as proposed in Figure 2, since such representation help identify the sequence of activities as well as their logical relationships.

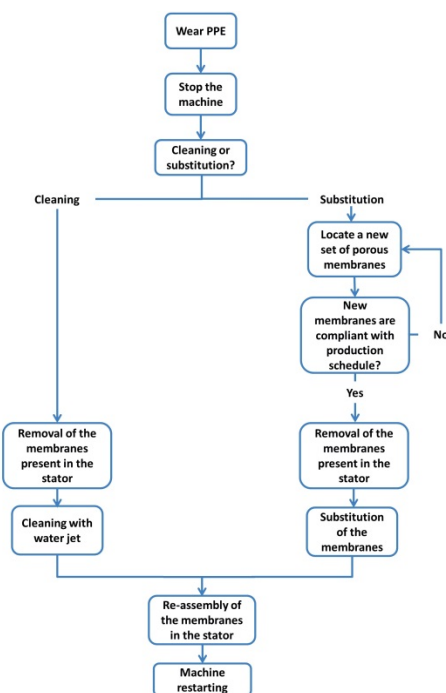


Figure 2: Main steps for the sieves cleaning/substitution.

As can be seen from Figure 2, the first activity the employee should carry out consists in wearing the required Personal Protective Equipment (PPE). In this case, we recall that the main risk is to come into contact with hot products; accordingly, the required PPE are protective and heat resistant gloves, compliant with EN 407, and a protective screen.

The second step of the task is to stop the machine. In order to do this, the following actions have to be carried out:

- from the electric panel of the machine, turn off the product flow by acting on button 13 (see Figure 3);
 - close the manual ball valve located on the product supply pipeline (B);
 - close the manual valve located on the juice outlet section (C);
 - open the drain valve (D);
 - open the manual butterfly two valves on the water supply pipeline (A), so to pre-wash the stator chamber;
 - from the electrical panel, stop the machine by pushing button 11;
- turn the main switch (6) to position “0”. This switch is an interlocking device with guard locking. This is a supplementary safe measure that ensures the reachability of the stator when its hazardous movements are stopped. Selection and installation of this safety device have moreover to minimize the possibility of defeating in reasonably foreseeable manner (see requirements contained in the standard EN ISO 14119:2013). Figure 3 and Figure 4 show the main components of the electrical panel and of the machine on which the operator must act to properly carry out the operations previously described.



Figure 3: Machine electrical panel.

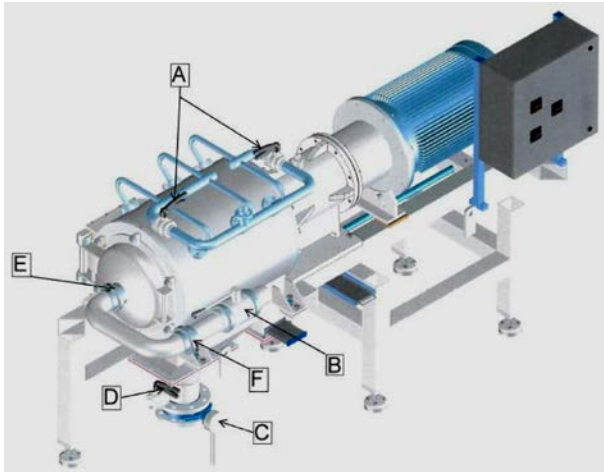


Figure 4: Machine representation.

The components listed in Figures 3 and 4 are detailed in Table 1.

Table 1: Description of the components listed in Figures 3 and 4.

Electrical panel		Machine representation	
No.	Description	No.	Description
1	Voltmeter	A	Water supply butterfly valve
2	Voltmetric switch	B	Product supply ball valve
3	Keyboard	C	Juice outlet valve
4	Increase rotor rotation speed	D	Drain valve
5	Decrease rotor rotation speed	E	Coupling between product pipe and stator chamber
6	Main switch	F	Coupling in product supply pipe
7	Anomalies indicator		
8	Machine start		
9	Cork		
10	Product feed indication		
11	Machine stop		
12	Local control/remote control switch		
13	Enabling product feed		
14	Emergency stop		

Once the machine is stopped, the operator has to choose whether to carry out a simple cleaning of the porous sieves or their full replacement. In this latter case, he/she has to pick the new pair of sieves and check if they are compliant with the kind of product scheduled to be processed after the machine restarts.

At this point, the employee should remove the sieves located in the stator chamber. The actions required to properly perform this operation are the following:

- unscrew the coupling E (see Figure 4 and Table 1);
- loosen the coupling F (see Figure 4 and Table 1), so as to remove the product pipeline from the machine's cover;
- unscrew the cover locking nuts using a 30 mm wrench;
- open the machine's cover;
- screw the supplied pullers on the first sieve and remove it;
- repeat the last action on the second sieve.

Once the above set of tasks has been completed, the sieves can be cleaned or, if damaged, replaced with the new ones. Finally, the sieve has to be re-assembled and the machine has to be restarted. It is self-evident that, to assemble the sieves and restart the machine, it is sufficient to follow backwards the actions listed above.

3.2. Step 2: Data collection

After the description and the analysis of the procedure retrieved from the maintenance and operating manual, we carried out a detailed data collection phase. This step is intended to gather all the relevant information that could be useful to develop the AR application. Examples of relevant pieces of information are technical drawings, photos of the whole machine or of some parts, and/or photos of the tools required to carry out the set of activities described in the previous sub-section. Videos reproducing the behavior of a trained operator, who is carrying out the sieves substitution, have also been recorded. To this extent, some visits at the company's site were carried out from May to July 2016.

Examples of information retrieved during site visits (e.g., pictures of some small particular features of the machine, tools used to lock the machine's cover) are proposed below.

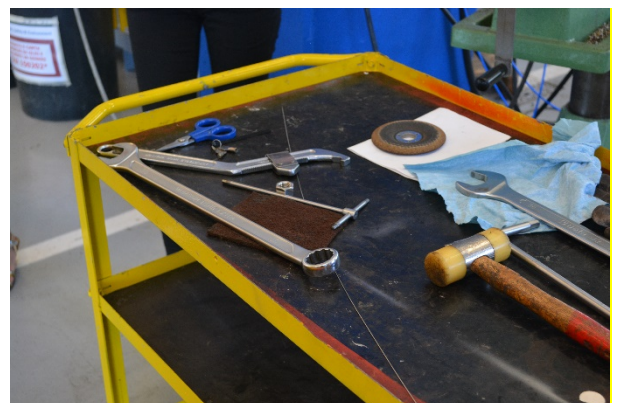


Figure 5: example of tools used during the targeted maintenance task.



Figure 6: the sieves to be substituted during the targeted maintenance task.

Photos and pictures are also useful to set up a feature-based tracking of the machine and its main parts. This means that machine and components can be recognised directly based on their shapes or other characteristics features, avoiding the use of markers (marker-less systems). Otherwise, AR systems typically make use of markers to identify either machines, equipment or safety devices. In the case in exam, however, these markers would need to be placed on the machine or on elements/parts of machine, which, however, could compromise its functioning. For instance, a marker could not be placed on the sieve, to recognise it, as the sieve is in direct contact with the food product. Moreover, the fruit is at hot temperature, meaning that the marker would be subject to relevant thermal excursions.

3.3. Step 3: Organization of the acquired information

In many cases, AR systems couple the 3D rendering of the machine being reproduced with a set of video or print instructions and a personal (voice) assistant. In the case under examination, all the above elements are planned to be included in the AR solution that will be developed for the targeted machine.

The design of the personal assistant, in particular, requires a further preliminary step, i.e. the classification of the information acquired by means of keywords or questions that the employee could ask when carrying out the task supported by the AR system. Indeed, personal assistants work by using a natural language user interface to answer questions, make recommendations, or perform actions, while retrieving the relevant information from a set of keywords.

There are several ways to organise data so that they can be used by a personal assistant. The simplest way is to identify the possible questions a non-expert employee could ask when carrying out the task of cleaning/replacing the sieves of the extractor. As an example, let's think about the first task of the list in section 3.1, i.e. "from the electric panel of the machine, turn off the product flow by acting on button 13". A

non-expert employee could ask, for instance, the following questions:

1. Where is button 13? What is button 13 for?
2. Where is the electric panel?
3. What is the correct movement for turning off the product flow?
4. ...

Obviously, the set of questions listed above is not exhaustive and is intended to provide only an example of possible indications a non-expert employees could ask when carrying out the first task of the targeted procedure. Nonetheless, some keywords can be easily identified from this set of sample questions, for instance "button 13", "electric panel", or "movement". Categorizing the data collected means giving them a sort of tag ("button 13", "electric panel", "movement"), so that the personal assistant is able to search the answer to the employee questions by screening the tags. To be more precise, anytime an employee asks, for instance, "where is button 13?", the personal assistant will identify the keyword "button 13" and will return the whole set of data which have been tagged with "button 13".

3.4. Step 4: Development of AR application

The next step is the development of the AR solution, including the 3D rendering of the machine being reproduced, the augmented information (print or video instructions) and the personal assistant. This task reflects software implementation and verification (or debugging). The AR solution can then be installed directly on the machine or used on a personal digital assistant (PDA), for instance for remote training of new employees.

The real development of the AR solution is a complex step and, actually, is not the focus of the present work. More precisely, for the targeted application the AR solution is being developed by other partners of the SISOM project (specifically, from the University of Calabria and University of Genoa). Therefore, the related details will be described in a separate work.

3.5. Step 5: Cost and benefit estimate

The last step of the framework consists in estimating the cost and benefit resulting from the use of the AR system in the targeted context. At the time of writing, as mentioned, the AR solution is still being developed, which prevents the possibility of providing a quantitative evaluation of the cost and benefit resulting from its application in the real scenario. Nonetheless, some indications about the potential cost and saving resulting from the use of an AR solution to support the task examined can be provided.

With respect to the cost of AR, the main components obviously include the cost for data collection (step 2), for the organization of the pieces of

information to make them usable by the personal assistant (step 3) and the cost for developing the AR solution (step 4). In addition, the AR solution needs to be either installed on the machine or tested through laboratory experiments. These costs are quite easy to be estimated, as most of them consist in manpower costs.

With respect to the expected benefits, it is worth mentioning that some authors in the literature have discussed (and sometimes also quantified) the benefits resulting from the use of AR systems in real cases. Among others, these benefits can include:

- Faster execution of the task by the employees (Sääski et al., 2008, Serván et al., 2012);
- Faster training of the employees on maintenance tasks (Besbes et al., 2012; Webel et al., 2013);
- Lower number of errors made by the employees when carrying out the task (Webel et al., 2013);
- Higher accuracy in assembly tasks (Rios et al., 2013);
- Decrease in the number of accidents or near misses related to the task supported by the AR system.

The above elements should be quantitatively evaluated in the specific context to assess the suitability of adopting the AR solution.

4. DISCUSSION AND CONCLUSIONS

The possibility of using AR system to support the execution of maintenance tasks has been widely explored in many sectors of manufacturing industry, as shown by the published literature. For instance Webel et al. (2013) have shown that AR systems could be helpful in the assembly and maintenances of machines used in the beverage sector. De Crescenzo et al. (2011) instead, presented a prototype, based on an AR system, to help operators in executing maintenance tasks on aircrafts. Other cases are reported for instance by Sääski et al., (2008) (agricultural machinery industry) and by Salonen et al. (2009) (automotive industry).

In most of the cases the adoption of an AR system was appreciated by the operators and it brought many benefits such as, for instance, faster execution of the tasks, lower number of errors and a decrease in the time required for a proper training of inexperienced operators (see section 3.5).

The same benefits are expected in this case too. However, as at the time of writing the implementation of the AR system has not been tested (yet), the capability of the solution developed to decrease the risks associated to the targeted task still has to be evaluated.

Obviously, to assess the convenience of adopting this kind of application, the benefits mentioned above should be quantified through experimental tests and related to the cost expected for the system

implementation. In general we can expect that this latter cost consists of five main components, i.e.:

1. cost for data collection;
2. cost for the organization of the pieces of information to make them usable during the development of the application;
3. cost for purchasing the hardware required to develop and implement the application;
4. cost for developing the AR solution;
5. cost for implementation and testing.

If we exclude the cost components 1 and 2, which are expected to have a limited impact on the total cost of the system (because they are representative of the operations that require less manpower to be carried out), the remaining cost components will be carefully estimated and then monitored during the application development.

Finally, a prototype will be built and tested, so that the cost/benefit ratio could be evaluated. In the case of favorable results, the natural next step will be the implementation of the system in the real industrial environment.

REFERENCES

- Besbes, B., Collette, S. N., Tamaazousti, M., Bourgeois, S., Gay-Bellile, V., 2012. An interactive augmented reality system: a prototype for industrial maintenance training applications. In *Mixed and Augmented Reality (ISMAR)*, 2012 IEEE International Symposium on (pp. 269-270). IEEE.
- Carmigniani, J., Furht, B., Anisetti, M., Ceravolo, P., Damiani, E., & Ivkovic, M., 2011. Augmented reality technologies, systems and applications. *Multimedia Tools and Applications*, 51(1), 341-377.
- De Crescenzo, F., Fantini, M., Persiani, F., Di Stefano, L., Azzari, P., Salti, S., 2011. Augmented reality for aircraft maintenance training and operations support. *IEEE Computer Graphics and Applications*, 31(1), 96-101.
- Geller, E.S., 2001. Behavior-based safety in industry: realizing the large-scale potential of psychology to promote human welfare. *Applied & Preventive Psychology*, 10, 87-105.
- Rios, H., González, E., Rodríguez, C., Siller, H. R., Contero, M., 2013. A Mobile Solution to Enhance Training and Execution of Troubleshooting Techniques of the Engine Air Bleed System on Boeing 737. *Procedia Computer Science*, 25, 161-170.
- Sääski, J., Salonen, T., Liinasuo, M., Pakkanen, J., Vanhatalo, M., Riitahuhta, A., 2008. Augmented reality efficiency in manufacturing industry: a case study. In *DS 50: Proceedings of NordDesign 2008 Conference*, Tallinn, Estonia, 21.-23.08. 2008.
- Salonen, T., Sääski, J., Woodward, C., Korkalo, O., Marstio, I., Rainio, K., 2009. Data pipeline from CAD to AR based assembly instructions. In

- ASME-AFM 2009 World Conference on Innovative Virtual Reality (pp. 165-168). American Society of Mechanical Engineers.
- Servan, J., Mas, F., Menéndez, J. L., Ríos, J., 2012. Assembly work instruction deployment using augmented reality. In *Key Engineering Materials* (Vol. 502, pp. 25-30). Trans Tech Publications.
- Webel, S., Bockholt, U., Engelke, T., Gavish, N., Olbrich, M., Preusche, C., 2013. An augmented reality training platform for assembly and maintenance skills. *Robotics and Autonomous Systems*, 61(4), 398-403.
- Wirth, O., Sigurdsson, S.O., 2008. When workplace safety depends on behavior change: Topics for behavioural safety research. *Journal of Safety Research*, 39, 589-598.
- Zhang, M., Fang, D., 2013. A continuous behavior-based safety strategy for persistent safety improvement in construction industry. *Automation in Construction* 34, 101-107

ACKNOWLEDGEMENTS

The research described in this paper has been funded by INAIL (the Italian institute for insurance and safety at the workplace) under the SISOM (*Sistemi Intelligenti Sicurezza Operatore Macchina*) project. We also thank the company CFT S.p.A., sited in Parma (Italy) for the support given to the experimental part of this research.

AUTHORS BIOGRAPHY

Simone SPANU is a scholarship holder at CERIT research center at the University of Parma. In March 2014 he has achieved a master degree in Mechanical Engineering for the Food Industry at the same university. His main fields of research concern industrial processes modelling and simulation, with a particular focus on the CFD simulation for the advanced design of food and beverage processing plants.

Massimo BERTOLINI graduated in 1999 in Mechanical Engineering at the University of Parma and received his Ph.D. in Production Systems and Industrial Plants from the same university in 2004. Since 2002 he has been a Lecturer in Industrial Plants at the Department of Industrial Engineering of the University of Parma. He is currently Associate professor of Operations management at the same university. His research activities mainly concern equipment maintenance, reliability, production planning, logistics and food safety. He has published more than 60 papers in international journals and conferences.

Eleonora BOTTANI is Associate professor of Industrial Logistics at the Department of Industrial Engineering of the University of Parma. She graduated (with distinction) in Industrial Engineering and Management in 2002, and got her Ph.D. in Industrial Engineering in 2006, both at the University of Parma. Her primary research interests are in the field of

logistics and supply chain management, while secondary research topics encompass safety and quality of industrial plants. She is author (or co-author) of approx. 130 scientific papers, referee for more than 60 international scientific journals, editorial board member of five scientific journals, Associate Editor for one of those journals, and Editor-in-Chief of a scientific journal.

Giuseppe VIGNALI is an Associate Professor at University of Parma. He graduated in 2004 in Mechanical Engineering at the University of Parma. In 2009, he received his Ph.D. in Industrial Engineering at the same university, related to the analysis and optimization of food processes. Since August 2007, he worked as a Lecturer at the Department of Industrial Engineering of the University of Parma. His research activities concern food processing and packaging issues and safety/security of industrial plant. Results of his studies related to the above topics have been published in more than 70 scientific papers, some of which appear both in national and international journals, as well in national and international conferences.

Francesco LONGO received his Ph.D. in Mechanical Engineering from University of Calabria in January 2006. He is currently Assistant Professor at the Mechanical Department of University of Calabria and Director of the Modelling & Simulation Center – Laboratory of Enterprise Solutions (MSC-LES). He has published more than 150 papers on international conferences and journals. His research interests include Modeling & Simulation tools for training procedures in complex environment, supply chain management and security. He is Associate Editor of the “Simulation: Transaction of the society for Modeling & Simulation International”. For the same journal he is Guest Editor of the special issue on Advances of Modeling & Simulation in Supply Chain and Industry. He is Guest Editor of the “International Journal of Simulation and Process Modelling”, special issue on Industry and Supply Chain: Technical, Economic and Environmental Sustainability. He is Editor in Chief of the SCS M&S Newsletter and he has served as General Chair and Program Chair for the most important international conferences in the simulation area.

Luciano DI DONATO graduated in 1992 in Electrical Engineering at the University of Federico II. He had a previous position as technical director for an electrical installation company and played professional service in the field of electrical construction sites. Since 1997 he is a researcher in INAIL and since 2015 he is Responsible of Machines and work equipment Lab in Department of Technological Innovation. His main fields of research concern safety of machinery and working equipment, the critical issues of electrical equipment of machines and the issue of defeating, misuse and reasonably foreseeable misuse related to safety distances and safety devices. He is author of about fifty papers published in

journals and many conference papers. He participated in many scientific committees and international meetings. He is member of National and European technical working groups for safety of machines and confined space with or without pollution. He is a Chair Person of CEN TC 146 Packaging machines – Safety.

Alessandra FERRARO graduated in 2004 in Mechanical Engineering at the University of Roma Tre. Started professional experience providing maintenance services for a leading chemical company, since 2011 she is a researcher in INAIL Department of Technological Innovation. Her primary research interest is in safety of machinery and working equipment, focusing on the critical issues of machines for lifting of people and on the topic of defeating, misuse and reasonably foreseeable misuse. She is author (or co-author) of papers in safety journals, she participated as speaker in many conferences, she is active in training on safety for technicians on the field.

Authors' Index

Askari	19	
Bertolini	70	
Blanco-Fernández	58	64
Bottani	26	70
DeFalco	49	
DiDonato	70	
Digiuni	26	
Elmasry	5	
Emam-Djomeh	19	
Ferrari	39	
Ferraro	70	
Hashemabadi	19	
Jiménez-Macías	58	64
Latorre-Biel	58	64
Leiva-Lázaro	58	64
Loia	49	
Longo	70	
Malekjani	19	
Marchini	26	
Martínez-Cámara	58	64
Montanari	26	32
Olaniyan	11	
Owolabi	11	
Pérezde la Parte	58	64
Rahmati	1	
Rarità	49	
Shahbazi	1	
Solari	32	
Spanu	39	70
Tagliavini	26	32
Tarek	5	
Tomasiello	49	
Vignali	39	70